EVALUATION OF THE CLEARSKY SMOKE DISPERSION ENSEMBLE FORECAST SYSTEM FOR AGRICULTURAL FIELD BURNING IN EASTERN WASHINGTON AND NORTHERN IDAHO

BY

KYLE MATTHEW HEITKAMP

A thesis submitted in partial fulfillment of
the requirements for the degree of

MASTER OF SCIENCE IN ENVIRONMENTAL ENGINEERING

WASHINGTON STATE UNIVERSITY
Department of Civil and Environmental Engineering

May 2006

To the Faculty of Washington State University:

The members of the Committee appointed to examine the dissertation/thesis of KYLE MATTHEW HEITKAMP find it satisfactory and recommend that it be accepted.

_____

(Chair)

_____

_____

ACKNOWLEDGMENT

I would like to acknowledge and thank all of the people that have been involved with my research. I would first like to thank the faculty, supporting staff, and graduate students of the Civil and Environmental department for a great academic experience at Washington State University. I am very grateful for the knowledge, guidance, and support provided to me by my committee members Drs. Brian Lamb, Joseph Vaughan, and Candis Claiborn. Special thanks go to Drs. Brian Lamb and Joseph Vaughan for devoting time to familiarize me with the computational components of my research.

I am grateful to everyone that assisted me in the planning and collection of data during the 2004 plume height measurement campaign. The planning and data collection team included: Dr. Brian Lamb, Dr. Candis Claiborn, Dr. Joseph Vaughan, Clint Bowman, Jorge Jimenez, Julie Simpson, Ranil Dhammapala, Scott Brewer, and Shawn Nolph.

I would also like to thank the ClearSky users (Idaho State Department of Agriculture, Idaho Department of Environmental Quality, Coeur d'Alene Tribes, Nez Perce Tribes, and Washington Department of Ecology) for their cooperation during the course of this research.

Last but not least, I would like to thank my family and friends for their support and encouragement during my research.

Support for this research was funded by the NW-AIRQUEST Consortium.

EVALUATION OF THE CLEARSKY SMOKE DISPERSION ENSEMBLE FORECAST SYSTEM FOR AGRICULTURAL FIELD BURNING IN EASTERN WASHINGTON AND NORTHERN IDAHO

ABSTRACT

By Kyle Matthew Heitkamp, M.S.
Washington State University
May 2006

Chair: Brian Lamb

An ensemble air quality forecast system (ensemble ClearSky) was developed to predict hourly surface level particulate matter concentrations downwind of agricultural field burns in eastern Washington and northern Idaho. A suite of 17 meteorological forecasts is used as input to a Lagrangian dispersion model (CALPUFF) along with a single $PM_{2.5}$ emissions scenario (representing agricultural field burns) to yield an ensemble of $PM_{2.5}$ dispersion forecasts. Thus, for a selected day, the ensemble ClearSky system produces a range of possible $PM_{2.5}$ forecasts by using 17 different, similarly possible, meteorological forecasts. The ensemble average (un-weighted average of ensemble members), individual ensemble members, and original ClearSky $PM_{2.5}$ forecasts were evaluated against observed $PM_{2.5}$ concentrations for two burn days during the 2004 burn season. The evaluation used observations from five monitoring sites on the August 17, 2004 burn day and seven monitoring sites on the September 8, 2004 burn day. Normalized mean error (NME) and unpaired peak prediction error (UPPE) were calculated for the $PM_{2.5}$ concentrations, and the mean absolute error (MAE) in wind direction was calculated for the forecast meteorology. For $PM_{2.5}$ prediction, the ensemble

average had lower NME values at 11 of the monitoring sites and lower UPPE values at five of the sites compared to original ClearSky.

With the exception of one monitoring site (Plummer, ID) where significant $PM_{2.5}$ over-prediction occurred, the lowest UPPE values ranged from 1% – 68% for the two burn days. The UPPE values for the ensemble average $PM_{2.5}$ forecasts ranged from 11% – 78%; and the UPPE values for the original ClearSky $PM_{2.5}$ forecasts ranged from 8% – 88 %. The lowest NME values ranged from 27% – 98% for the two burn days. The NME values for the ensemble average $PM_{2.5}$ forecasts ranged from 36% – 117%; and the NME values for the original ClearSky $PM_{2.5}$ forecasts ranged from 41% – 131%. The lowest MAE in wind direction values ranged from 13 – 73 degrees. Using the ensemble meteorology, the dispersion model was capable of predicting the maximum $PM_{2.5}$ concentrations within the range of 1% - 68% based upon the UPPE statistics.

TABLE OF CONTENTS

LIST OF TABLES

LIST OF FIGURES

CHAPTER 1

INTRODUCTION

1.1. Overview and Objectives

Agricultural burning is commonly used to remove crop residue after harvest in eastern Washington and northern Idaho. Wheat and Kentucky bluegrass (KBG) are two major crops grown in northern Idaho, while eastern Washington farmers chiefly grow wheat. Once these crops are harvested, farmers typically burn the crop residue on their fields. Burning agricultural fields is more cost-effective for farmers than other methods for clearing agricultural fields, including but not limited to: bailing, composting, and disking crop residue. Post harvest burning helps to control pests and plant diseases, maintains future harvest yield, and quickly removes the crop residue from the fields (ASI, 2003; ASI, 2004; Johnston et al., 2003).

Even though field burning is cost-effective, it releases many pollutants into the atmosphere. These pollutants include: particulate matter (PM), carbon dioxide (CO_2), carbon monoxide (CO), nitrogen oxides (NO plus NO_2, or NO_X), polycyclic aromatic hydrocarbons (PAHs), and a variety of other products of incomplete combustion (Crutzen and Andrea, 1990). The emissions from field burning can seriously degrade the local air quality of populated areas in eastern Washington and northern Idaho. Particulate matter with an aerodynamic diameter of less than 2.5 μm ($PM_{2.5}$) is a very important pollutant; the small particles can travel deep into human lungs and trigger respiratory health problems (Roberts and Corkill, 1998; Slaughter et al. 2003).

As a result of the potential air quality impact of field burning, both Washington and Idaho have developed field burn permitting systems to regulate when farmers are

allowed to burn their agricultural fields. The field burn permit system was created to help prevent cities and towns from being adversely impacted by air pollutants, specifically $PM_{2.5}$, emitted from field burning. First, burn managers for each state assemble databases of fields that are proposed to burn. Then, the burn managers use meteorological forecasts, air quality observations, and other information to help decide which farmers will be allowed to burn their fields. Once the burn managers have decided on fields to burn, they issue a burn call to the farmers. The burn call provides the farmers with restrictions for burning his fields including but not limited to: burnable acreage, start time, and finish time. Complete descriptions of the smoke management programs in Washington and Idaho are presented in WA DOE (2004) and ISDA (2004), respectively.

The ClearSky smoke dispersion forecast system for agricultural burning was developed at Washington State University and operated during the 2002 — 2005 agricultural burn seasons for eastern Washington and northern Idaho. ClearSky was developed to provide burn managers with an additional tool for making burn decisions. The project website (www.clearsky.wsu.edu) contains databases of field location, acreage, and crop type. Burn managers log into their respective database on the ClearSky website and create burn scenarios for the next day by selecting individual fields, burn start times, and acres to burn. At night, the burn scenarios are used to create scenario emission data files which are used in a dispersion modeling system to simulate plume transport for each scenario. ClearSky is automated and runs during the night using burn scenarios and the most recent numerical meteorological forecast. The next morning, the burn managers can view predicted surface $PM_{2.5}$ concentrations resulting from the burn

scenarios the burn managers created a day earlier. Jain (2004) provides a full description of the operational ClearSky system.

Previous evaluations of ClearSky found that small differences in the model-predicted wind direction can affect whether a simulated smoke plume impacts an air monitoring station or misses the station by a few kilometers (Jain, 2004). In order to improve the ClearSky system, uncertainties in meteorological forecasts must be represented. We hypothesize that ensemble techniques can be used to represent uncertainties in the forecast meteorology. The primary objective of this research is to improve air quality forecasts of $PM_{2.5}$ concentrations from agricultural burning in eastern Washington and northern Idaho. The approach for this objective is to use a suite of meteorological forecasts within the ClearSky system to produce ensemble forecasts of $PM_{2.5}$ concentrations. These ensemble $PM_{2.5}$ forecasts should represent the range of expected $PM_{2.5}$ plumes produced by agricultural burning. This thesis presents an evaluation of the ensemble $PM_{2.5}$ results in comparison to the deterministic results produced by the original ClearSky system. Measured $PM_{2.5}$ surface concentrations available from Washington and Idaho monitoring networks are used for this evaluation.

This thesis is divided into four chapters. The Introduction chapter provides a description of the current deterministic ClearSky model, a summary of the 2003 ClearSky evaluation, and a literature review of ensemble techniques used in both numerical weather prediction and air quality modeling. The second chapter is a summary of a short field study to obtain plume rise measurements from field burns for evaluation of the ClearSky plume rise estimates. Chapter three, Evaluation of the ensemble ClearSky System, provides a description of the ensemble ClearSky system and results from the

2004 ensemble ClearSky system evaluation. Chapter four contains a brief summary of research results and possible future research areas.

1.2. Description of Current ClearSky System

The ClearSky forecast system is comprised of four parts: meteorological forecast model, meteorological processor, field emissions, and dispersion model. The meteorological forecast is produced at the University of Washington (UW) using the Penn State/ National Center for Atmospheric Research (NCAR) Mesoscale Meteorological Model Version 3.6.3 (MM5) (Grell et al., 1995). The MM5 forecast is completed for an outer horizontal domain with 36-km cells and for two nested domains (with 12-km and 4-km cells) with 36 vertical sigma levels. MM5 uses the 00 UTC Global Forecast System (GFS) for initial and boundary conditions. More information on the UW MM5 set-up is available in Mass et al. 2003 and on the UW-MM5 web site: http://www.atmos.washington.edu/mm5rt/

Hours 12 – 36 UTC from the 4-km MM5 forecast are then processed using CALMM5/CALMET. CALMET recalculates the vertical wind velocity to satisfy the continuity equation for each grid cell (Scire et al., 2000). The forecast meteorology was further improved by replacing the planetary boundary layer (PBL) parameters calculated by CALMET with the MM5 PBL parameters passed through by MCIP, the Models-3/CMAQ meteorology preprocessor (O'Neill and Lamb, 2004). The PBL variables replaced by MCIP include: friction velocity, PBL height, convective velocity scale, air temperature, Monin-Obukhov length, roughness length, and terrain elevation. The surface elevations, three-dimensional wind components (calculated by CALMET), and

PBL parameters (passed through by MCIP) are blended into a single meteorological data file (calmet.dat).

Once the burn manager picks fields to simulate burning, two $PM_{2.5}$ emission source files are created. An agricultural burn can be viewed as two separate sources, a flame front (buoyant line source) and a smoldering field (buoyant area source). $PM_{2.5}$ emissions are calculated using the field size in acres, crop type (KBG or Wheat), estimated field fuel loadings, and $PM_{2.5}$ emission factors based on cereal grains (ASI, 2003) and KBG (ASI, 2004). $PM_{2.5}$ emissions are calculated from emission factors, the mass of crop residue burned, and an estimate of the time required to burn a field. The $PM_{2.5}$ emission factors for burning wheat stubble and KBG are 3.7g/kg and 28.5g/kg, respectively. In ClearSky, fuel loadings are available from a field databases for eastern Washington; however, the rest of the ClearSky domain uses assumed fuel loadings of~ 2.5 Ton/ac (wheat stubble) and ~3.5 Ton/ac (KBG). It is also assumed, based upon field observations, that the typical burn time is approximately 100 ac/hr. The total $PM_{2.5}$ emitted from any one field is weighted 80% and 20% between the buoyant line source and the buoyant area source. Even though more $PM_{2.5}$ is created by the pre (drying) and post (smoldering) combustion phases, the flaming combustion phase produces turbulent convective air motions that entrain large amounts of $PM_{2.5}$ from the pre and post combustions phases and then emit the $PM_{2.5}$ to the atmosphere (Ward, 2001). ASI (2003) and ASI (2004) were also used to determine specific plume rise parameters for both the buoyant line source and the buoyant area source. See Table 1 for the summary of input parameters for the buoyant line and buoyant area sources.

Table 1.1: Emission parameters for buoyant line and buoyant area sources

Buoyant Area Source	**Value**
Effective Height of Emissions (m)	0.5
Plume Temperature (K)	324
Effective Rise Velocity (m/s)	1.4
Initial Vertical Spread (m)	100
Buoyant Line Source	
Line Height (m)	0.5
Distance Between Sources (m)	5
Average Source Width (m)	5
Average Line Width (m)	5
Exit Velocity (m/s)	2.2
Plume Temperature (K)	361

The processed meteorological data (calmet.dat) and emission files (buoyant line and area sources) are used as inputs for CALPUFF, a three-dimensional Lagrangian puff dispersion model (Scire et al., 1999). CALPUFF uses puffs to simulate the emission, diffusion, and transport of $PM_{2.5}$ plumes created from agricultural field burns. Each hour, a three dimensional computational grid (4 km by 4 km with heights in meters of z = 20, 36, 73, 109, 146, 220, 295, 408, 523, 677, 1034, 1746, 3451, and 5805) is used to calculate the transport and dispersion of individual puffs. Scire et al. (2000) presents the basic Gaussian equation for calculating the instantaneous concentration of pollutant at a surface receptor due to a single puff:

$$C = \frac{Q}{2\pi\sigma_x\sigma_y} g \exp\left[-d_a^2/\left(2\sigma_x^2\right)\right]\exp\left[-d_c^2/\left(2\sigma_y^2\right)\right]$$

$$g = \frac{2}{\left(2\pi\right)^{\frac{1}{2}}\sigma_z} \sum_{n=-\infty}^{\infty} \exp\left[-\left(H_e + 2nh\right)^2/\left(2\sigma_z^2\right)\right]$$

where,

C is the ground level concentration (g/m3),

Q is the pollutant mass (gram) in the puff,

σ_x is the standard deviation (m) of the Gaussian distribution in the along wind direction,

σ_y is the standard deviation (m) of the Gaussian distribution in the crosswind direction,

σ_z is the standard deviation (m) of the Gaussian distribution in the vertical direction,

d_a is the distance (m) from the puff center to the receptor in the along wind direction,

d_c is the distance (m) from the puff center to the receptor in the cross wind direction,

g is the vertical factor (m^{-1}) of the Gaussian equation,

H_e effective height (m) above the ground of the puff center, and

h is the mixed layer height (m).

$PM_{2.5}$ concentrations are calculated for receptor cells (4-km by 4-km) covering the entire ClearSky domain. The hourly averaged surface level $PM_{2.5}$ concentrations are then written into a data file (conc.dat). The conc.dat file is converted into a network Common Data Form (netCDF) format and hourly tile plots of surface $PM_{2.5}$ concentrations are created using the Package for Analysis and Visualization of Environmental Data (PAVE). PAVE utilizes netCDF files to create different visualizations of air quality data. After all of the above processes are completed, the burn managers can view the tile plots of $PM_{2.5}$ concentrations through the ClearSky website. An example is shown in Figure 1.

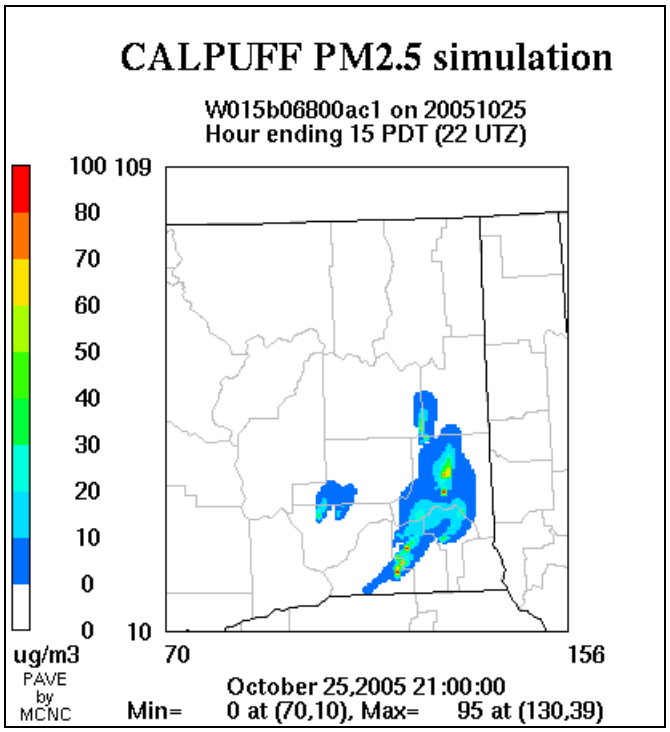

Figure 1.1: Example map of hourly surface $PM_{2.5}$ concentration contours predicted by ClearSky for October 25, 2005 over eastern Washington.

1.3. 2003 Evaluation of ClearSky

Jain (2004) evaluated the performance of the ClearSky modeling system for the 2003 burn season. Twenty burn days were re-run using ClearSky with the actual burn information (acres burned and start time when available) for fields burned each day. The predicted hourly $PM_{2.5}$ concentrations were compared against hourly-observed $PM_{2.5}$ concentration data collected at 20 air quality sites in eastern Washington and northern Idaho. CALPUFF was run using 4-km by 4-km cells for the meteorological grid and 1-km by 1-km cells for the receptor grid. For evaluation purposes, the range of predicted $PM_{2.5}$ concentrations was extracted for a 4-km square around each air quality site. For hours when an observation site registered elevated $PM_{2.5}$ concentrations, the predicted

and observed meteorological parameters (wind speed and wind direction) were also compared.

Each of the 20 burn days was evaluated for $PM_{2.5}$ concentrations and meteorological parameters at individual air quality sites within the ClearSky domain; and depending on the mean errors of wind direction, each burn day was placed in one of three categories.

1. Modeled and observed wind directions agree (mean absolute error less than 26^{o}) and ClearSky predicted $PM_{2.5}$ concentrations impacts at several monitoring stations where $PM_{2.5}$ impacts were observed.
2. Modeled and observed wind directions do not agree (mean absolute error less than 95^{o}) and ClearSky did not predict $PM_{2.5}$ concentration impacts at any monitoring sites where $PM_{2.5}$ impacts were observed.
3. Modeled and observed wind directions agree but ClearSky does not predict any $PM_{2.5}$ concentrations at monitoring sites where elevated $PM_{2.5}$ impacts were observed.

Overall, seven of the burn days fell into the first category. Many of the modeled plumes did not predict a $PM_{2.5}$ impact at the monitoring station because the predicted plumes missed the station by a few kilometers. However, for many of these situations, the $PM_{2.5}$ concentrations in the modeled plumes were very similar to the $PM_{2.5}$ concentrations recorded at the monitoring station. The results showed that small differences in predicted versus observed wind direction can affect whether a $PM_{2.5}$ impact is predicted at a monitoring station. The 2003 evaluation concludes with describing the need for more accurate forecast meteorology. Specifically, the evaluation recommends using ensemble forecast meteorology in future evaluations of the ClearSky modeling system. The next section of this paper will present and discuss ensemble techniques used for meteorological forecasts and air quality models.

1.4. Ensemble Literature Review

This section summarizes the background and the benefits of using ensemble forecasting, including some practical examples of ensemble air quality forecasting. The use of ensemble forecasting techniques in air quality modeling systems is a relatively new development (last 10 years); although many ensemble techniques used in air quality forecasting are based on ensemble Numerical Weather Prediction (NWP) techniques.

1.4.1. Ensemble Background

The atmosphere is considered chaotic in nature and consequently there are fundamental limits to atmospheric prediction, so that even the smallest changes in initial conditions can, over a period of time, create significantly large changes in the atmosphere. So uncertainties in initial conditions can create large errors in forecast meteorology (Lorenz, 1963). Instead of relying on a single deterministic forecast to represent the atmosphere, a stochastic-dynamic forecast like an ensemble forecast can be used to approximate atmospheric variance information (Epstein, 1969). Leigh (1974) developed a simple method of stochastic dynamic prediction by selecting a number of different initial conditions (IC) and creating multiple forecasts. Leigh (1974) found that combining as few as eight different forecasts developed a noticeable improvement in meteorological forecasts. Uncertainties in meteorological forecasting are not limited to initial conditions. Other sources of uncertainty within NWP models include: numerics, formulation, and physical parameterization (Tribbia and Baumhefner, 1988).

In the early 90's the US National Centers for Environmental Prediction (NCEP) and the European Center for Medium-Range Weather Forecasts (ECMWF) implemented daily global ensemble meteorological forecasts. The NCEP and ECMWF global

forecasts use different methods of perturbing initial conditions. The NCEP ensemble forecast system details and a discussion on the breeding method used to create perturbations can be found in Toth and Kalnay (1993). The ECMWF system details and a discussion on the singular-vectors approach to creating initial condition perturbations can be found in Molteni (1996).

The forecast ensemble technique that shows the most potential is the multi-model approach (Hou et al., 2001; Wandishin et al., 2001). The multi-model ensemble approach accounts for the errors associated with initial conditions and errors associated with individual NWP models. The authors conclude that results from multi-model ensemble forecasting capture more atmospheric uncertainties when compared to results from a single NWP model using multiple perturbations of initial conditions.

1.4.2. Air Quality Forecasting

Air quality forecasts (AQFs) provide the public and the government with valuable information to help them make daily decisions on how to protect human health. Many AQF techniques are used to predict air pollutant concentrations, ranging from simple statistical methods to complex deterministic three-dimensional air quality models. Statistical methods have little, if any, incorporation of chemical or physical pollutant processes; furthermore, statistical methods only apply to areas with large datasets of historical air pollution events (EPA, 2003). Three-dimensional deterministic air quality models try to simulate pollutants in the atmosphere by using meteorology, pollutant emissions, transportation, reactions, and deposition. With the development of NWP models, enhanced three-dimensional meteorological data sets are available for use in air quality models (Dabbert et al., 2004). More recently, deterministic air quality models

have began to be used as forecasting tools due to high performance computing at low costs. Over the last few years, several deterministic AQF systems have been developed (McHenry et al., 2004; O'Neill et al., 2003; Vaughan et al., 2004).

Dabberdt and Miller (2000) and Dabberdt et al. (2004) confirm the potential applications of AQF systems and propose using ensemble techniques to represent the uncertainties in the atmosphere and the air quality models. These air quality ensemble techniques can be quite similar to techniques currently utilized by ensemble NWP systems.

1.4.3. Ensemble Air Quality Models

This subsection will present ensemble techniques that can be used in AQF systems and specific examples of the different ensemble techniques. Most of the authors agree that deterministic air quality predictions, while valuable, cannot reliably represent pollutant interactions with the atmosphere.

Straume et al. (1998) used a Lagrangian dispersion model, the Severe Nuclear Accident Program (SNAP), and an ensemble of meteorological files to create multiple realizations of two tracers released and measured during the European Tracer Experiment (ETEX). The ETEX field campaign included measurements of two tracers released in France during 1994 (Nodop et al., 1998). The ECMWF produced an ensemble of 33 meteorological forecasts by perturbing the initial conditions of a control meteorological forecast. The 33 forecasts were then reprocessed for different grid and time resolutions using the High Resolution Limited Area Model (HIRLIM), a NWP model, and then each forecast was used separately for SNAP. Straume et al. (1998) evaluated the spread of ensemble tracer concentrations by calculating the root-mean-square error (RMSE) using

the modeled tracer concentrations from the control forecast and the modeled tracer concentrations from each of the ensemble members. Overall, the authors found there was a large spread of concentrations when looking at all of the ensemble members. The RMSE ranged from 1—10% when comparing the ensemble members to the control forecast. The trajectories modeled and observed match quite well, but the modeled concentrations were over-predicted most of the time when compared to the field measurements.

Dabberdt and Miller (2000) show results from a probabilistic simulation of an actual three-hour accidental release of sulfuric acid gas in the San Francisco Bay Area. The authors argue that since little data are available for directing emergency responses, ensemble techniques are necessary for producing useful air quality forecasts. The authors employed a non-steady-state puff dispersion model driven by a diagnostic mass-consistent wind field model. The ensemble contained 162 members created from combinations of perturbed wind speed (±15%), wind direction (±5 degrees), source strength (±15%), plume rise (±15%), and stability (first or second choice of stability class). The results clearly show the wealth of information gained by using an ensemble approach and how emergency responders could use the ensemble results.

Galmarini et al. (2001) utilized RTMOD (Real Time Model Evaluation), a procedure to help evaluate ensemble forecasting of long-range dispersion during nuclear emergencies. The authors assembled a suite of 20 dispersion models produced by different organizations around the world. The ensemble predicted transport and concentrations of radioactive releases in the atmosphere using different dispersion models coupled with different NWP meteorology. The ensemble results were compared to

observations from the ETEX field campaign (Nodop et al., 1998). The authors concluded that using a suite of different dispersion models can be very useful in representing AQF uncertainty, determining concentrations probabilities, and helping modelers check for general tendencies in their air quality predictions.

Straume (2001) extends the earlier work of Straume et al. (1998). The author compared her previous SNAP results to results from 34 dispersion models that participated in the ETEX field campaign, and concluded that the ensemble mean was more reliable than the control forecast at estimating arrival time and trajectory of the tracer to the receptors. However, the ensemble mean was less reliable at predicting non-arrival events, when the ensemble mean predicted impacts that were not observed at monitoring stations. A probable reason behind these conclusions is that the ensemble mean is the "smear" of all ensemble results; in other words, the ensemble mean removes the maximum and the minimum by averaging the results from the entire ensemble.

Warner et al. (2002) developed ensemble simulations to determine the transport and dispersion of a possible toxic gas release during the 1991 Gulf War in Iraq. An ensemble of 12 MM5 meteorological forecasts was created using different initial conditions, boundary-layer parameterizations, and surface physics schemes. The Second Order Closure integrated Lagrangian puff dispersion model (SCIPUFF) was used to calculate surface level dosages of the toxic gas. The vertical wind field variances, calculated from the ensemble meteorology, were used directly in SCIPUFF to calculate surface level dosages. Overall, the authors found ensemble techniques could be used to quantify the uncertainties in the meteorology and that ensemble dosage probabilities were more useful than any single deterministic forecast.

Draxler (2003) used a single dispersion model, Hybrid Single-Particle Lagrangian Integrated Trajectory (HYSPLIT), and a single meteorological forecast to develop an ensemble system. The meteorology forecast was provided by NCEP and an ensemble of 27 members was created by shifting the meteorology fields horizontally (± 1 grid) and vertically (± 250 meters). The ensemble simulated average daily tracer concentrations that were collected during the Across North America Tracer Experiment, ANATEX (Draxler et al., 1991). The ensemble trajectory results accounted for approximately 41 — 47% of the variance in the measurement data; but the residual shows that this ensemble technique did not account for all the uncertainties associated with dispersion modeling and forecast meteorology.

Delle Monache and Stull (2003) developed the first ensemble for pollutant transport and photochemical reactions. The ensemble utilized four chemical transport models including: European Monitoring and Evaluation Programme (EMEP), European Air Pollutant Dispersion (EURAD), Long-Term Ozone Simulation (LOTOS), and Regional Eulerian Model with three different chemistry schemes (REM3). Each model required different emissions data; and each model utilized a different meteorological forecast. EMEP and LOTOS used a NWP model with observations representing mixing heights; EURAD utilized MM5 forecasts; and the REM3 meteorological fields were derived entirely from observations. Delle Monache and Stull (2003) simulated an ozone episode from July 31 – August 5, 1990. Ozone observations were compared to individual ensemble concentrations and ensemble average concentrations using statistical measures (gross error and unpaired peak prediction accuracy). Over the entire episode period, the ensemble average outperformed any single ensemble member; the mean ensemble

concentrations were closer to the observed concentrations when compared to any single ensemble member.

Galmarini et al. (2004a) reviewed techniques for creating ensemble dispersion forecast systems. The authors focused on describing a suite of 17 dispersion models used to simulate the transport of radionuclides released into the atmosphere over Europe. The dispersion models were operated by different organizations across the world, and each dispersion model utilized a different a different NWP model. Specific information about the different dispersion and NWP models are provided in Galmarini et al. (2004a).

Galmarini et al. (2004b) compared tracer concentration results from a suite of dispersion air quality models to tracer concentrations observed during the ETEX tracer experiment (Nodop et al., 1998). The suite of dispersion models was described in Galmarnin et al. (2004a). The ensemble modeled results showed the median tracer concentration (50^{th} percentile of all ensemble modeled results) was a better tracer forecast when compared to results from any single ensemble member. The authors concluded that no single deterministic tracer forecast adequately simulated tracers released. An ensemble of dispersion models and meteorology must be used to represent the uncertainties in dispersion models and the uncertainties associated with NWP forecasts.

Mckeen et al. (2005) described a real-time ensemble ozone forecast system with a domain covering northeastern U.S. The ensemble ozone forecast system contains ozone concentrations simulated by seven air quality forecast models; moreover, the ensemble ozone forecast system calculated an ensemble mean ozone concentration and an ensemble median ozone concentration from the seven ensemble members simulations of hourly ozone forecasts. The different chemical transport models and NWP models used

by each ensemble member were described in Mckeen et al. (2005). The ensemble ozone forecast system simulated hourly surface ozone concentrations for July 6 – August 30, 2004. The hourly predicted ozone concentrations were compared to hourly ozone concentration observations from 358 monitoring sites within the northeast U.S. The correlation coefficient, mean bias, and root-mean-square-error for the maximum eight-hour average ozone concentrations predicted and observed were evaluated. Overall, the ensemble median and average concentrations proved to be more accurate forecasts when compared to any single air quality model from the ensemble.

Pagowski et al. (2005) developed a method of weighting individual members of an ensemble to calculate weighted ensemble averaged ozone concentrations. The method is based on minimization of the least-squares error between the modeled and observed ozone concentrations. The weighting method was demonstrated for ensemble modeled ozone concentrations and observed ozone concentrations from Mckeen et al. (2005). With sufficient observations for an entire modeling domain, weighting factors can be calculated for individual ensemble models. The authors showed the weighted ensemble average was more accurate than any single ensemble member; in addition, the weighted ensemble average was more accurate than the non-weighted ensemble average.

O'Neill and Lamb (2005) developed a suite of ozone forecast systems to forecast ozone concentrations in the Pacific Northwest region of the U.S. The ozone forecasts are simulated by four ensemble members. The four members were developed from utilizing two different grid models, three different chemical mechanisms, and three different meteorological simulations. Also, two ensemble averages (one-hour and 8-hour) were calculated from the ozone concentrations simulated by the ensemble members. Statistical

measures (normalized gross error, normalized bias, and index of agreement) were calculated for the individual ensemble members and the ensemble averages using observed ozone concentrations from 12 monitoring stations. The eight-hour ensemble average was the best performer, most often, when compared to all other ensemble members. Also, the overall modeling uncertainty could be measured by taking the standard deviation of all the ensemble hourly ozone concentrations about the ensemble hourly average.

Mallet and Sportisse (2006) developed an air quality model ensemble to represent the uncertainties in a single chemical transport model due to physical parameterizations and model numerics. The authors created an ensemble of 20 model members by using a single model control configuration and by varying 19 parameters, one at a time, of the model control configuration. Some of the parameters included: chemical mechanisms, turbulent closure theories, deposition velocities, emission distributions, time steps, vertical grid resolution, and horizontal grid resolution. A 2004 summer ozone episode was simulated for the control model parameter configuration and the 19 ensemble members (varied model parameters). The ozone concentrations simulated by the ensemble members were compared to each other and to the ozone concentrations simulated by the control model simulation. The comparison demonstrated that the chemical transport model was more sensitive to the turbulent closure theory and chemistry mechanisms. The authors were able to represent some, but not all, of the uncertainties of a chemical transport model due to different physical parameterizations and numerics; more importantly, the authors showed that ensemble techniques can be used to represent some of the uncertainties in a chemical transport model.

1.5. References

ASI (Air Sciences Inc.), 2003. Final Report: Cereal grain crop open field burning emissions study, Project 152-02. Available at http://www.ecy.wa.gov/programs/air/pdfs/FinalWheat_081303.pdf

ASI, 2004. Quantifying post-emissions from bluegrass seed production field burning. Available at http://www.ecy.wa.gov/programs/air/pdfs/bluegrass_final_report.pdf

Crutzen, P. J., and Andrea, M. O., 1990. Biomass burning in the tropics: impact on atmospheric chemistry and biogeochemical cycles. *Science* 250, 1669-1678.

Dabberdt, W. F., and Miller, E., 2000. Uncertainty, ensembles and air quality dispersion modeling: Applications and challenges. *Atmospheric Environment* 34, 4667-4673.

Dabberdt, W. F., Carroll, M. A., Baumgardner, D. , Carmichael, G., Cohen, R., Dye, T., Ellis, J., Grell, G., Grimmond, S., Hanna, S., Irwin, J., Lamb, B., Madronich, S., Mcqueen, J., Meagher, J., Odman, T., Pleim, J., Schmid, H. P., and Westphal, D. L., 2004. Meteorological Research Needs for Improved Air Quality Forecasting - Report of the 11th Prospectus Development Team of the Us Weather Research Program. *Bulletin of the American Meteorological Society* 85, 563-586.

Delle Monache, L. D. and Stull, R. B., 2003. An ensemble air-quality forecast over western Europe during an ozone episode. *Atmospheric Environment* 37, 3469-3474.

Draxler, R. R., Dietz, R., Lagomarsino, R. J., and Start, G., 1991. Acroos Nort America Experiment (ANATEX): sampling and analysis. *Atmospheric Environment* 25, 2815-2836.

Draxler, R. R., 2003. Evaluation of an ensemble dispersion calculation. *Journal of Applied Meteorology* 42, 308-317.

Environmental Protection Agency (EPA), 2003. Guidelines for developing an air quality (Ozone and PM2.5) forecasting program. Technical Report EPA-456/R-03-002, U.S. Envrionmental Protection Agency.

Epstein, E. S., 1969. Stochastic dynamic prediction. *Tellus* 21, 739-759.

Galmarini, S., Bianconi, R., Bellasio, R., and Graziani, G., 2001. Forecasting the Consequences of Accidental Releases of Radionuclides in the Atmosphere From Ensemble Dispersion Modelling. *Journal of Environmental Radioactivity* 57, 203-219.

Galmarini, S., Bianconi, R., Klug, W., Mikkelsen, T., Addis, R., Andronopoulos, S., Astrup, P., Baklanov, A., Bartniki, J., Bartzis, J. C., Bellasio, R., Bompay, F., Buckley, R., Bouzom, M., Champion, H., D'amours, R., Davakis, E., Eleveld, H., Geertsema, G. T., Glaab, H., Kollax, M., Ilvonen, M., Manning, A., Pechinger, U., Persson, C., Polreich, E., Potemski, S., Prodanova, M., Saltbones, J., Slaper, H., Sofiev, M. A., Syrakov, D., Sorensen, J. H., Van Der Auwera, L., Valkama, I., and Zelazny, R., 2004a. Ensemble Dispersion Forecasting - Part I: Concept, Approach and Indicators. *Atmospheric Environment* 38(28), 4607-4617.

Galmarini, S., Bianconi, R., Addis, R., Andronopoulos, S., Astrup, P., Bartzis, J. C., Bellasio, R., Buckley, R., Champion, H., Chino, M., D'amours, R., Davakis, E., Eleveld, H., Glaab, H., Manning, A., Mikkelsen, T., Pechinger, U., Polreich, E., Prodanova, M., Slaper, H., Syrakov, D., Terada, H., and Van Der Auwera, L., 2004b. Ensemble Dispersion Forecasting - Part II: Application and Evaluation. *Atmospheric Environment* 38, 4619-4632.

Grell, G. A., Dudhia, J., and Stauffer, D. R., 1995: A description of the fifth-generation Penn State/NCAR mesoscale model (MM5). NCAR Tech. Note NCAR/TN-398+STR, 122 pp.

Hou, D. C., Kalnay, E., and Droegemeier, K. K., 2001. Objective verification of the SAMEX'98 ensemble forecasts. *Monthly Weather Review* 129, 73-91.

Idaho State Department of Agriculture (ISDA), 2004. Idaho Crop Residue Disposal Smoke Management Program 2004 Season Review. Prepared by ISDA, Idaho Department of Environmental Quality, Nez Perce Tribe, Coeur d'Alene Tribe, and Kootenai Tribe of Idaho. Available at http://www.idahoag.us/Categories/Environment/Smoke/Documents/AnnualSummary2004.pdf

Jain, R., 2004. Modeling Transport and Dispersion of Smoke Plumes from Agricultural Field Burning in Eastern Washington and Northern Idaho, M.S. Thesis, Washington State University, Pullman, WA, U.S.A.

Johnson, R. C., Johnston, W. J., and Golob, C. T., 2003. Residue management, seed production, crop development, and turf quality in diverse Kentucky bluegrass germplasm. *Crop Science* 43, 1091-1099.

Leith, C. E., 1974. Theoretical skill of Monte Carlo forecasts. *Monthly Weather Review* 102, 409-418.

Lorenz, E. N., 1963. Deterministic non-periodic flow. *Journal of the Atmospheric Sciences* 20, 130-141.

Mallet, V., and Sportisse, B., 2006. Uncertainty in a chemistry-transport model due to physical parameterizations and numerical approximations: An ensemble approach applied to ozone modeling. *Journal of Geophysical Research*, 111, D01302, doi:10.1029/2005JD006149.

Mass, C. F., Albright, M., Ovens, D., Steed, R., Maciver, M., Grimit, E., Eckel, T., Lamb, B., Vaughan, J., Westrick, K., Storck, P., Colman, B., Hill, C., Maykut, N., Gilroy, M., Ferguson, S. A., Yetter, J., Sierchio, J. M., Bowman, C., Stender, R., Wilson, R., and Brown, W., 2003. Regional environmental prediction over the Pacific Northwest. *Bulletin of the American Meteorological Society* 84, 1353-1366.

Mchenry, J. N., Ryan, W. F., Seaman, N. L., Coats, C. J., Pudykiewicz, J., Arunachalam, S., and Vukovich, J. M., 2004. A real-time Eulerian photochemical model forecast system. *Bulletin of the American Meteorological Society* 85, 525-548.

Mckeen, S., Wilczak, J., Grell, G., Djalalova, I., Peckham, S., Hsie, E. Y., Gong, W., Bouchet, V., Menard, S., Moffet, R., Mchenry, J., Mcqueen, J., Tang, Y., Carmichael, G. R., Pagowski, M., Chan, A., Dye, T., Frost, G., Lee, P., and Mathur, R., 2005. Assessment of an ensemble of seven real-time ozone forecasts over eastern North America during the summer of 2004. *Journal of Geophysical Research* 110, D21307, doi:10.1029/2005JD005858.

Molteni, F. and Palmer, T. N., 1993. Predictability and finite-time instability of the northern winter circulation. *Quarterly Journal of Royal Meteorological Society* 119, 269-298.

Nodop, K., Connolly, R., and Girardi, F., 1998. The field campaigns of the European Tracer Experiment (ETEX): overview and results. *Atmospheric Environment* 32, 4095-4108.

O'neill, S. M. and Lamb, B. K., 2005. Intercomparison of the Community Multiscale Air Quality Model and Calgrid Using Process Analysis. *Environmental Science & Technology* 39, 5742-5753.

O'Neill, S. M., Ferguson, S. A., Peterson, J., and Wilson R., 2003. The BlueSky Smoke Modeling Framework (www.BlueSkyRAINS.org). In *American Meteorological Society, 5th Symposium on Fire and Forest Meteorology*. Orlando, Florida.

Pagowski, M., Grell, G. A., McKeen, S. A., Dévényi, D., Wilczak, J. M., Bouchet, V., Gong, W., McHenry, J., Peckham, S., McQueen, J., Moffet, R., and Tang Y., 2005. A simple method to improve ensemble-based ozone forecasts. *Geophysical Research Letters*, 32, L07814, doi: 10.1029/2004GL022305.

Roberts, R. A. and Corkill, J., 1998. Grass Seed Field Smoke and Its Impart on Respiratory Health. *Journal of Environmental Health* 60, 10-16.

Scire, J. S., Robe, F. R., Fernau, M. E., and Yamartino, R. J., 2000a. A user's guide for the CALMET meteorological model (version 5), Earth Tech Inc., Concord, MA.

Scire, J. S., Strimaitis, D. G., and Yamartino, R. J., 2000b. A user's guide for the CALPUFF dispersion model (version 5), Earth Tech Inc., Concord, MA.

Slaughter, J. C., Lumley, T., Sheppard, L., Koenig, J. Q., and Shapiro, G. G., 2003. Effects of Ambient Air Pollution on Symptom Severity and Medication Use in Children With Asthma. *Annals of Allergy Asthma & Immunology* 91, 346-353.

Straume, A. G., Koffi, E. N., and Nodop, K., 1998. Dispersion Modeling Using Ensemble Forecasts Compared to Etex Measurements. *Journal of Applied Meteorology* 37, 1444-1456.

Straume, A. G., 2001. A more extensive investigation of the use of ensemble forecasts for dispersion model evaluation. *Journal of Applied Meteorology* 40, 425-445.

Toth, Z. and Kalnay, E., 1993. Ensemble forecasting at NMC: the generation of perterbations. *Bulletin of the American Meteorological Society* 74, 2317-2330.

Tribbia, J. J. and Baumhefner, D. P., 1988. The reliability of improvements in deterministic short-range forecasts in the presence of initial state and modeling deficiencies. *Monthly Weather Review* 116, 2276-2288.

Vaughan, J., Lamb, B., Frei, C., Wilson, R., Bowman, C., Figueroa-Kaminsky, C., Otterson, S., Boyer, M., Mass, C., Albright, M., Koenig, J., Collingwood, A., Gilroy, M., and Maykut, N., 2004. A numerical daily air quality forecast system for the Pacific Northwest. *Bulletin of the American Meteorological Society* 85**,** 549-561.

Ward, D., 2001. "Chapter 3. Combustion Chemistry and Smoke." Forest Fires: Behavior and Ecological Effects, Academic Press, San Diego, CA, 55-75.

Wandishin, M. S., Baldwin, M. E., and Mullen, S. L., 2005. Short-Range Ensemble Forecasts of Precipitation Type. *Weather and Forecasting* 20, 609-626.

Warner, T. T., Sheu, R. S., Bowers, J. F., Sykes, R. I., Dodd, G. C., and Henn, D. S., 2002. Ensemble Simulations With Coupled Atmospheric Dynamic and Dispersion Models: Illustrating Uncertainties in Dosage Simulations. *Journal of Applied Meteorology* 41, 488-504.

Washington Department of Ecology (WA DOE), 2004. Cereal grain crops: best management practices/emission reduction guidance. Availabe at http://www.ecy.wa.gov/programs/air/pdfs/Cereal_BMPs.pdf.

CHAPTER 2

2004 CLEARSKY FIELD BURN STUDY OF PLUME RISE

2.1. Introduction

During 2004, a field campaign was completed to evaluate ClearSky, a smoke dispersion forecast system for agricultural field burning. The focus of the campaign was to collect plume rise measurements from agricultural field burns. The plume rise measurements were then compared to the plume rise predicted by the Lagrangian dispersion model CALPUFF, which is part of the ClearSky system. Plume height validation is important because those CALPUFF calculations determine how large the smoke plume becomes, the distance the smoke plume travels, and the smoke plume location relative to surface receptors. Field measurement methods, field burn modeling methods, plume height measured and modeled results, and a discussion of results are presented in this chapter.

ClearSky (Jain, 2004) is an automated smoke dispersion forecast system which simulates agricultural field burns in eastern Washington and northern Idaho. In operation, burn coordinators create burn scenarios of the fields they want to burn the next day. These burn scenarios are created on the project website (www.clearsky.wsu.edu) and are then converted to $PM_{2.5}$ emission files for input into CALPUFF, a Lagrangian dispersion model (Scire et al., 2000b). Hourly meteorological fields for a Pacific Northwest domain with 4-km grid cells are produced by the Penn State/National Center for Atmospheric Research (NCAR) fifth generation Mesoscale Meteorological Model (MM5) (Grell et al., 1995). The MM5 forecasts are produced by the University of Washington MM5 forecast system (Mass et al., 2003). The 4-km MM5 forecast is

processed by CALMM5/CALMET to create a meteorology input for CALPUFF (Scire et al., 2000a). The forecast meteorology is further improved by replacing the planetary boundary layer (PBL) parameters calculated by CALMET with the MM5 PBL parameters passed through by MCIP, the Models-3/CMAQ meteorology preprocessor (O'Neill et al., 2005). CALPUFF simulates the emission and transport of $PM_{2.5}$ from agricultural burns and calculates the surface level $PM_{2.5}$ concentrations for each burn scenario. The hourly surface level $PM_{2.5}$ concentrations predicted by ClearSky are then displayed for review by the burn coordinators through a graphical interface on the project website.

Plume heights were measured during nine field burns over four days of the 2004 agricultural burn season. The dates for the plume height measurement campaign included July 30, August 20, September 8, and September 29, 2004. Four wheat stubble field burns were observed in eastern Washington and five Kentucky bluegrass field burns were observed in northern Idaho. Field sizes varied from 32 to 157 acres in size. Table 2.1 contains date, location, start time, end time, size, and crop type of each observed field burn.

2.2. Methodology

During each field burn, plume height measurements were taken utilizing an aircraft and also from the ground. For this study, the top of plume heights were measured because of the difficulty in determining the plume centerline height. The air-crew made observations of top of plume height, vertical temperature profiles, and took photographs throughout each field burn. The ground-crew measured the top of plume heights and deployed instruments to measure surface air temperatures, surface wind speeds, surface

wind directions, wind speed and direction vertical profiles, and obtain field burn photographs. A fuel sample was also collected before and after each field burn.

2.2.1. Aircraft Measurements

The air-crew consisted of a pilot and one to two researchers. The main purpose of the air-crew was to measure the top of plume height throughout each field burn. The top of plume height measurements were estimated using the airplane altimeter. As the pilot circled around the burning field, another crew member watched to see when the plane altitude and the plume height were equal, and then recorded the plane altimeter and their geographic location with a waypoint on a handheld Global Positioning Satellites (GPS) unit. The time, altitude, and waypoint number were written on a data collection sheet.

The air temperature was also collected on the airplane using a data logging device called a Temperature External HOBO. The HOBO collected air temperature measurements, every four seconds, from a thermistor mounted outside of the airplane. Measurement times were thus recorded by both the handheld GPS and HOBO. By matching the measurement times from the GPS and HOBO, vertical temperature profiles were developed.

The air-crew also took photographs of the fields and the smoke plumes. These photographs record what the crew saw when they made their measurements. The air-crew also noted anything else of potential value to the field study. If the farmer burned the field in a particular manner (heading fire, backing fire, etc.), the air-crew described the method.

2.2.1. Surface Measurements

The ground-crew consisted of one to two researchers setting up equipment and collecting data. The main purpose of the ground-crew was to collect measurements of the top of plume heights, wind speeds, and wind directions.

Top of plume heights were measured from the ground using a handheld clinometer and a handheld GPS unit. The clinometer was used to measure the elevation angle between the ground (zero degrees) and the top of the plume. A ground data collection sheet was used to record the time and clinometer readings. The geographic location of the surface location used for plume height measurements was determined using the GPS unit. These data permitted calculation of the distance to the center of the field from the surface location as well as the trigonometric estimation of the top of plume height. See Figure 2.1. This top of plume height measurement technique assumed that the plume only traveled vertically from the center of the field.

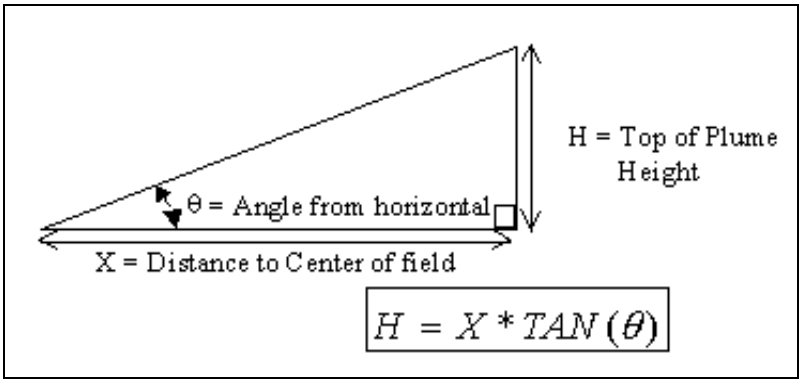

Figure 2.1: Trigonometry used to determine top of plume height.

A WNT model 170 ultrasonic anemometer was used to measure wind speed and wind direction. Every three seconds the anemometer reported a wind speed and wind direction measurement and these data were captured and stored on a portable laptop. A second HOBO was used as a data logger for the air temperature. The anemometer and

HOBO were mounted 1.5 m above ground level using a tripod. The HOBO collected a temperature reading every four to eight seconds depending on the configuration settings for each field burn. The anemometer was oriented towards geographic North using a compass and the magnetic declination of the area. The anemometer was sited carefully, to prevent the surface winds from being influenced by nearby trees and buildings.

A sonic detection and ranging (sodar) instrument was used to measure wind speed and wind direction at different altitudes. The sodar was only available for the last field study day (September 29, 2004). The sodar was a Scintec Flat Array Sodar model MFAS. The MFAS was used to measure both wind speed and wind direction vertical profiles. The sodar also was also oriented towards geographic North using a compass and the magnetic declination of the area; and the sodar was leveled with a bubble level to minimize errors in the data. The sodar made measurements from 30 meters up to 400 meters in increments of 10 meters. With an averaging time of 10 minutes, the sodar reported wind speed and wind direction to a laptop.

Two fuel samples were taken from each field, one before the field burn and one after the field burn. Each sample was taken from a one meter by one meter sampling area and placed in a plastic bag to be analyzed. The sample consisted of any residue above the ground. The field samples were analyzed for Residual Moisture Content (RMC) determined by:

$$RMC = \frac{(W_{field} - W_{OD})}{W_{OD}} * 100\%$$

where W_{field} is the fresh weight of each sample and W_{OD} is the weight of each sample after drying in an oven. Using the RMC value, the entire fresh sample weight was converted to an oven dried weight and then a fuel loading was calculated by:

$$Loading = \frac{W_{OD}}{A_{Sample}}$$

where W_{OD} is equal to the weight of the entire sample after drying in an oven and A_{Sample} is equal to the sample area (one meter by one meter square).

The ground-crew also took photographs of the fields and the smoke plumes. These photographs helped to document what the ground-crew saw when they were making their measurements. The ground-crew also described anything else of potential value to the field study (general wind direction, plume behaviors, etc.).

2.2.3. ClearSky Rerun for Field Study Dates

Predicted plume heights from CALPUFF were determined by rerunning ClearSky for each field burn. CALPUFF was configured to produce a plume log detailing each puff released by the field burns. In ClearSky, a buoyant line source and buoyant area source were used to represent an active fire front and a smoldering field respectively. CALPUFF calculated centerline plume heights for the buoyant line and buoyant area sources and also calculated the corresponding Gaussian vertical dispersion coefficient (sigma-z). The top of plume heights were estimated by adding the centerline plume height and the value of 2.15 times the sigma-z value (distance from the centerline to the top edge of the plume). For buoyant line sources, CALPUFF calculates only the final plume height and final plume distance values, but CALPUFF calculates the entire evolution of plume height with distance for buoyant area sources. Top of plume heights estimated from CALPUFF and top of plume heights measured by the ground-crew were both expressed above ground level (AGL). The top of plume heights observed from the airplane had to be converted from above sea level (plane altimeter) to AGL in order to be compared with estimated top of plume heights. The average elevation of each field was

determined from a topographic map, for each burn site, and used to convert above sea level top of plume heights to AGL top of plume heights.

2.3 Results

The equipment used in the air and surface measurements varied from one study day to another and sometimes equipment malfunctioned. Table 2.2 shows a summary of the equipment that collected data during each of the field campaign days. A summary of the average values for the surface measurements for temperature, wind speed, wind direction, and fuel loading are presented in Table 2.3. The dry weight field loading for wheat stubble (Days 1 and 4) ranged from 2.0 to 4.7 tons per acre; ClearSky currently uses from 2 to 6 tons per acre. The dry weight field loading for Kentucky bluegrass (Day 2) was 1.6 tons per acre, while ClearSky currently uses 2.8 tons per acre.

Table 2.1: 2004 Field burn campaign overview

Day	Field	Date	Location (County)	Start Time (PDT)	End Time (PDT)	Size (Acres)	Crop Type
Day 1	Field 1	7/30/2004	Franklin, WA	10:59	12:30	120	Irr. Spring Wheat
	Field 2			14:56	15:31	110	Irr. Spring Wheat
Day 2	Field 1	8/20/2004	Nez Perce, ID	13:18	14:27	88	KBG
	Field 2			14:36	15:12	32	KBG
	Field 3			15:17	16:18	105	KBG
Day 3	Field 1	9/8/2004	Lewis, ID	12:05	13:03	76	KBG
	Field 2			13:50	15:05	157	KBG
Day 4	Field 1	9/29/2004	Columbia, WA	11:54	12:55	122	Winter Wheat
	Field 2			14:53	15:58	122	Winter Wheat

Table 2.2: 2004 Field campaign equipment overview

Day	Field	Air	Ground				
		Hobo	Clinometer	Hobo	Sonic Anemometer	Sodar	Field Sample
Day 1	Field 1	X		X	X		X
	Field 2	X		X	X		X
Day 2	Field 1		X	X	X		X
	Field 2		X	X	X		X
	Field 3		X	X	X		X
Day 3	Field 1	X	X	X	X		
	Field 2	X	X	X			
Day 4	Field 1	X	X	X		X	X
	Field 2	X	X	X	X	X	X

Table 2.3: Summary of field burn surface observations

Day	Field	Temp. (C)	Sonic Anemometer		Field Loading[a](Ton/Acre)	
			W. S. (m/s)	W.D. (degrees)	Pre-Burn	Post-Burn
Day 1	Field 1	29	3.4	184	4.7	
	Field 2	36	2.6	99	4.0	
Day 2	Field 1	33	1.2	268	1.6	0.3
	Field 2	34	0.4	322	1.6	0.3
	Field 3	34	1.1	293	1.6	0.3
Day 3	Field 1	25	1.4	83		
	Field 2	27				
Day 4	Field 1	29			2.3	0.2
	Field 2	29	3.5	243	2.0	0.4

[a]Field Loadings are calculated on a dry weight basis

Air and ground data collection sheets along with predicted and measured top of plume heights from the eighth field burn (September 29, 2004 – Field 1) are shown in this chapter for purposes of illustration. Tables 2.4 and 2.5 show the data collection sheets for September 29, 2004 and describe the field burn and top of plume height measurements. Figure 2.2 shows CALPUFF calculated top of plume heights for the buoyant area source, final top of plume height for the buoyant line source, and the ranges of top of plume heights measured from the air and ground. See Appendix A for the data collection sheets and CALPUFF calculated top of plume height figures for each of the nine field burns. The final top of plume rises for the buoyant line and buoyant area sources were approximately 200 m and 420 m respectively. The range of measured top of plume heights from the aircraft was 320 m – 1400 m and range measured from the ground was 150 m – 770 m. The air and ground top of plume height measurements were up to three times higher than the range of CALPUFF-modeled top of plume heights.

Table 2.4: 9/29/04, Field 1 - Top of Plume Heights Measured from the Plane

Time (PDT)	Burn Description	Top of Plume AGL (m)
11:54	Burn start, northern edge	
12:20		320
12:21		320
12:22		381
12:25		503
12:26		655
12:30	1/3 of field ignited	655
12:36		1082
12:38		1234
12:39		1387
12:40	Another 1/3 of field ignited	
12:46	Last 1/3 of field ignited	
12:54	Burn Finished	
Average Elevation of Field 1 = 655 meters above sea level		

Table 2.5: 9/29/04, Field 1 - Top of Plume Heights from Surface Measurements

Time (PDT)	Burn Description	Top of Plume AGL (m)
11:54	Burn start, northern edge	
12:18		148
12:21		171
12:25		191
12:28		218
12:30	1/3 of field ignited	
12:33		372
12:37		237
12:41	Another 1/3 of field ignited	368
12:42		439
12:43	Last 1/3 of field ignited	494
12:49		774
12:52		386
12:54	Burn Finished	
Distance Between Field Center And Ground-crew = 590 m		

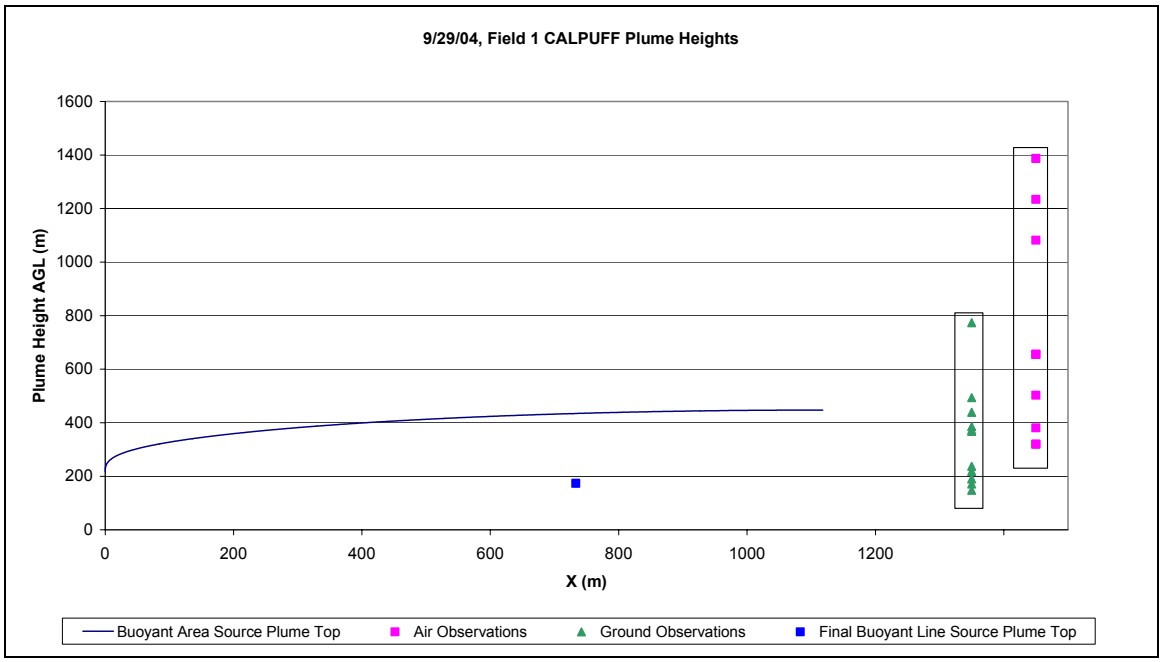

Figure 2.2: CALPUFF plume heights versus downwind distance (X) and the ranges of air and ground observations are displayed in the boxes on the right side of the plot.

Similar results were also found for most of the field burns. Figure 2.3 shows a summary chart of maximum top of plume heights measured and final top of plume heights modeled. The chart shows considerable variability between the predicted plume heights and the individual observations. There was large variability between the air and ground measurements for top of plume heights. CALPUFF under predicted the top of plume heights for six field burns compared to measurements. CALPUFF predicted top of plume heights within the same range as measurements for three field burns.

Because CALPUFF under-predicted top of plume heights for most of the field burns, an effort was made to improve the plume emission parameters. The emission parameters for the buoyant line and area source were updated to the plume emission parameters from a 2003 ClearSky evaluation discussed in Jain (2004). These updated

emission parameters were based upon agricultural field burning studies completed by Washington State University and with collaboration from Air Sciences Inc. and the Missoula Fire Sciences Laboratory (ASI, 2003; ASI, 2004). Table 2.6 presents the previous and the updated emission parameter values. With the new emission parameters, the plume exit temperatures were lowered and the exit velocities were increased for both buoyant line and buoyant area sources. Figure 2.4 shows a summary chart of maximum top of plume heights measured and final top of plume heights modeled using the updated emission parameters.

Table 2.6: Previous and Updated ClearSky Emissions Parameters

Buoyant Area Source	**Previous Value**	**Updated Value**
Effective Height of Emissions (m)	0.5	0.5
Temperature (K)	333	324
Effective Rise Velocity (m/s)	0.01	1.4
Initial Vertical Spread (m)	100	100
Buoyant Line Source		
Line Height (m)	1	0.5
Average Line Width (m)	5	5
Exit Velocity (m/s)	0.5	2.2
Temperature (K)	573	361

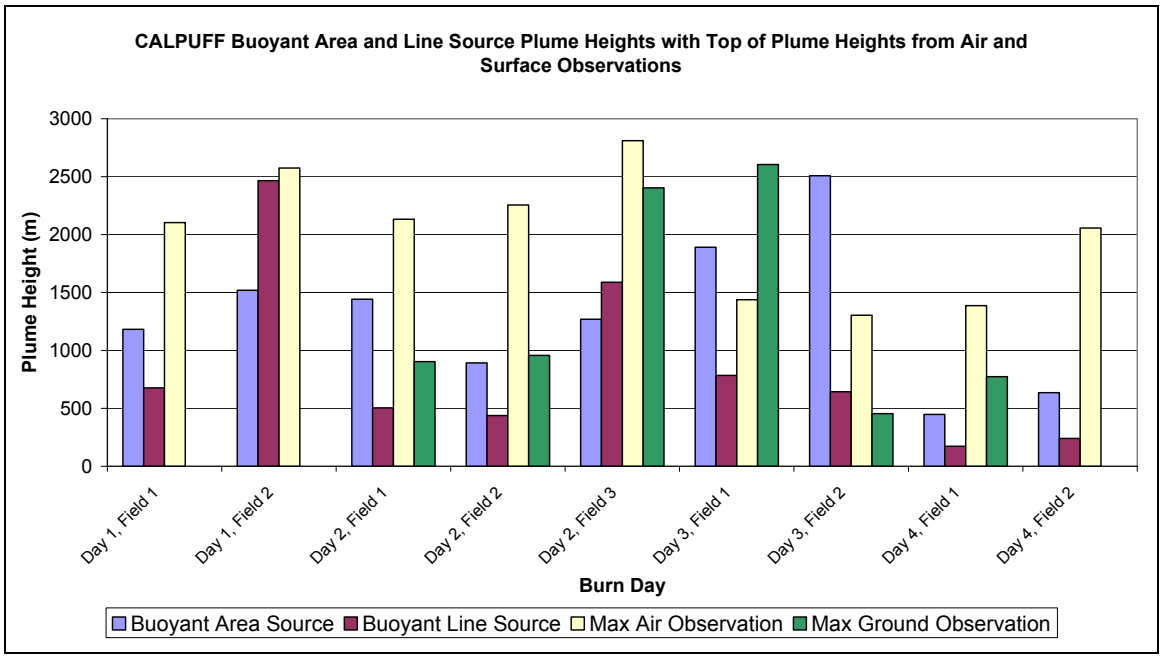

Figure 2.3: Ranges of both CALPUFF plume heights and measured plume heights for each field burn.

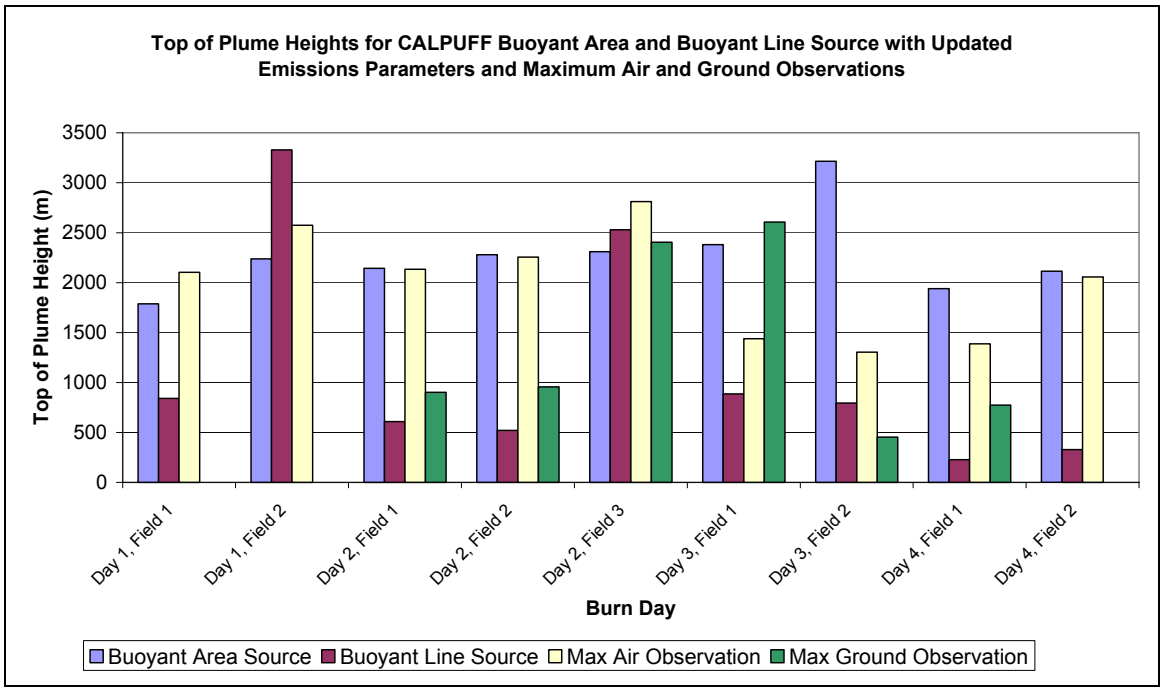

Figure 2.4: Ranges of both CALPUFF plume heights, with updated emissions parameters, and measured plume heights for each field burn.

2.4. Discussion

The updated emission parameters increased the top of plume heights for both the buoyant area and the buoyant line sources when compared to the top of plume heights calculated using the previous emissions parameters. Moreover, with the new emission parameters CALPUFF calculated top of plume heights closer to those measured compared to the previous results shown in Figure 2.3. The updated emissions parameters were therefore incorporated into ClearSky for the 2005 and subsequent burn seasons.

For future plume height studies, more accurate plume height measurement techniques should be incorporated. Both methods used in this study were quite subjective. The top of plume height measurements taken from the aircraft depended on the researcher to determine when the aircraft was close to the same altitude as the top of the plume. Two researchers could easily estimate different altitudes for the top of plume height. The ground measurements of top of plume height were probably less accurate than the air measurements due to the errors and assumptions incorporated into the ground-crew measurements. Different researchers would probably measure different values for the angle between the ground and the top of plume height. Also, the ground measurements assumed the ground distance (x) to the plume was constant. The distance from the measurement site to the center of the field was used to calculate the top of plume heights. This assumption was not good for burn days when the winds transported the smoke plumes away from the center of the fields, causing the top of plume height calculation to either over predict or under predict the top of plume height. For future studies, a light detection and ranging (lidar) system could be utilized for the top of plume height measurements. The lidar would provide a more accurate measure of the distance

and the angle to the top of plume height and therefore produce better measurements of top of plume heights.

2.5. References

ASI (Air Sciences Inc.), 2003. Final Report: Cereal grain crop open field burning emissions study, Project 152-02. Available at http://www.ecy.wa.gov/programs/air/pdfs/FinalWheat_081303.pdf

ASI, 2004. Quantifying post-emissions from bluegrass seed production field burning. Available at http://www.ecy.wa.gov/programs/air/pdfs/bluegrass_final_report.pdf

Grell, G. A., Dudhia, J., and Stauffer, D. R., 1995: A description of the fifth-generation Penn State/NCAR mesoscale model (MM5). NCAR Tech. Note NCAR/TN-398+STR, 122 pp.

Jain, R., 2004. Modeling Transport and Dispersion of Smoke Plumes from Agricultural Field Burning in Eastern Washington and Northern Idaho, M.S. Thesis, Washington State University, Pullman, WA, U.S.A.

Mass, C. F., Albright, M., Ovens, D., Steed, R., Maciver, M., Grimit, E., Eckel, T., Lamb, B., Vaughan, J., Westrick, K., Storck, P., Colman, B., Hill, C., Maykut, N., Gilroy, M., Ferguson, S. A., Yetter, J., Sierchio, J. M., Bowman, C., Stender, R., Wilson, R., and Brown, W., 2003. Regional Environmental Prediction Over the Pacific Northwest. *Bulletin of the American Meteorological Society* 84(10), 1353-1366.

O'neill, S. M. and Lamb, B. K., 2005. Intercomparison of the Community Multiscale Air Quality Model and Calgrid Using Process Analysis. *Environmental Science & Technology* 39, 5742-5753.

Scire, J. S., Robe, F. R., Fernau, M. E., and Yamartino, R. J., 2000a. A user's guide for the CALMET meteorological model (version 5), Earth Tech Inc., Concord, MA.

Scire, J. S., Strimaitis, D. G., and Yamartino, R. J., 2000b. A user's guide for the CALPUFF dispersion model (version 5), Earth Tech Inc., Concord, MA.

CHAPTER 3

EVALUATION OF AN ENSEMBLE SMOKE DISPERSION FORECAST SYSTEM FOR AGRICULTURAL BURNING IN EASTERN WASHINGTON AND NORTHERN IDAHO

3.1. Introduction

Agricultural burning is commonly used to remove crop residue after harvest in eastern Washington and northern Idaho. Wheat and Kentucky bluegrass (KBG) are two major crops grown in northern Idaho, while eastern Washington farmers grow mainly wheat. Once these crops are harvested, farmers will typically burn the leftover crop residue on their fields. Burning agricultural fields is more cost-effective for farmers than other methods for clearing agricultural fields including: bailing, composting, and disking crop residue. Post harvest burning helps to control pests and plant diseases, maintains future harvest yield, and quickly removes the crop residue from the fields (ASI, 2003; ASI, 2004; Johnson et al., 2003).

Agricultural field burning emits many pollutants into the atmosphere including: particulate matter (PM), carbon dioxide (CO_2), carbon monoxide (CO), nitrogen oxides (NO plus NO_2, or NO_X), polycyclic aromatic hydrocarbons (PAHs), and a variety of other products of incomplete combustion (Crutzen and Andrea, 1990). Particulate matter with an aerodynamic diameter of less than 2.5 μm ($PM_{2.5}$) is a very important pollutant; the small particles can travel deep into human lungs and trigger respiratory health problems (Slaughter et al., 2003; Roberts et al., 1998). The particulate emissions from field burning can reduce visibility on highways and seriously degrade the local air quality of populated areas in eastern Washington and northern Idaho.

As a result of the potential air quality impact of field burning, both Washington and Idaho have developed smoke management programs to manage and regulate when farmers are allowed to burn their agricultural fields. Smoke management programs were created to regulate agricultural field burning and also to prevent cities and towns from being adversely impacted by air pollutants, specifically $PM_{2.5}$, emitted from field burning. Burn managers use meteorology forecasts, air quality observations, and other information to help decide which farmers will be allowed to burn their fields. Complete descriptions of the smoke management programs in Washington and Idaho are presented in WA DOE (2004) and ISDA (2004), respectively.

ClearSky is an automated smoke dispersion forecast system that was developed at Washington State University and operated during the 2002 – 2005 agricultural burn seasons for eastern Washington and northern Idaho. A technical description of the ClearSky system is presented in Jain (2004); a summary detailing the major components of ClearSky is presented below.

ClearSky was developed to provide burn coordinators with an additional tool for making burn decisions. In operation, burn coordinators create burn scenarios of the fields they may allow to burn the next day. These burn scenarios are created on the project website (www.clearsky.wsu.edu) and are then converted to $PM_{2.5}$ emission files for input into CALPUFF, a Lagrangian dispersion model (Scire et al., 2000b). Hourly meteorological fields for a Pacific Northwest domain with 4-km grid cells are produced by the Penn State/National Center for Atmospheric Research (NCAR) fifth generation Mesoscale Meteorological Model (MM5) (Grell et al., 1995). The MM5 forecasts were run by the University of Washington MM5 forecast system (Mass et al., 2003). The

MM5 forecast is processed by CALMM5/CALMET to create a forecast meteorology input for CALPUFF (Scire et al., 2000a). The forecast meteorology is further improved by replacing the planetary boundary layer (PBL) parameters calculated by CALMET with the MM5 PBL parameters passed through by MCIP, the Models-3/CMAQ meteorology preprocessor (O'Neill et al., 2005). CALPUFF simulates the emission and transport of $PM_{2.5}$ from agricultural burns and calculates the surface level $PM_{2.5}$ concentrations for each burn scenario. The hourly surface level $PM_{2.5}$ concentrations predicted by ClearSky are then displayed for review by the burn coordinators through a graphical interface on the project website.

Jain (2004) presented an evaluation of ClearSky for 20 burn days during the 2003 agricultural burn season. Forecast $PM_{2.5}$ concentrations from ClearSky were compared to $PM_{2.5}$ concentrations measured at 20 air quality monitoring sites in Washington and Idaho. At monitoring sites where elevated $PM_{2.5}$ concentrations were observed, a comparison of model-predicted and observed wind directions was also completed. Many of the forecast $PM_{2.5}$ plumes missed air quality monitoring stations where elevated $PM_{2.5}$ concentrations were observed. The evaluation found that small differences between the model-forecast and actual wind directions could determine whether a simulated smoke plume impacts an air monitoring station or misses the station by a few kilometers. For the remainder of this paper, ClearSky, as described above, will be referred to as original ClearSky.

Dabberdt et al. (2004) described how ensemble meteorological forecasts present a range of possible atmospheric conditions; in addition, these ensemble meteorological forecasts can be used in air quality dispersion models to represent meteorological forecast

uncertainties and to account for uncertainty in the transport and diffusion of air pollutants. Forecast meteorology ensembles can be developed by changing initial conditions, boundary conditions, individual model parameterizations, and using different Numerical Weather Prediction (NWP) models (Molteni et al., 1996; Toth et al., 1997; Grimit et al., 2002; Wandishin et al., 2005).

Ensemble techniques can also be applied to air quality modeling. Two major ensemble approaches have been applied to pollutant/tracer dispersion forecasts. The first approach represents the uncertainties in forecast meteorology by utilizing a suite of meteorological forecasts and one dispersion model. Methods for creating a suite of meteorological forecasts include:

- shifting the meteorological data from a single forecast ±1 grid point horizontally and ±250 m vertically (Draxler, 2003);
- perturbing meteorological variables (wind speed, wind direction, etc.) of a single forecast (Dabberdt et al., 2000);
- perturbing the initial and boundary conditions of a NWP model (Straume et al., 1998); and
- changing initial conditions, physical parameterizations, and surface physics schemes of a NWP model (Warner et al., 2002).

The second approach uses suites of both meteorological forecasts and dispersion models to represent the uncertainties in forecast meteorologies and different diffusion modeling concepts (Galmarini et al., 2001; Straume, 2001; Galmarini et al., 2004a; Galmarini et al., 2004b). Ensemble ozone forecasts have been created using a single meteorological forecast and multiple parameterizations of one chemical transport model

(Mallet et al., 2006) or a suite of meteorological forecasts and chemical transport models (Delle Monache et al., 2003; Mckeen et al., 2005; O'Neill et al., 2005). In this paper, we present an ensemble $PM_{2.5}$ forecasting approach. The ClearSky ensemble system utilizes a suite of MM5 meteorological forecasts for input into a single dispersion model (CALPUFF) to improve the prediction of surface level $PM_{2.5}$ concentrations from agricultural field burns in eastern Washington and northern Idaho.

3.2. Methodology

An ensemble smoke dispersion forecast system, ensemble ClearSky, was created to produce probabilistic surface-level $PM_{2.5}$ concentration forecasts for agricultural burning in eastern Washington and northern Idaho. Ensemble ClearSky is similar to the original ClearSky and likewise uses a single $PM_{2.5}$ emission scenario, CALMET and MCIP meteorological processors, and the dispersion model CALPUFF. However, ensemble ClearSky generates 17 $PM_{2.5}$ forecasts of one field burn scenario by utilizing a suite of 17 different MM5 forecasts, whereas original ClearSky simulated one $PM_{2.5}$ forecast using a single MM5 forecast. Figure 3.1 displays a schematic of ensemble ClearSky. The suite of 17 MM5 forecasts, with 12-km resolution over the Pacific Northwest, is produced nightly by the University of Washington Mesoscale Ensemble (UWME). The UWME produces two sets of forecasts:

- CORE (uses different initial and boundary conditions, but the same MM5 physics configuration) and
- CORE+ (uses different initial and boundary conditions and varies the MM5 physics configuration).

There are eight different sources of data used for the initial conditions and the boundary conditions of the CORE and CORE+ ensembles. The initial and boundary condition data sources are provided by global forecast, global analysis, and mesoscale models including:

- National Center for Environmental Prediction (GFS),
- National Center for Environmental Prediction (ETA),
- Canadian Meteorology Center GEM (CMCG),
- United Kingdom Met Office Unified Model (UKMO),
- Taiwanese Central Weather Bureau GFS (TCWB),
- Australian Bureau of Meteorology (GASP),
- U.S. Navy Fleet Numerical Meteorological and Oceanographic Center (NGPS),
- Japanese Meteorological Administration GSM (JMA), and
- Centroid (CENT) – The grid average of the eight data sets.

Altogether, 17 MM5 forecasts are produced daily by the UWME. More information about UWME is available in Mass et al. (2003) and on the UWME website: http://www.atmos.washington.edu/~ens/uwme_info.html.

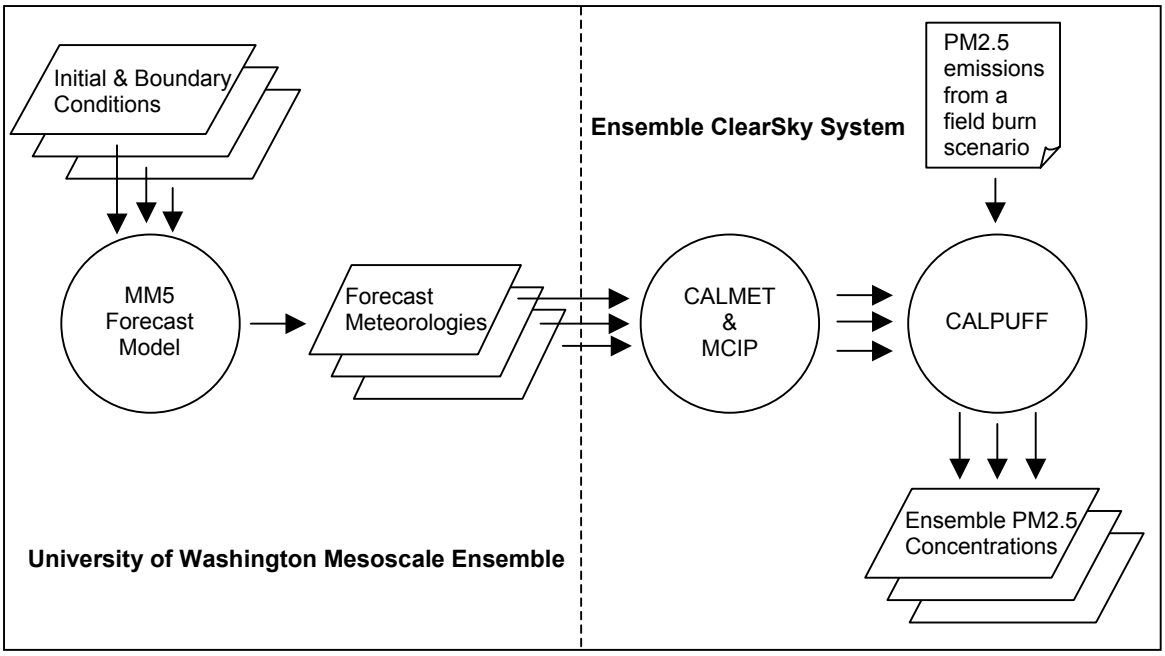

Figure 3.1: Schematic representation of the UWME and the ensemble ClearSky system with multiple rectangles representing multiple ensemble members.

CALPUFF was run with 12-km grid spacing (ensemble ClearSky) and 4-km grid spacing (original ClearSky) to match their respective MM5 forecasts. $PM_{2.5}$ concentrations were determined for both ensemble and original ClearSky by sampling with one-kilometer resolution over the modeling domains. The forecast, $PM_{2.5}$ concentrations used for evaluation calculations were extracted from the one-kilometer sampling grids.

Ensemble ClearSky and original ClearSky were used to simulate fires during two burn days (August 17 and September 8, 2004) during the 2004 agricultural burn season. These burn days were selected because of the large acreage burned and $PM_{2.5}$ impacts at monitoring sites. A total of 5990 and 18400 acres were burned in eastern Washington and northern Idaho during August 17, 2004 and September 8, 2004 respectively. $PM_{2.5}$ emission files were created for both burn days using burn logs which contain completed

field burn information (field location, acres, crop, burn start time, etc.). It should be noted that start times were not available for all field burns, so typical start times were assigned to some field burns. The $PM_{2.5}$ forecasts were identified and labeled by the meteorological forecast used in the CALPUFF simulation. For example, if the GFS meteorological forecast from the CORE+ ensemble was used, the resulting $PM_{2.5}$ forecast was identified as GFS+. An ensemble average, the un-weighted hourly mean $PM_{2.5}$ concentration of all ensemble ClearSky members, was also calculated.

The ensemble member $PM_{2.5}$ forecasts, ensemble average $PM_{2.5}$ forecast, and the original ClearSky $PM_{2.5}$ forecast were all compared to hourly $PM_{2.5}$ concentrations observed at 23 air quality monitoring sites located in eastern Washington and northern Idaho. Only monitoring sites that observed $PM_{2.5}$ impacts were used to evaluate ensemble and original ClearSky forecasts. The comparison of predicted and observed $PM_{2.5}$ concentrations was used to determine if ensemble ClearSky provided a more accurate $PM_{2.5}$ forecast than original ClearSky. In previous ensemble ozone and ensemble tracer studies, the ensemble average was proven to be the most accurate forecast, when compared to any single forecast (Straume, 2001; Delle Monache et al., 2003; Mckeen et al., 2005; O'Neill et al., 2005). The following two statistical measures were calculated for individual ensemble members, ensemble average, and original ClearSky $PM_{2.5}$ concentrations at selected monitoring sites:

Normalized Mean Error (NME)

$$= \frac{\sum_{i=1}^{N} | C_p(x,t_i) - C_o(x,t_i) |}{\sum_{i=1}^{N} C_o(x,t_i)} * 100\ \%$$

and

Unpaired Peak Prediction Error (UPPE)

$$= \frac{C_p(x,t')_{\max} - C_o(x,t')_{\max}}{C_o(x,t')_{\max}}$$

where N is the number of hourly concentrations at a given monitoring station, $C_o(x,t_i)$ is the observed concentration at the monitoring station located at x for hour t_i, $C_p(x,t_i)$ is the predicted concentration at the monitoring station located at x for hour t_i, $C_o(x,t')_{max}$ is the maximum 1-hr observed concentration at a specific monitoring station over one burn day, and $C_p(x,t')_{max}$ is the maximum 1-hr predicted concentration at a specific monitoring station over one burn day. NME is a rigorous analysis that matches predicted and observed $PM_{2.5}$ concentrations in both time and space, whereas the UPPE analysis compares the maximum observed and maximum predicted concentrations at a single site.

The mean absolute error (MAE) of the wind direction was calculated for individual meteorological forecasts (ensemble ClearSky members and original ClearSky) and for the ensemble average of the suite of meteorological forecasts using measured wind directions from monitoring sites where elevated $PM_{2.5}$ concentrations were observed. The MAE of wind direction is defined as:

$$MAE = \frac{1}{N}\sum_{i=1}^{N}\left|WD_p(x,t_i) - WD_o(x,t_i)\right|$$

where N is the number of hourly concentrations at a given monitoring station, $WD_p(x,t_i)$ is the predicted wind direction at the monitoring station located at x for hour t_i, and $WD_o(x,t_i)$ is the observed wind direction at the monitoring station located at x for hour t_i. If the calculated MAE is greater than 180 degrees (maximum error in wind direction), the absolute value of MAE minus 360 degrees is calculated for each hour and then the sum of the absolute errors is averaged over the total number of hours. This correction is used because the error in predicted versus observed wind direction can not be greater than 180

degrees (opposite) of each other. This statistical analysis shows how the ensemble meteorology forecasts and the original ClearSky meteorology compared to observed wind directions.

3.3. Results

Ensemble ClearSky simulated one burn scenario for August 17, 2004 using a suite of 16 meteorological forecasts; one meteorological forecast, CENT, was not available from the UWME. Observed and predicted $PM_{2.5}$ concentrations for August 17, 2004 were compared at five air quality monitoring sites located in Idaho (Coeur d'Alene, Pinehurst, Post Falls, Rathdrum, and Reubens). Figures 3.2 and 3.3 show observed wind directions and wind speeds for August 17, 2004 respectively. The wind speeds ranged from 1 – 7 m/s and the wind directions ranged from 230 – 316 degrees. The wind direction was defined as the direction the wind was coming from. Figure 3.4 shows time series of observed $PM_{2.5}$ concentrations at the five monitoring stations. Peak observed $PM_{2.5}$ concentrations ranged from ~ 40 $\mu g/m^3$ at Rathdrum, ID to ~ 20 $\mu g/m^3$ at Pinehurst, ID. Figure 3.5 shows the distribution of monitoring stations and surface concentration contours of $PM_{2.5}$ concentrations, for 13:00 PST, predicted by original ClearSky for eastern Washington and northern Idaho. The Environmental Protection Agency established a National Ambient Air Quality Standard (NAAQS) for $PM_{2.5}$ for a 24-hour averaging period (65 $\mu g/m^3$). None of the monitoring stations exceeded the NAAQS for 24-hour $PM_{2.5}$ because smoke from field burns typically impact a monitoring station for only a few hours, and these higher $PM_{2.5}$ concentrations are then averaged with many hours when low $PM_{2.5}$ concentrations were recorded at the monitoring station. Background $PM_{2.5}$ concentrations were also determined for each site according to

observed $PM_{2.5}$ concentrations, the assigned background $PM_{2.5}$ concentration for each site include:

- Coeur d'Alene, ID – 6 $\mu g/m^3$;
- Pinehurst, ID – 7 $\mu g/m^3$;
- Post Falls, ID – 0.1 $\mu g/m^3$;
- Rathdrum, ID – 14 $\mu g/m^3$; and
- Reubens, ID – 3 $\mu g/m^3$.

Ensemble ClearSky simulated one burn scenario for September 8, 2004 using a suite of 15 meteorological forecasts; two meteorological forecasts, CENT and TCWB+, were not available from the UWME. Observed and predicted $PM_{2.5}$ concentrations for September 8, 2004 were compared at seven air quality monitoring sites, two sites located in Washington (Pullman and Walla Walla) and five sites were located in Idaho (Coeur d'Alene, Pinehurst, Moscow, Plummer, and Reubens). Observed wind directions and wind speeds for September 8, 2004 are shown in Figures 3.6 and 3.7 respectively. The wind speeds ranged from 2 – 8 m/s and the wind directions varied considerably between monitoring sites, ranging from 150 – 310 degrees. Figure 3.8 shows time series of observed $PM_{2.5}$ concentrations at the seven monitoring stations. Peak observed $PM_{2.5}$ concentrations ranged from approximately 80 $\mu g/m^3$ at Reubens, ID to 10 $\mu g/m^3$ at Walla Walla, WA. Again, no monitoring stations exceeded the NAAQS for 24-hour $PM_{2.5}$. Figure 3.9 shows the distribution of monitoring stations and surface concentration contours of $PM_{2.5}$ concentrations, for 12:00 PST, predicted by original ClearSky for eastern Washington and northern Idaho. Background $PM_{2.5}$ concentrations were also

determined for each monitoring site according to observed $PM_{2.5}$ concentrations, the assigned background $PM_{2.5}$ concentration for each site include:

- Coeur d'Alene, ID – 0.1 $\mu g/m^3$;
- Moscow, ID – 3 $\mu g/m^3$;
- Pinehurst, ID – 3 $\mu g/m^3$;
- Plummer, ID – 0.1 $\mu g/m^3$;
- Pullman, WA – 3 $\mu g/m^3$;
- Reubens, ID – 0.1 $\mu g/m^3$; and
- Walla Walla, WA – 3 $\mu g/m^3$.

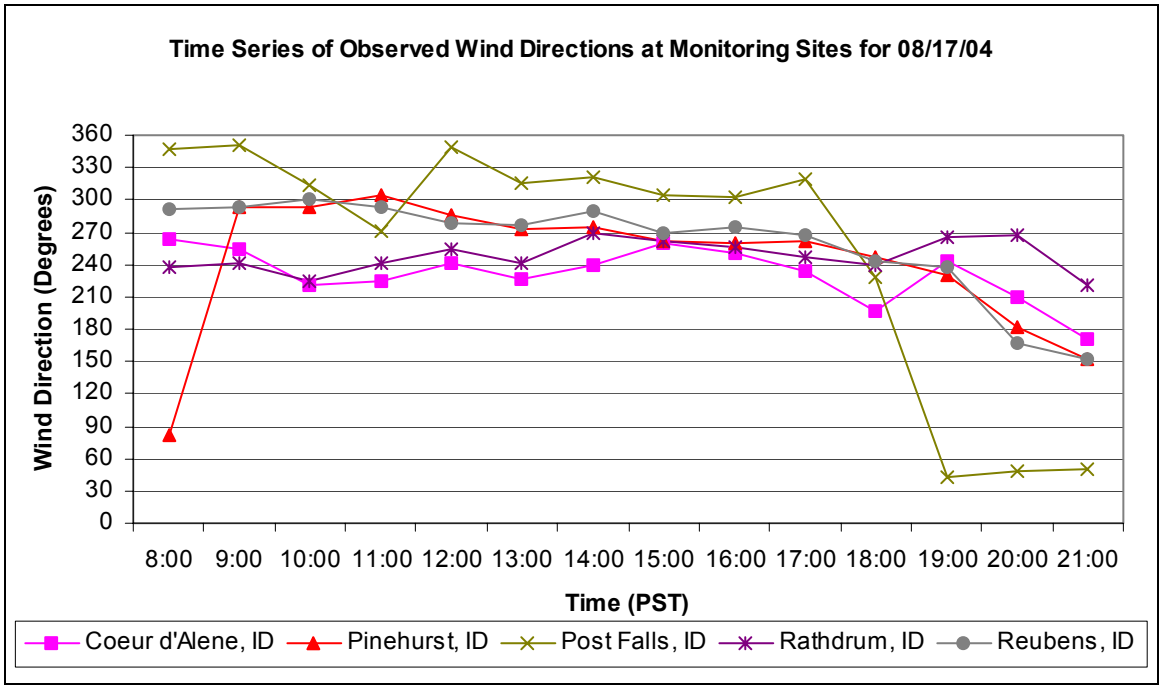

Figure 3.2: Time series of observed wind directions at five monitoring sites for August 17, 2004.

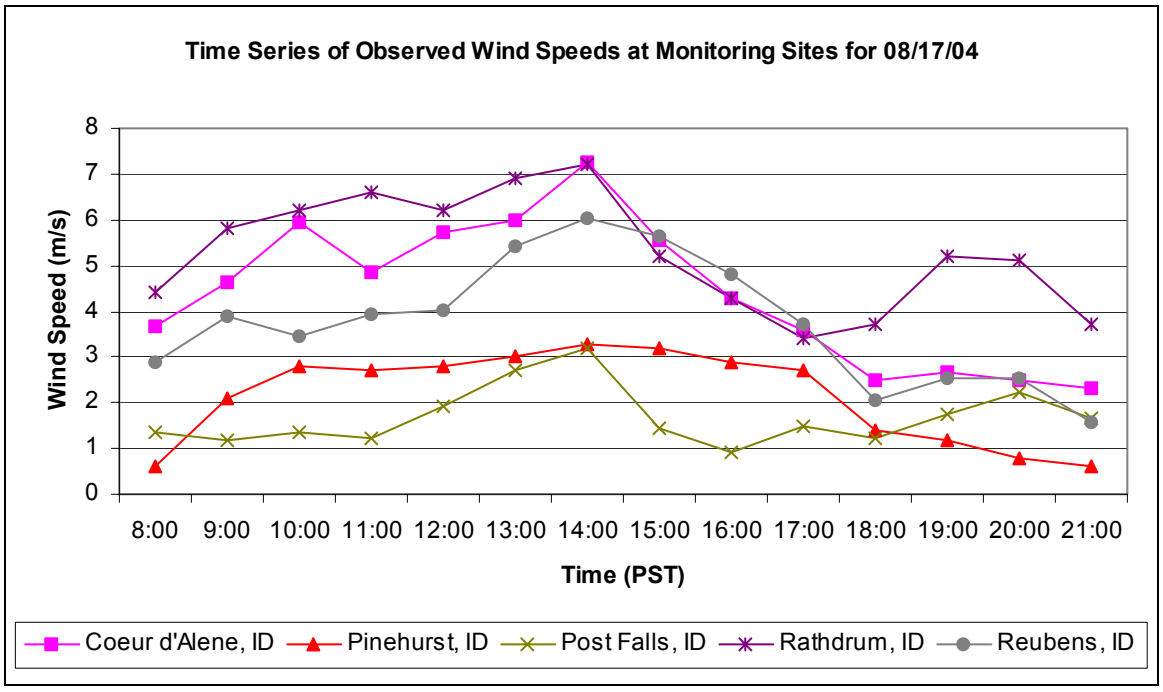

Figure 3.3: Time series of observed wind speeds at five monitoring sites for August 17, 2004.

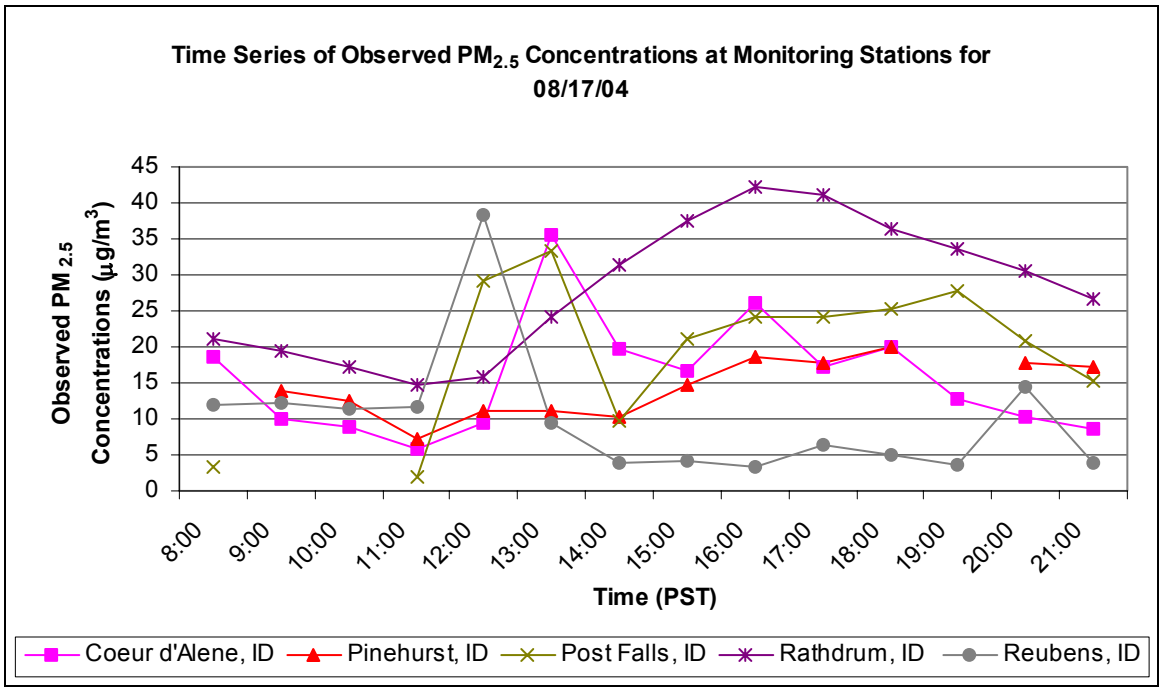

Figure 3.4: Time series of observed $PM_{2.5}$ concentrations at five monitoring stations for August 17, 2005.

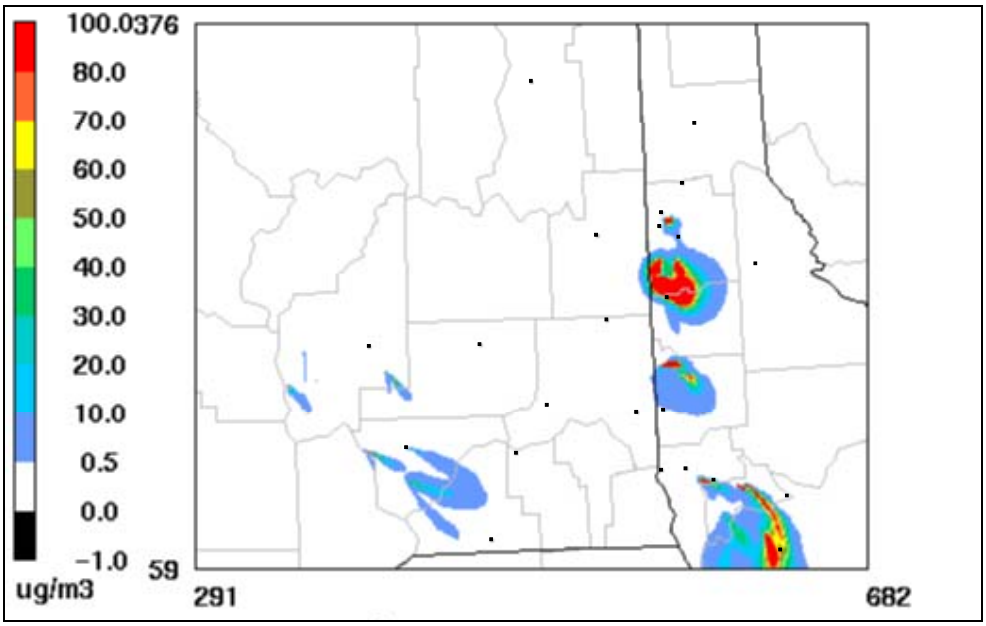

Figure 3.5: Surface concentration contours of $PM_{2.5}$ concentrations predicted by original ClearSky for 13:00 PST on August 17, 2004. The black squares represent $PM_{2.5}$ monitoring stations.

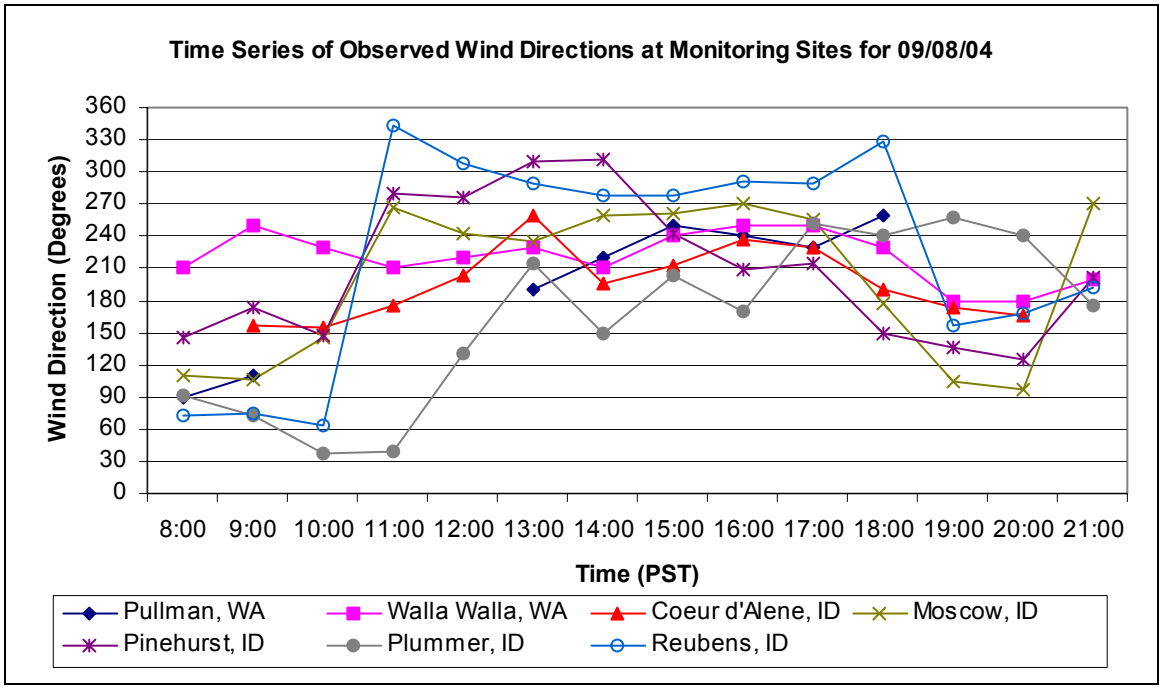

Figure 3.6: Time series of observed wind directions at seven monitoring sites for September 8, 2004.

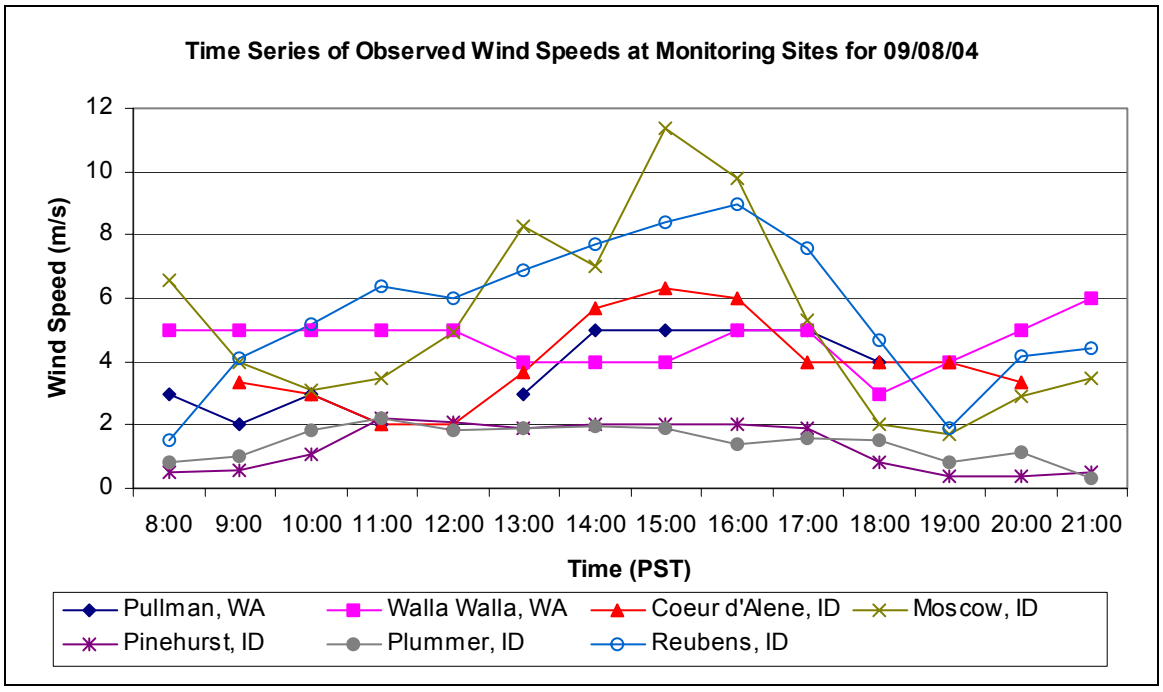

Figure 3.7: Time series of observed wind speeds at seven monitoring sites for September 8, 2004.

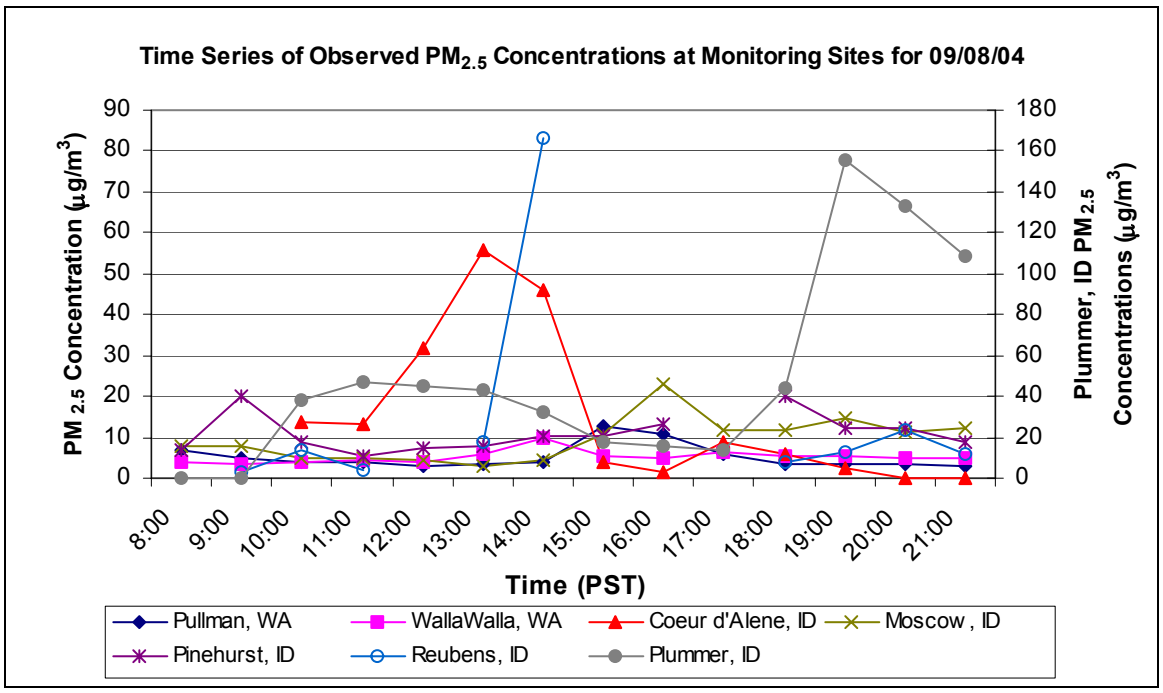

Figure 3.8: Time series of observed $PM_{2.5}$ concentrations at seven monitoring sites for September 8, 2004. Concentrations from the Plummer, ID monitoring site are shown on a secondary (right) y-axis.

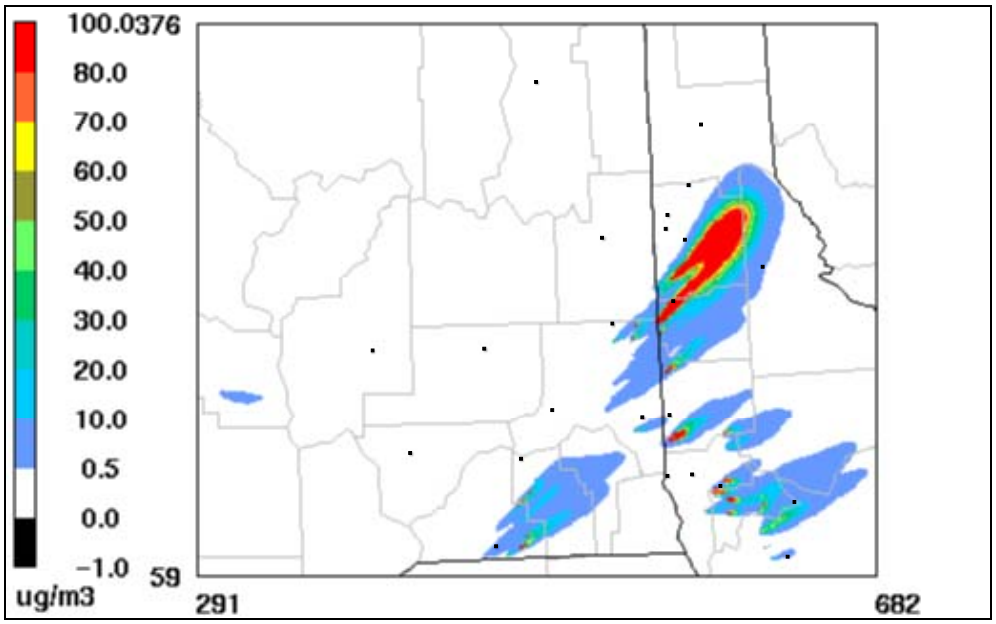

Figure 3.9: Surface concentration contours of $PM_{2.5}$ concentrations predicted by original ClearSky for 12:00 PST on September 8, 2004. The black squares represent $PM_{2.5}$ monitoring stations.

$PM_{2.5}$ forecasts from ensemble ClearSky simulations were viewed two ways: tile plots of $PM_{2.5}$ concentrations and time series plots of $PM_{2.5}$ concentrations. Hourly concentration contour maps of $PM_{2.5}$ concentrations displayed the spatial extent of the $PM_{2.5}$ plumes for a given burn scenario. Figure 3.10 displays one hour, 12:00 PST, surface $PM_{2.5}$ concentration contours, for an area near Coeur d'Alene, ID, showing five individual ensemble member plume forecasts and the ensemble average for the September 8, 2004 burn scenario. The contour maps show that each of the $PM_{2.5}$ forecasts simulated by ensemble ClearSky was different and that the ensemble average was a smear of all the individual ensemble member forecasts. Figure 3.10 also shows that the UKMO ensemble member plume missed a monitoring site while other members (ETA, GFS +, TCWB, and GASP) impacted the monitoring site.

The surface concentration contour maps can also be used to show the maximum ECS simulated $PM_{2.5}$ concentrations for each hour of the forecast. The hourly maximum $PM_{2.5}$ concentrations for each grid cell were determined by comparing and recording the maximum $PM_{2.5}$ concentrations predicted at each grid by all of the ECS members. Figures 3.11 and 3.12 show the maximum ensemble member-predicted $PM_{2.5}$ surface concentrations for 13:00 PST of August 17, 2004 and 12:00 PST of September 8, 2004. The maximum predicted $PM_{2.5}$ concentration contour maps represent all of the possible plume trajectories and provide a worse case scenario when compared to Figures 3.5 and 3.9 which show the $PM_{2.5}$ forecasts simulated by OCS.

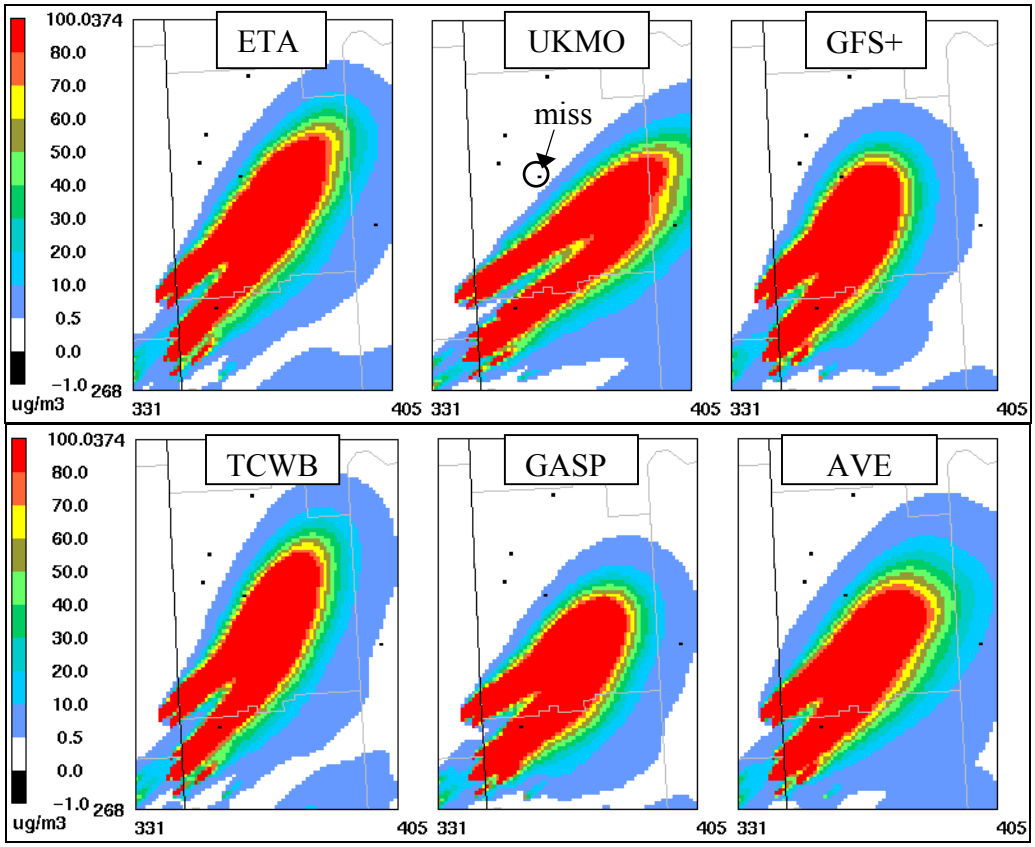

Figure 3.10: Surface concentration contour maps of $PM_{2.5}$ plumes near Coeur d'Alene, ID at 12:00 PST for September 8, 2004. Observation sites are shown as small black boxes. The bottom right map shows the ensemble average (AVE).

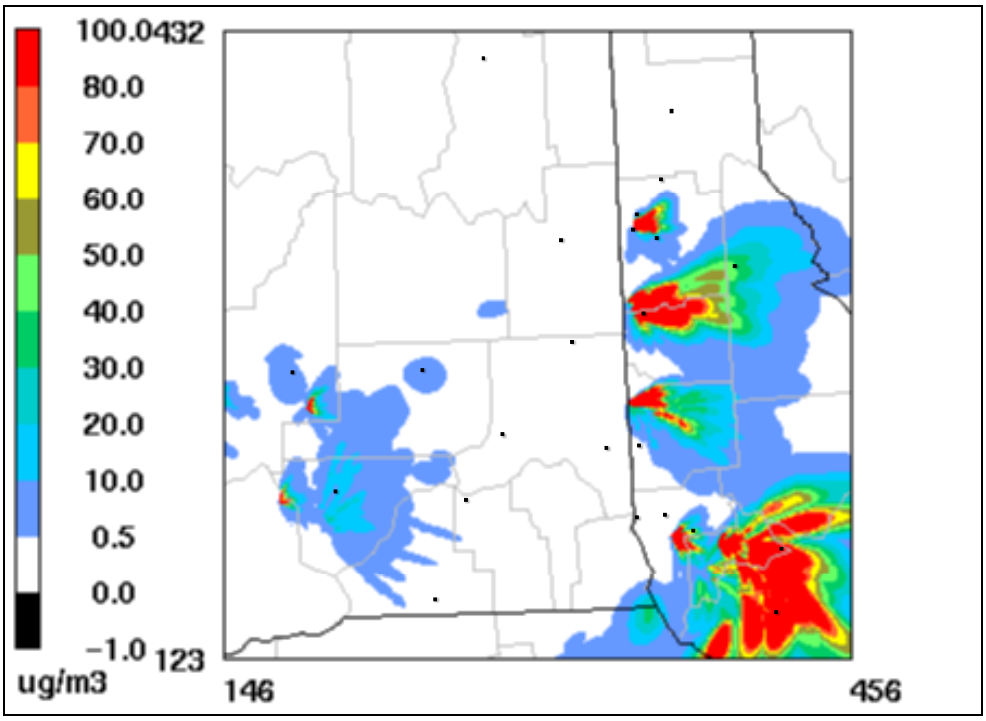

Figure 3.11: Surface concentration contour map of the maximum ensemble member-predicted $PM_{2.5}$ concentrations at 13:00 PST for August 17, 2004. Black boxes represent $PM_{2.5}$ monitoring stations.

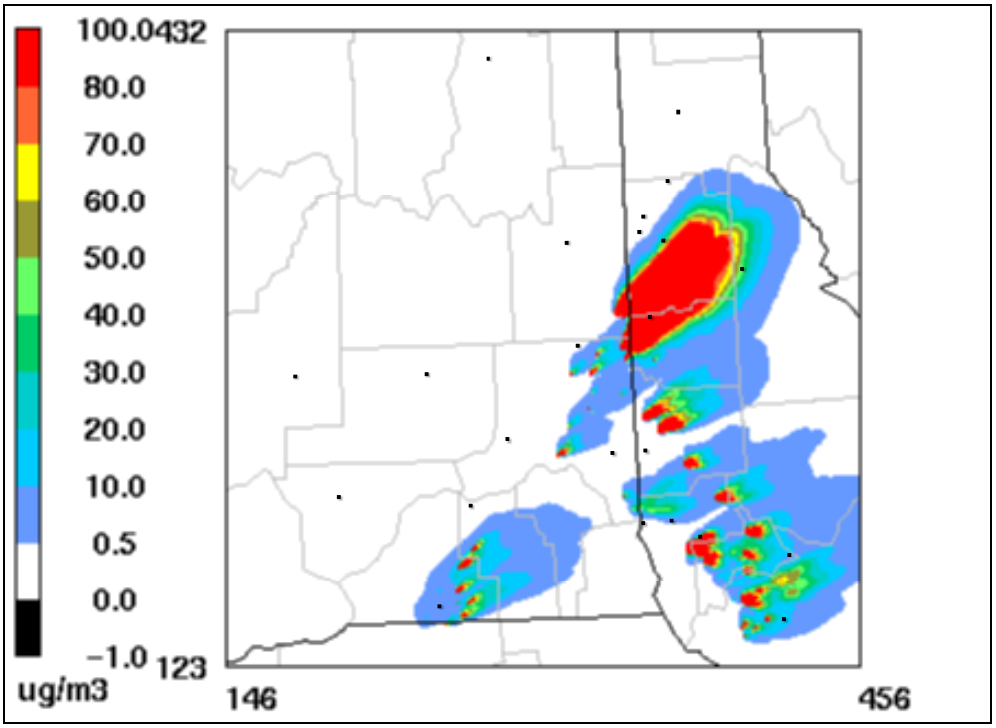

Figure 3.12: Surface concentration contour map of the maximum ensemble member-predicted $PM_{2.5}$ concentrations at 12:00 PST for September 8, 2004. Black boxes represent $PM_{2.5}$ monitoring stations.

A time series of the ensemble $PM_{2.5}$ forecasts for one monitoring site shows the spread of possible $PM_{2.5}$ forecasts for a given burn scenario. Figure 3.13 displays a time series of predicted and observed $PM_{2.5}$ concentrations for August 17, 2004 at the Reubens, ID monitoring site. The ensemble $PM_{2.5}$ forecasts as shown include the addition of the assigned background $PM_{2.5}$ concentration. The $PM_{2.5}$ time series plot for Reubens, ID shows four ensemble members (JMA, UKMO, UKMO+, and TCWB) that predict maximum $PM_{2.5}$ concentrations similar to the observed maximum $PM_{2.5}$ concentration (38 $\mu g/m^3$). Original ClearSky and the ensemble average predicted 4.5 $\mu g/m^3$ and 10 $\mu g/m^3$ for the maximum $PM_{2.5}$ concentration respectively. Nine

ensemble ClearSky members predicted low (less than 5 $\mu g/m^3$) $PM_{2.5}$ concentrations at Reubens, ID, and effectively lowered the ensemble average $PM_{2.5}$ concentrations. Time series plots were also created for the predicted and observed wind directions. Figure 3.14 displays time series of observed and predicted wind directions for August 17, 2004 at the Reubens, ID monitoring site. Figure 3.15 displays time series of observed and predicted wind speeds for August 17, 2004 at the Reubens, ID monitoring site. Figures 3.14 and 3.15 show the range of possible wind directions and wind speeds from the suite of 16 meteorological forecasts along with observations and the meteorological forecast for original ClearSky. At each of the selected monitoring sites, time series plots for wind direction, wind speed, and $PM_{2.5}$ concentration are displayed in Appendix B (August 17, 2004) and in Appendix C (September 8, 2004).

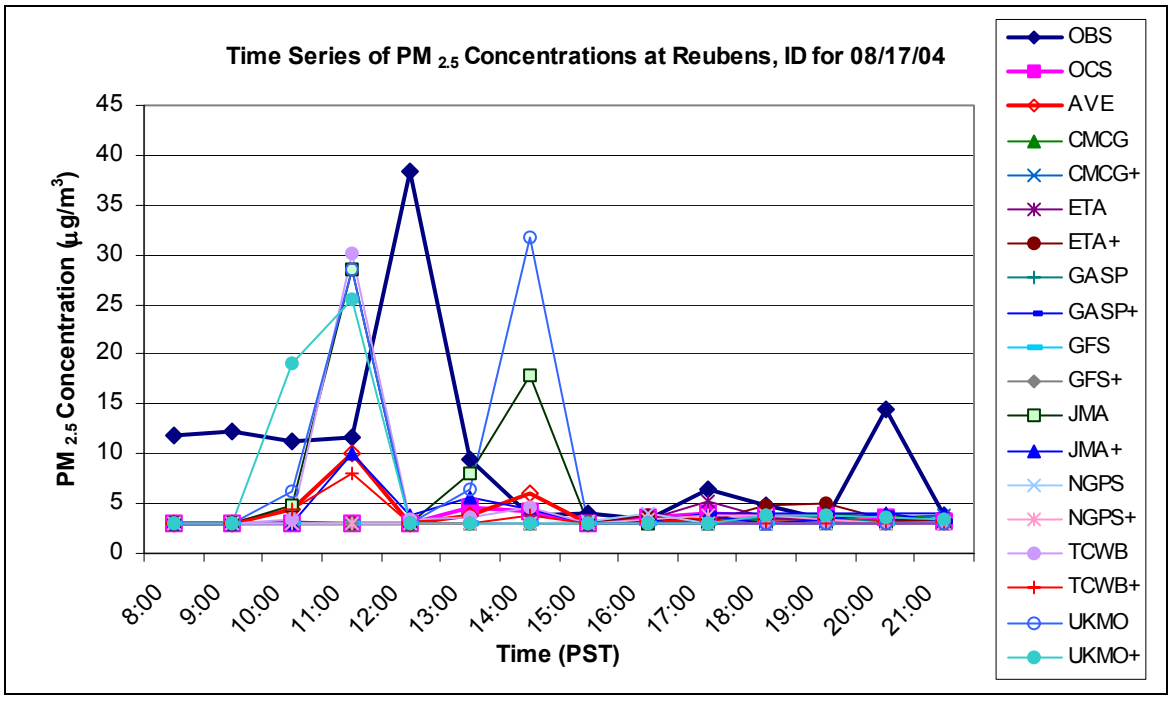

Figure 3.13: Time series of ensemble $PM_{2.5}$ concentrations at Reubens, ID monitoring site for August 17, 2004. Observations (OBS), original ClearSky (OCS), and ensemble average (AVE) are shown with the 16 ensemble ClearSky members.

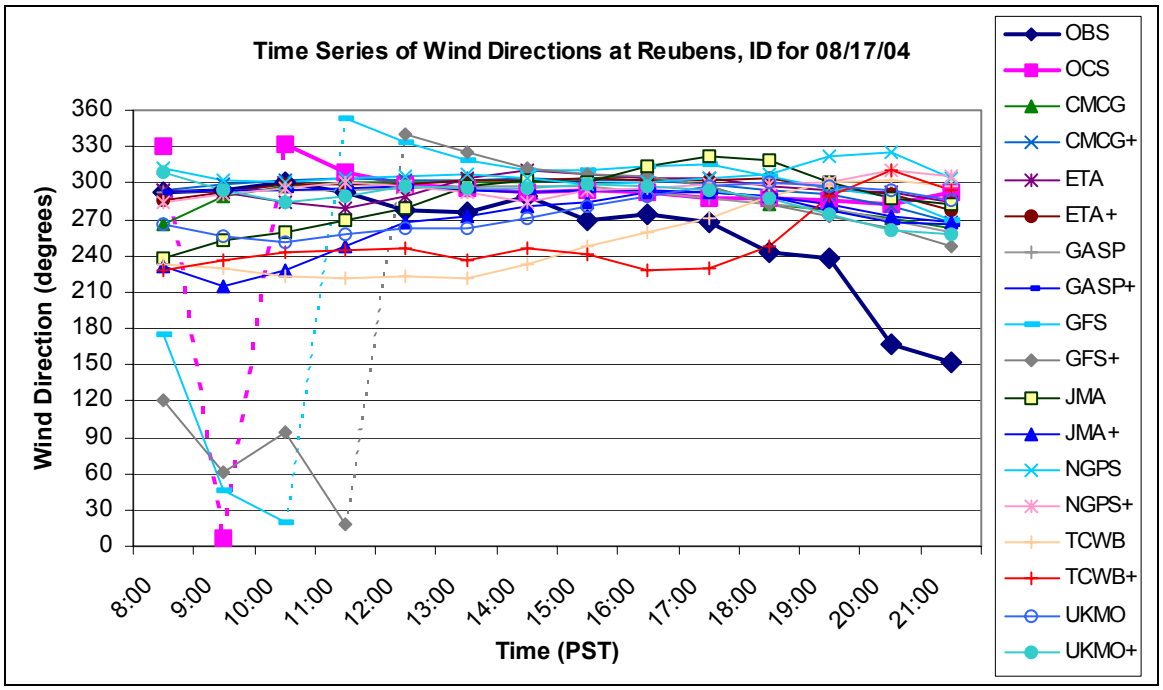

Figure 3.14: Time series of wind directions at Reubens, ID monitoring site for August 17, 2004. Observations (OBS) and original ClearSky (OCS) are shown with the 16 ensemble ClearSky members. Dashed lines indicate wind direction shifted across the top or bottom of the plot (360 degrees in circle).

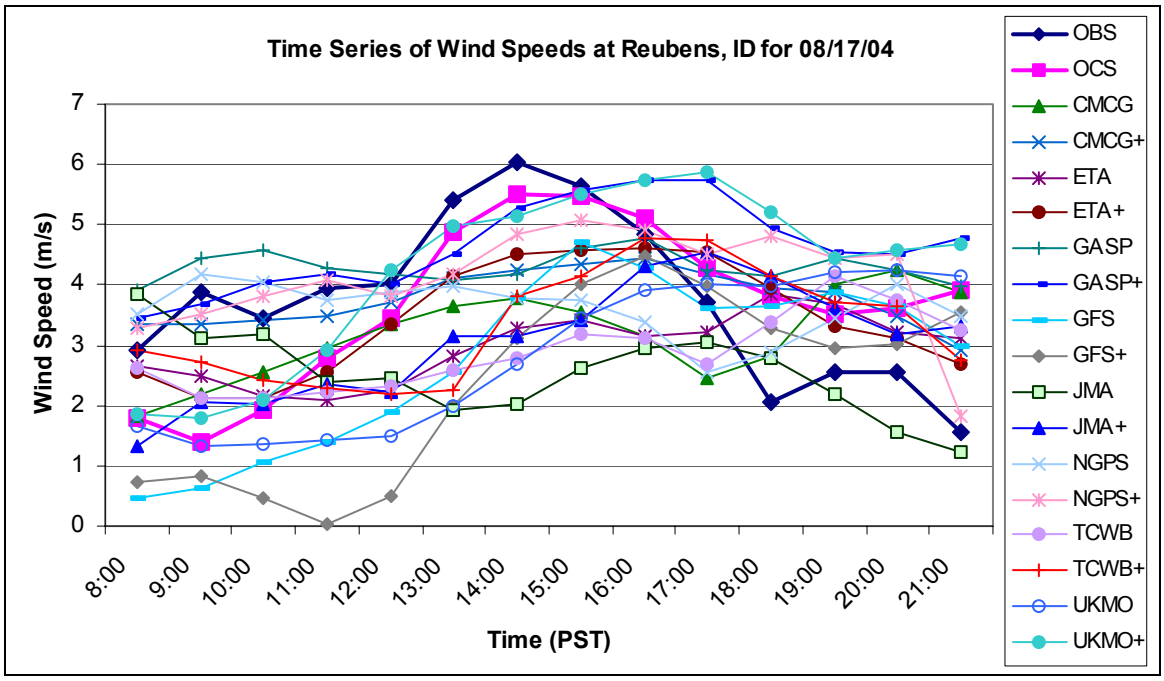

Figure 3.15: Time series of wind speeds at Reubens, ID for August 17, 2004. Observations (OBS) and original ClearSky (OCS) are shown with the 16 ensemble ClearSky members.

A statistical analysis of the predicted $PM_{2.5}$ concentrations and predicted wind directions was completed for both burn day simulations. The UPPE and NME were calculated for individual ensemble members, the ensemble average, original ClearSky, using the observed $PM_{2.5}$ concentrations at each monitoring site. The NME and UPPE values for August 17, 2004 are shown in Tables 3.1 and 3.2. The NME and UPPE values for September 8, 2004 are shown in Tables 3.3 and 3.4. The ensemble average had lower UPPE values than original ClearSky at all monitoring sites except at the Coeur d'Alene, ID monitoring site for the August 17, 2005 $PM_{2.5}$ forecasts. The original ClearSky had lower UPPE values compared to the ensemble average at all monitoring sites except at the Plummer, ID and Walla Walla, WA monitoring sites for the September 8, 2004 $PM_{2.5}$

forecasts. The ensemble average had lower NME values compared to original ClearSky at all but one monitoring sites for both burn days; original ClearSky had the lowest NME value at Pinehurst, ID for September 8, 2004.

The UPPE values calculated at the Pinehurst, ID monitoring site during August 17, 2004 ranged from 9% (ETA+) to 405% (CMCG). The large errors at the site were due to four ensemble members (CMCG, TCWB, TCWB+, and UKMO) over predicting the peak $PM_{2.5}$ concentrations as much as five times the observed peak $PM_{2.5}$ concentration (~20 $\mu g/m^3$).

Some of the UPPE values calculated at the Pinehurst, ID site and all of the UPPE values calculated at the Plummer, ID site were greater than 100% for September 8, 2004. The observed peak $PM_{2.5}$ concentration was ~20 $\mu g/m^3$ at the Pinehurst, ID site and six ensemble members (CMCG, CMCG+, GASP, NGPS+, UKMO, and UKMO+) over predicted the peak $PM_{2.5}$ concentration by as much as a factor of 3.5. The observed peak $PM_{2.5}$ concentration was ~50 $\mu g/m^3$ at the Plummer, ID site during the morning burn period, and all of the ensemble members over predicted the peak $PM_{2.5}$ concentration by up to a factor of nine. During the time of the peak concentrations observed at Plummer, the observed wind directions were from the northeast, while all of the predicted wind directions for Plummer were from the southwest. Thus, the plume impact observed at Plummer was probably due to a different field compared to the impacts predicted with the ensemble system. At the same time, the predicted wind speeds were also approximately twice as high as observed. These higher wind speeds would decrease plume rise from a field burn and increase surface concentrations.

Table 3.1: Normalized Mean Error (in %) for hourly $PM_{2.5}$ concentrations from 8:00 – 21:00 PST on August 17, 2004 (Bold values represent the best $PM_{2.5}$ forecast at that monitoring site)

	Coeur d'Alene, ID	**Pinehurst, ID**	**Post Falls, ID**	**Rathdrum, ID**	**Reubens, ID**	**Overall**
OCS	73	51	100	50	60	67
AVE	58	50	95	49	56	62
CMCG	53	141	95	50	62	80
CMCG+	**52**	46	95	50	63	61
ETA	61	45	97	50	61	63
ETA+	56	**40**	95	50	62	61
GASP	62	45	97	50	63	63
GASP+	62	48	**91**	50	61	62
GFS	62	63	98	50	63	67
GFS+	62	46	100	**47**	63	64
JMA	61	71	98	50	74	71
JMA+	62	49	97	50	**53**	62
NGPS	61	51	94	50	63	64
NGPS+	57	48	96	49	62	62
TCWB	60	90	97	50	69	73
TCWB+	62	101	98	50	64	75
UKMO	62	129	97	50	84	84
UKMO+	62	42	96	50	65	63

OCS = Original ClearSky, AVE = Ensemble Average

Table 3.2: Unpaired Peak Prediction Error (in %) for maximum $PM_{2.5}$ concentrations from 8:00 – 21:00 PST on August 17, 2004 (Bold values represent the best $PM_{2.5}$ forecast at that monitoring site)

	Coeur d'Alene, ID	**Pinehurst, ID**	**Post Falls, ID**	**Rathdrum, ID**	**Reubens, ID**	**Overall**
OCS	50	64	100	67	88	74
AVE	68	24	71	64	74	60
CMCG	50	405	66	67	90	135
CMCG+	48	46	59	67	90	62
ETA	79	16	76	67	86	65
ETA+	57	**9**	66	67	87	57
GASP	83	40	80	67	90	72
GASP+	**2**	47	**36**	67	89	48
GFS	83	61	86	66	92	78
GFS+	83	52	100	**21**	91	70
JMA	81	109	88	66	25	74
JMA+	83	58	76	67	74	72
NGPS	81	63	63	65	89	72
NGPS+	21	47	78	61	90	60
TCWB	79	108	80	67	21	71
TCWB+	82	269	84	67	79	116
UKMO	83	338	78	67	**17**	117
UKMO+	83	35	74	67	34	58

OCS = Original ClearSky, AVE = Ensemble Average

Table 3.3: Normalized Mean Error (in %) for hourly $PM_{2.5}$ concentrations from 8:00 – 21:00 PST on September 8, 2004 (Bold values represent the best $PM_{2.5}$ forecast at that monitoring site)

	Coeur d'Alene, ID	**Moscow, ID**	**Pinehurst, ID**	**Plummer, ID**	**Pullman, WA**	**Reubens, ID**	**WallaWalla, WA**	**Overall**
OCS	93	67	80	113	41	131	63	84
AVE	84	64	97	87	36	117	59	78
CMCG	100	66	161	104	40	116	63	93
CMCG+	100	65	156	109	39	**98**	62	90
ETA	89	65	79	83	37	138	62	79
ETA+	88	63	75	**56**	35	119	58	71
GASP	98	65	124	123	39	129	58	91
GASP+	**60**	65	86	123	39	109	49	76
GFS	87	64	72	84	38	104	62	73
GFS+	83	62	71	85	35	119	56	73
JMA	93	65	100	96	39	129	63	83
JMA+	84	62	95	86	35	127	58	78
NGPS	93	**59**	78	63	**27**	111	**49**	69
NGPS+	95	64	120	94	38	128	59	85
TCWB	103	63	**62**	70	42	123	60	75
TCWB+ [‡]								
UKMO	100	66	127	97	41	123	63	88
UKMO+	100	68	140	103	42	98	62	88

OCS = Original ClearSky, AVE = Ensemble Average

[‡] No MM5 forecast available for this ensemble member

Table 3.4: Unpaired Peak Prediction Error (in %) for maximum $PM_{2.5}$ concentrations from 8:00 – 21:00 PST on September 8, 2004 (Bold values represent the best $PM_{2.5}$ forecast at that monitoring site)

	Coeur d'Alene, ID	**Moscow, ID**	**Pinehurst, ID**	**Plummer, ID**	**Pullman, WA**	**Reubens, ID**	**WallaWalla, WA**	**Overall**
OCS	75	69	20	711	59	8	8	136
AVE	78	77	70	429	61	45	11	110
CMCG	100	79	239	789	70	28	8	188
CMCG+	100	74	246	832	66	49	8	196
ETA	81	74	26	535	58	16	2	113
ETA+	49	71	**2**	**280**	40	46	15	72
GASP	96	77	149	693	70	21	4	159
GASP+	29	81	89	693	55	38	52	148
GFS	78	73	13	509	62	**3**	10	107
GFS+	11	77	7	423	58	20	6	86
JMA	86	75	81	498	62	29	5	120
JMA+	67	72	69	433	57	30	**1**	104
NGPS	12	70	26	343	**34**	59	57	86
NGPS+	85	76	144	525	66	29	4	133
TCWB	**1**	**68**	49	364	76	42	10	87
TCWB+ ‡								
UKMO	100	76	179	608	71	23	7	152
UKMO+	100	85	170	503	76	83	14	147

OCS = Original ClearSky, AVE = Ensemble Average

‡ No MM5 forecast available for this ensemble member

The MAE of wind direction was calculated for the individual ensemble ClearSky members and the original ClearSky meteorological forecasts. The MAE of wind direction values for August 17, 2004 are shown in Table 3.3 and the MAE of wind direction values for September 8, 2004 are shown in Table 3.4. The NGPS meteorological forecast had lower wind direction MAE values at one monitoring site (Rathdrum, ID) for August 17, 2004 and at three monitoring sites (Pinehurst, ID; Plummer, ID; and Pullman, WA) for September 8, 2004. The original ClearSky meteorological forecast had the lowest wind direction MAE value at only one site for September 8, 2004. Tables 3.5 and 3.6 show that no single meteorological forecast better predicted wind directions at every monitoring site for both burn days.

Scatter plots were created from NME of $PM_{2.5}$ concentrations versus the MAE of wind direction at all of the monitoring sites. Figures 3.16 displays the scatter plot for August 17, 2004 and Figure 3.17 displays the scatter plot for September 8, 2004. For the majority of the monitoring sites, the concentration NME increases as the wind direction MAE increases. These findings show that larger errors in forecast wind direction can cause larger errors in the predicted $PM_{2.5}$ concentrations.

Table 3.5: Mean Absolute Error of Wind Direction (in degrees) for 8:00 – 21:00 PST on August 17, 2004 (Bold values represent the most accurate meteorological forecast at that monitoring site)

	Coeur d'Alene, ID	**Pinehurst, ID**	**Post Falls, ID**	**Rathdrum, ID**	**Reubens, ID**	**Overall**
OCS	52	85	93	73	44	70
CMCG	22	49	105	34	35	49
CMCG+	**20**	40	101	21	36	44
ETA	26	40	98	30	41	47
ETA+	27	38	92	17	39	43
GASP	21	45	98	17	**29**	42
GASP+	32	**33**	95	27	30	43
GFS	27	42	101	25	70	53
GFS+	25	35	95	26	74	51
JMA	25	42	98	23	51	48
JMA+	29	38	77	33	46	45
NGPS	35	45	85	**16**	47	45
NGPS+	29	39	96	22	40	45
TCWB	**20**	47	95	18	62	49
TCWB+	**20**	42	99	20	57	48
UKMO	26	51	113	40	45	55
UKMO+	36	36	**73**	40	32	43

OCS = Original ClearSky

Table 3.6: Mean Absolute Error of Wind Direction (in degrees) for 8:00 – 21:00 PST on September 8, 2004

(Bold values represent the most accurate meteorological forecast at that monitoring site)

	Coeur d'Alene, ID	**Moscow, ID**	**Pinehurst, ID**	**Plummer, ID**	**Pullman, WA**	**Reubens, ID**	**WallaWalla, WA**	**Overall**
OCS	**28**	65	59	72	56	68	18	52
CMCG	40	71	60	72	68	65	18	56
CMCG+	38	70	58	75	68	65	15	56
ETA	38	55	61	72	50	76	19	53
ETA+	31	**50**	52	73	42	70	25	49
GASP	41	59	62	70	53	74	21	54
GASP+	39	74	65	71	47	79	20	56
GFS	36	58	58	70	51	77	20	53
GFS+	38	62	61	70	59	**63**	19	53
JMA	38	55	60	72	48	70	19	52
JMA+	36	**50**	56	70	40	70	15	48
NGPS	30	54	**51**	**68**	**21**	71	21	45
NGPS+	37	55	59	72	48	72	**13**	51
TCWB	32	64	52	71	60	71	23	53
TCWB+ ‡								
UKMO	39	69	63	75	65	69	16	56
UKMO+	41	69	61	74	66	64	15	56

OCS = Original ClearSky

‡ No MM5 forecast available for this ensemble member

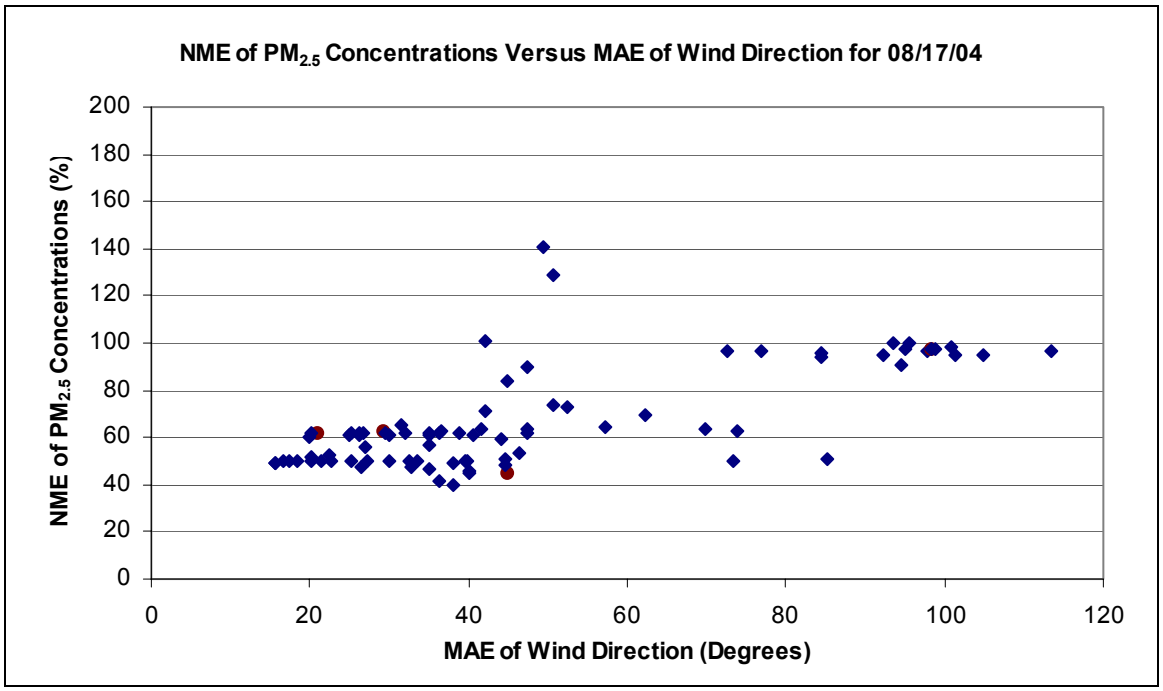

Figure 3.16: Scatter-Plot of normalized mean error of $PM_{2.5}$ concentrations versus mean absolute error of wind direction for August 17, 2004.

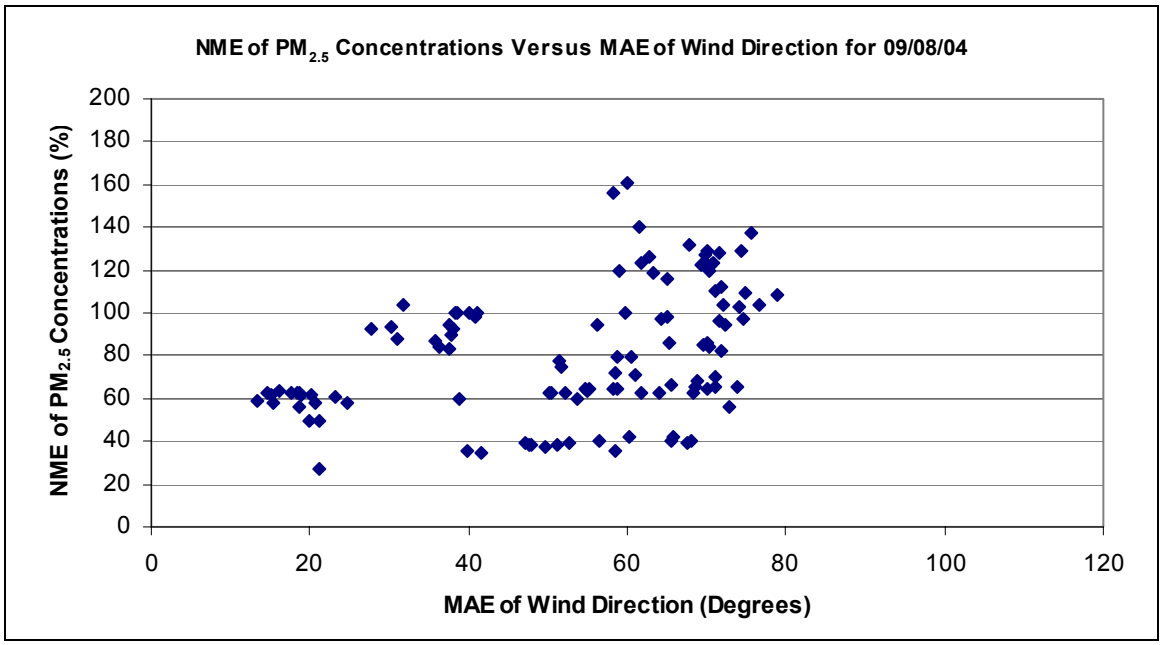

Figure 3.17: Scatter-Plot of normalized mean error of $PM_{2.5}$ concentrations versus MAE of wind direction for September 8, 2004.

3.4. Discussion

The results presented in the previous section show that ensemble ClearSky produces a better $PM_{2.5}$ forecast than original ClearSky. The ensemble average $PM_{2.5}$ concentrations are generally more accurate than the deterministic $PM_{2.5}$ forecasts produced by original ClearSky. The ensemble $PM_{2.5}$ forecasts utilize up to 17 different MM5 forecasts and provided a wealth of useful information including: the range of potential $PM_{2.5}$ concentrations at any particular site, multiple visualizations of $PM_{2.5}$ plume transport, and representation of some of the uncertainties in the forecast meteorology.

The ensemble average forecast $PM_{2.5}$ concentrations were not more accurate than forecasts from some ensemble ClearSky members, this can be explained by how the ensemble average is calculated. Individual ensemble member $PM_{2.5}$ plumes either impacted the monitoring site or missed the monitoring site all together and, more often than not, the $PM_{2.5}$ plumes missed the monitoring station and lowered the ensemble average $PM_{2.5}$ concentrations. Past studies that concluded the ensemble average was better than any single member were completed for ozone plumes (Delle Monache et al., 2003; Mckeen et al., 2005; O'Neill et al., 2005) and a large release of tracer gas (Straume, 2001). These ozone and tracer plumes are much wider than a $PM_{2.5}$ plume from an agricultural field burn and therefore are less apt to miss a monitoring station completely. For this reason, the ensemble average may not be the best predictor of $PM_{2.5}$ concentrations from agricultural burns; nevertheless, when looking at monitoring sites for a specific burn day, no one ensemble ClearSky member was clearly superior at predicting the $PM_{2.5}$ concentrations at each monitoring site.

Of the $PM_{2.5}$ forecasts available for August 17, 2004 burn day, three $PM_{2.5}$ forecasts (CMCG+, ETA+, and UKMO+) had the lowest average NME (61%), the ETA+ $PM_{2.5}$ forecast had the lowest average UPPE (57%), and four meteorological forecasts (ETA+,GASP, GASP+, and UKMO+) had the lowest average MAE in wind direction (42 – 43 degrees). Of the available $PM_{2.5}$ forecasts available for September 8, 2004 burn day, the NGPS $PM_{2.5}$ forecast had the lowest average NME (69%), the ETA+ $PM_{2.5}$ forecast had the lowest average UPPE (72%), and the NGPS meteorological forecast had the lowest average MAE in wind direction (45 degrees). These results show that the best meteorological forecast produced the lowest average NME for both burn days, and the best meteorological forecast produced the lowest average UPPE for the August 17, 2004 burn day.

With the exception of the Plummer site where significant overprediction occurred, the lowest UPPE values ranged from 1% – 68% for the two burn days. The average UPPE (without the Plummer site) was 18%. This indicates that given the correct meteorology, the dispersion model can predict maximum $PM_{2.5}$ concentrations to within 18%. This is significant since it provides confidence in the overall set of assumptions regarding the $PM_{2.5}$ emissions and plume rise parameters. The UPPE values for the ensemble average $PM_{2.5}$ forecasts ranged from 11% – 78%; and the UPPE values for the original ClearSky $PM_{2.5}$ forecasts ranged from 8% –88%.

The lowest NME values ranged from 27% – 98% for the two burn days. The NME values for the ensemble average $PM_{2.5}$ forecasts ranged from 36% – 117%; and the NME values for the original ClearSky $PM_{2.5}$ forecasts ranged from 41% – 131%. Averaged over both days, the OCS overall NME was 76%, the ensemble average overall

NME was 70%, and the best single member overall NME was 65%. The lowest MAE in wind direction values ranged from 13 – 73 degrees.

Because field burn start times were assigned to some fields, the timing of peak predicted $PM_{2.5}$ concentrations could be shifted by one or more hours. Therefore, the calculated NME values may not have a strong statistical significance for the two burn days because the predicted and observed $PM_{2.5}$ concentrations were paired in time for the calculation. The calculated UPPE values were a better statistical calculation because the predicted and observed $PM_{2.5}$ concentrations were not paired in time.

Overall, the results show that a suite of meteorological forecasts is still necessary to represent the uncertainties in the forecast meteorology. The suite of 17 meteorological forecasts represent some of the uncertainties in the forecast meteorology, but as Figure 3.14 shows, the range of possible wind directions did not vary greatly between the different meteorological forecasts. The grid resolution may be too coarse to resolve surface features that could influence the wind direction predictions. The current ensemble ClearSky configuration provides better $PM_{2.5}$ forecasts than the original ClearSky, but future research should be focused on improving the forecast meteorology by increasing grid resolution or by perturbing wind directions, at individual grid cells, over a specified range (± 20 degrees).

3.5. References

ASI (Air Sciences Inc.), 2003. Final Report: Cereal grain crop open field burning emissions study, Project 152-02. Available at http://www.ecy.wa.gov/programs/air/pdfs/FinalWheat_081303.pdf

ASI, 2004. Quantifying post-emissions from bluegrass seed production field burning. Available at http://www.ecy.wa.gov/programs/air/pdfs/bluegrass_final_report.pdf

Crutzen, P. J., and Andrea, M. O., 1990: Biomass burning in the tropics: impact on atmospheric chemistry and biogeochemical cycles. *Science*, 250, 1669-1678.

Dabberdt, W. F. and Miller, E., 2000. Uncertainty, Ensembles and Air Quality Dispersion Modeling: Applications and Challenges. *Atmospheric Environment* 34, 4667-4673.

Dabberdt, W. F., Carroll, M. A., Baumgardner, D. , Carmichael, G., Cohen, R., Dye, T., Ellis, J., Grell, G., Grimmond, S., Hanna, S., Irwin, J., Lamb, B., Madronich, S., Mcqueen, J., Meagher, J., Odman, T., Pleim, J., Schmid, H. P., and Westphal, D. L., 2004. Meteorological Research Needs for Improved Air Quality Forecasting - Report of the 11th Prospectus Development Team of the Us Weather Research Program. *Bulletin of the American Meteorological Society* 85, 563-586.

Delle Monache, L. and Stull, R. B., 2003. An Ensemble Air-Quality Forecast Over Western Europe During an Ozone Episode. *Atmospheric Environment* 37, 3469-3474.

Draxler, R. R., 2003. Evaluation of an Ensemble Dispersion Calculation. *Journal of Applied Meteorology* 42, 308-317.

Galmarini, S., Bianconi, R., Bellasio, R., and Graziani, G., 2001. Forecasting the Consequences of Accidental Releases of Radionuclides in the Atmosphere From Ensemble Dispersion Modelling. *Journal of Environmental Radioactivity* 57, 203-219.

Galmarini, S., Bianconi, R., Klug, W., Mikkelsen, T., Addis, R., Andronopoulos, S., Astrup, P., Baklanov, A., Bartniki, J., Bartzis, J. C., Bellasio, R., Bompay, F., Buckley, R., Bouzom, M., Champion, H., D'amours, R., Davakis, E., Eleveld, H., Geertsema, G. T., Glaab, H., Kollax, M., Ilvonen, M., Manning, A., Pechinger, U., Persson, C., Polreich, E., Potemski, S., Prodanova, M., Saltbones, J., Slaper, H., Sofiev, M. A., Syrakov, D., Sorensen, J. H., Van Der Auwera, L., Valkama, I., and Zelazny, R., 2004a. Ensemble Dispersion Forecasting - Part I: Concept, Approach and Indicators. *Atmospheric Environment* 38, 4607-4617.

Galmarini, S., Bianconi, R., Addis, R., Andronopoulos, S., Astrup, P., Bartzis, J. C., Bellasio, R., Buckley, R., Champion, H., Chino, M., D'amours, R., Davakis, E., Eleveld, H., Glaab, H., Manning, A., Mikkelsen, T., Pechinger, U., Polreich, E., Prodanova, M., Slaper, H., Syrakov, D., Terada, H., and Van Der Auwera, L., 2004b. Ensemble Dispersion Forecasting - Part II: Application and Evaluation. *Atmospheric Environment* 38, 4619-4632.

Grell, G. A., Dudhia, J., and Stauffer, D. R., 1995: A description of the fifth-generation Penn State/NCAR mesoscale model (MM5). NCAR Tech. Note NCAR/TN-398+STR, 122 pp.

Grimit, E. P. and Mass, C. F., 2002. Initial Results of a Mesoscale Short-Range Ensemble Forecasting System Over the Pacific Northwest. *Weather and Forecasting* 17, 192-205.

Idaho State Department of Agriculture (ISDA), 2004: Idaho Crop Residue Disposal Smoke Management Program 2004 Season Review. Prepared by ISDA, Idaho Department of Environmental Quality, Nez Perce Tribe, Coeur d'Alene Tribe, and Kootenai Tribe of Idaho. Available at http://www.idahoag.us/Categories/Environment/Smoke/Documents/AnnualSummary2004.pdf.

Jain, R., 2004. Modeling Transport and Dispersion of Smoke Plumes from Agricultural Field Burning in Eastern Washington and Northern Idaho, M.S. Thesis, Washington State University, Pullman, WA, U.S.A.

Johnson, R. C., Johnston, W. J., and Golob, C. T., 2003. Residue Management, Seed Production, Crop Development, and Turf Quality in Diverse Kentucky Bluegrass Germplasm. *Crop Science* 43, 1091-1099.

Mallet, V. and Sportisse, B., 2006. Uncertainty in a Chemistry-Transport Model Due to Physical Parameterizations and Numerical Approximations: an Ensemble Approach Applied to Ozone Modeling. *Journal of Geophysical Research-Atmospheres* 111, D01302, doi:10.1029/2005JD006149.

Mass, C. F., Albright, M., Ovens, D., Steed, R., Maciver, M., Grimit, E., Eckel, T., Lamb, B., Vaughan, J., Westrick, K., Storck, P., Colman, B., Hill, C., Maykut, N., Gilroy, M., Ferguson, S. A., Yetter, J., Sierchio, J. M., Bowman, C., Stender, R., Wilson, R., and Brown, W., 2003. Regional Environmental Prediction Over the Pacific Northwest. *Bulletin of the American Meteorological Society* 84, 1353-1366.

Mckeen, S., Wilczak, J., Grell, G., Djalalova, I., Peckham, S., Hsie, E. Y., Gong, W., Bouchet, V., Menard, S., Moffet, R., Mchenry, J., Mcqueen, J., Tang, Y., Carmichael, G. R., Pagowski, M., Chan, A., Dye, T., Frost, G., Lee, P., and Mathur, R., 2005. Assessment of an Ensemble of Seven Real-Time Ozone Forecasts Over Eastern North America During the Summer of 2004. *Journal of Geophysical Research-Atmospheres* 110, D21307, doi:10.1029/2005JD005858.

Molteni, F., Buizza, R., Palmer, T. N., and Petroliagis, T., 1996. The ECMWF Ensemble Prediction System: Methodology and Validation. *Quarterly Journal of the Royal Meteorological Society* 122, 73-119.

O'neill, S. M. and Lamb, B. K., 2005. Intercomparison of the Community Multiscale Air Quality Model and Calgrid Using Process Analysis. *Environmental Science & Technology* 39, 5742-5753.

Roberts, R. A. and Corkill, J., 1998. Grass Seed Field Smoke and Its Impart on Respiratory Health. *Journal of Environmental Health* 60, 10-16.

Scire, J. S., Robe, F. R., Fernau, M. E., and Yamartino, R. J., 2000a. A user's guide for the CALMET meteorological model (version 5), Earth Tech Inc., Concord, MA.

Scire, J. S., Strimaitis, D. G., and Yamartino, R. J., 2000b. A user's guide for the CALPUFF dispersion model (version 5), Earth Tech Inc., Concord, MA.

Slaughter, J. C., Lumley, T., Sheppard, L., Koenig, J. Q., and Shapiro, G. G., 2003. Effects of Ambient Air Pollution on Symptom Severity and Medication Use in Children With Asthma. *Annals of Allergy Asthma & Immunology* 91, 346-353.

Straume, A. G., Koffi, E. N., and Nodop, K., 1998. Dispersion Modeling Using Ensemble Forecasts Compared to Etex Measurements. *Journal of Applied Meteorology* 37, 1444-1456.

Straume, A. G., 2001. A More Extensive Investigation of the Use of Ensemble Forecasts for Dispersion Model Evaluation. *Journal of Applied Meteorology* 40, 425-445.

Toth, Z., Kalnay, E., Tracton, S. M., Wobus, R., and Irwin, J., 1997. A Synoptic Evaluation of the Ncep Ensemble. *Weather and Forecasting* 12, 140-153.

Wandishin, M. S., Baldwin, M. E., and Mullen, S. L., 2005. Short-Range Ensemble Forecasts of Precipitation Type. *Weather and Forecasting* 20, 609-626.

Warner, T. T., Sheu, R. S., Bowers, J. F., Sykes, R. I., Dodd, G. C., and Henn, D. S., 2002. Ensemble Simulations With Coupled Atmospheric Dynamic and Dispersion Models: Illustrating Uncertainties in Dosage Simulations. *Journal of Applied Meteorology* 41, 488-504.

Washington Department of Ecology (WA DOE), 2004. Cereal grain crops: best management practices/emission reduction guidance available at http://www.ecy.wa.gov/programs/air/pdfs/Cereal_BMPs.pdf.

CHAPTER 4

SUMMARY OF RESEARCH FINDINGS AND POSSIBLE FUTURE RESEARCH

4.1. Summary

Two research projects were completed to enhance the ClearSky smoke dispersion forecast system for agricultural burning. The first project was a field campaign designed to measure plume rise from agricultural field burns and compare the measured heights to model calculated plume rise. The second project involved using a suite of 17 meteorological forecasts to represent a range of possible meteorological conditions of the atmosphere. The results for each of the research projects will be summarized along with possible research ideas to further improve each of the two projects.

Chapter 2 provided a full description of the field burn campaign and modeling methods. Top of plume height measurements collected during the field campaign were successfully used to evaluate the top of plume height calculations utilized within ClearSky. It was determined that the previous emission parameters (representing a burning field) underestimated top of plume heights for almost all the observed field burns where top of plume heights were measured. The emission parameters were updated and the resulting top of plume heights matched the measured top of plume heights better than the previous emission parameters. The updated emission parameters were then incorporated into the operational ClearSky and also used in the ensemble ClearSky research described in Chapter 3.

One possible future research project to further plume height evaluation is to use better techniques to measure the plume heights. A field campaign utilizing a light

detection and ranging (lidar) instrument would provide more accurate top of plume height measurements to compare with plume heights calculated within ClearSky.

Chapter 3 provided a full description of the ensemble techniques used to enhance the original ClearSky $PM_{2.5}$ forecasts. A suite of up to 17 meteorological forecasts was used to produce multiple $PM_{2.5}$ concentration forecasts. The ensemble average $PM_{2.5}$ concentrations were also calculated from the available $PM_{2.5}$ forecasts. The individual ensemble ClearSky members, ensemble average, and original ClearSky (one possible forecast) $PM_{2.5}$ forecasts were all evaluated against observed $PM_{2.5}$ concentrations at up to 23 monitoring stations in eastern Washington and northern Idaho for two field burn days (August 17, 2004 and September 8, 2004). The ensemble average $PM_{2.5}$ forecasts proved to be closer to observed $PM_{2.5}$ concentrations when compared to the original ClearSky $PM_{2.5}$ forecasts at most monitoring sites. However, the peak ensemble average $PM_{2.5}$ concentrations were lower than peak $PM_{2.5}$ observations. The ensemble members that predicted the $PM_{2.5}$ plumes would miss the monitoring stations effectively lowered the ensemble average $PM_{2.5}$ concentrations. It is significant that for the best single member the maximum $PM_{2.5}$ concentration was predicted to within an average of 18%. This provides some confidence in the overall set of assumptions involved in modeling the emissions and plume rise from agricultural field burns.

A statistical analysis was completed for ensemble ClearSky (individual members and ensemble average) and original ClearSky $PM_{2.5}$ forecasts. This analysis showed that different individual ensemble members predicted the peak $PM_{2.5}$ concentrations best for each monitoring site. This finding is important because it shows that no one $PM_{2.5}$

forecast was best and that multiple $PM_{2.5}$ forecasts were needed to show a range of possible $PM_{2.5}$ trajectories from a field burn scenario.

Future evaluations of ensemble ClearSky would likely be improved by using actual field burn start times. The evaluation of ensemble and original ClearSky presented in Chapter 3 did not have burn start times for all of the fields burned during the two evaluation dates. Burn start times were assigned to fields that did not have burn start times noted in their specific burn log. The errors in the timing of the peak predicted $PM_{2.5}$ concentrations could certainly be explained by burn start times being off by one to a few hours.

Even though the ensemble average was an easily applied method of combining all of the individual ensemble ClearSky results, other techniques like the weighted ensemble average, could be used to combine the individual $PM_{2.5}$ forecasts. The weighted ensemble average uses weighting factors to give certain ensemble members that perform well more weight than other members that do not perform as well. These techniques can only be applied if there is a large enough sample of observed versus predicted $PM_{2.5}$ concentrations at monitoring sites within the modeling domain. A large sample size will produce better weighting factors for the individual ensemble member $PM_{2.5}$ forecasts. Continual evaluation of the individual ensemble results to observations could also help determine specific members that perform better or worse than others. The suite of meteorological forecasts could then be decreased from the possible 17 to a smaller number of meteorological forecasts that frequently preformed better compared to the other forecasts.

One point of interest is that the current suite of 17 meteorological forecasts did not predict a large range of predicted wind directions. Instead the member-predicted wind direction varied only slightly (~30 degrees) at most of the monitoring sites for both burn days. One possible new ensemble technique for predicting $PM_{2.5}$ trajectories from agricultural burns would be to perturb the wind direction on the sub-grid cell scale. By changing wind directions over a certain range (± 20 degrees) for each grid cell in the modeling domain, a large spread of possible plume trajectories should be predicted. This variation would seem to simulate sub-scale wind uncertainties associated with convective eddies and/or local terrain.

Another research area is to look at other ways of viewing and combining ensemble data. A major issue with ensemble air quality forecasting is how to view air quality predictions from multiple forecasts. This matter was discussed in many papers and typically the forecast user/users decided upon one or more ways of viewing the ensemble forecasts. Future research could look into other methods of combining ensemble ClearSky forecasts into an understandable and practical format for the burn managers in eastern Washington and northern Idaho.

APPENDIX A

2004 Field Burn Plume Height Measurement Campaign

Case Study 1 (July 30, 2004 – Field 1)

Table A.1: 7/30/04, Field 1- Top of Plume Heights From Plane

Time (PDT)	Burn Description	Top of Plume AGL (m)
10:59	Burn Start, eastern edge	
11:11		31
11:13		107
11:16		92
11:17		107
11:20		122
11:21		92
11:15		122
11:25		122
11:55	Backing fire started	
12:03		1128
12:06		1189
12:07		1250
12:18		2103
12:21	Burn finished	
Average Elevation Of Field 1 = 274 meters ASL		

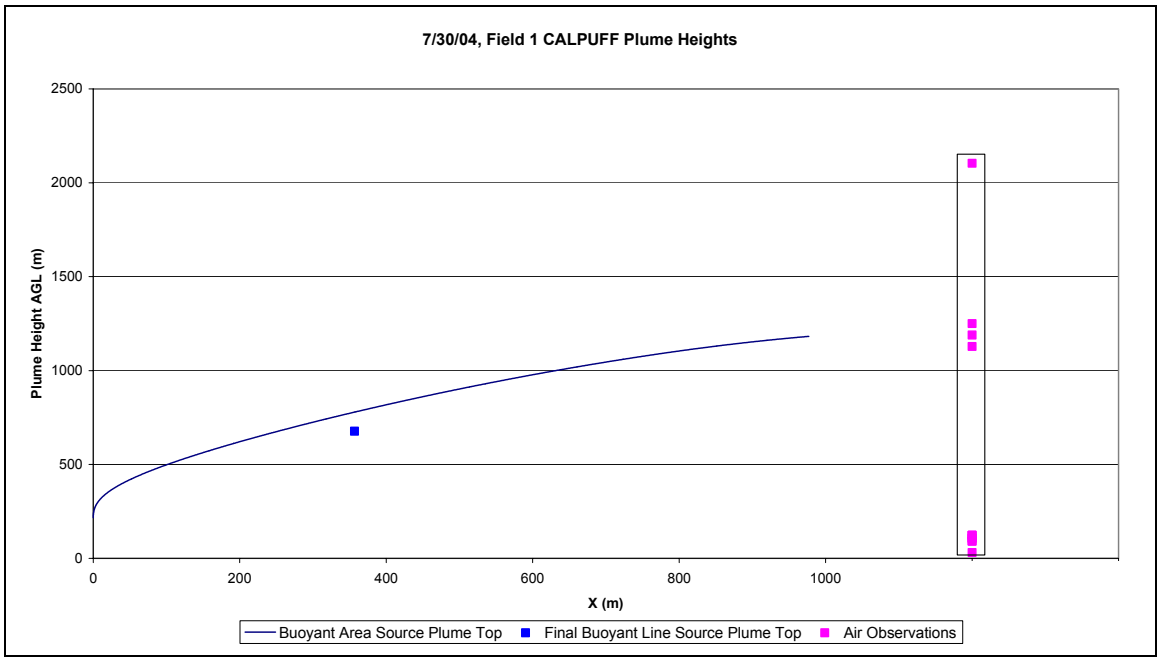

Figure A.1: CALPUFF plume heights versus downwind distance (X) and the range of air observations are displayed in a box on the right side of the graph.

Case Study 2 (July 30, 2004 – Field 2)

Table A.2: 7/30/04, Field 2 - Top of Plume Heights From Plane

Time (PDT)	Burn Description	Top of Plume AGL (m)
14:56	Burn start, north & east edge of field	
14:58		562
15:01		898
15:05	1/4 of field lit	
15:08		1324
15:10		1538
15:11		1751
15:20		2208
15:21		2330
15:22		2422
15:24		2574
15:29	Burn Completed	
Average Elevation Of Field 2 = 291 meters ASL		

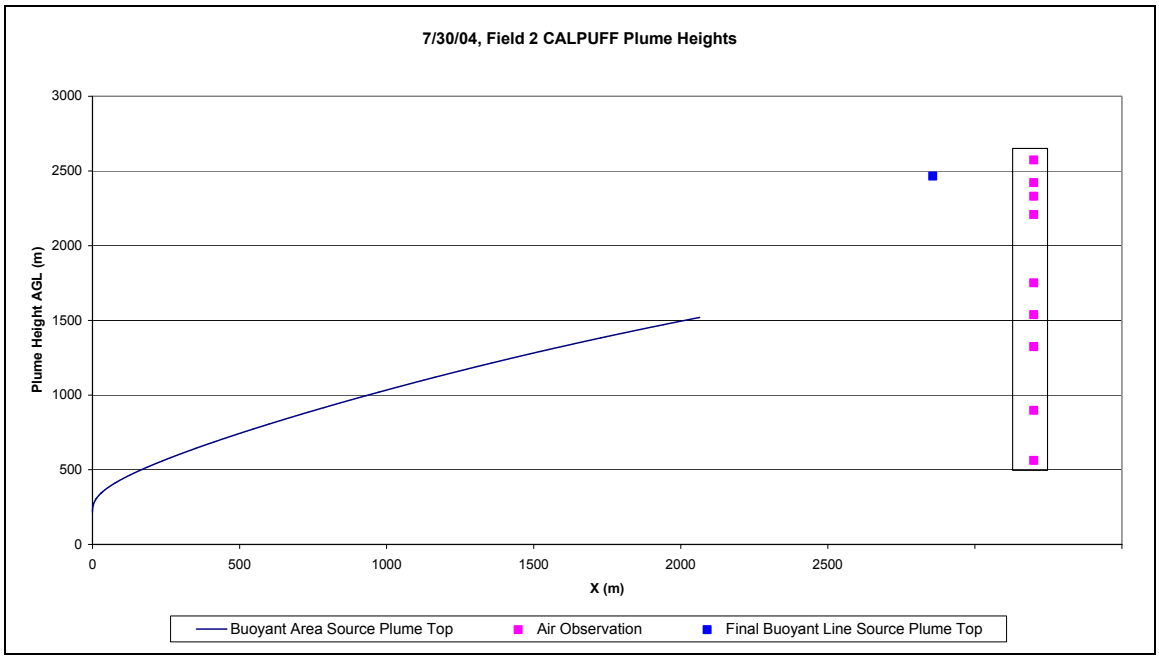

Figure A.2: CALPUFF plume heights versus downwind distance (X) and the range of air observations are displayed in a box on the right side of the graph.

Case Study 3 (August 20, 2004 – Field 1)

Table A.3: 8/20/04, Field 1 - Top of Plume Heights From Plane

Time (PDT)	Burn Description	Top of Plume AGL (m)
13:18	Burn Started	
13:19		122
13:19		152
13:20		305
13:21		457
13:22		762
13:23		853
13:25		1219
13:27		1524
13:28		1524
13:29		1676
13:31		1829
14:23		2134
14:27	Burn Finished	
Average Elevation Of Field 1 = 975 meters ASL		

Table A.4: 8/20/04, Field 1 - Top of Plume Heights From Surface

Time (PDT)	Burn Description	Top of Plume AGL (m)
13:18	Burn Started	
13:32		604
13:34		903
13:42		1580
13:50		903
14:27	Burn Finished	
Distance Between Field Center And Ground-crew = 1300 m		

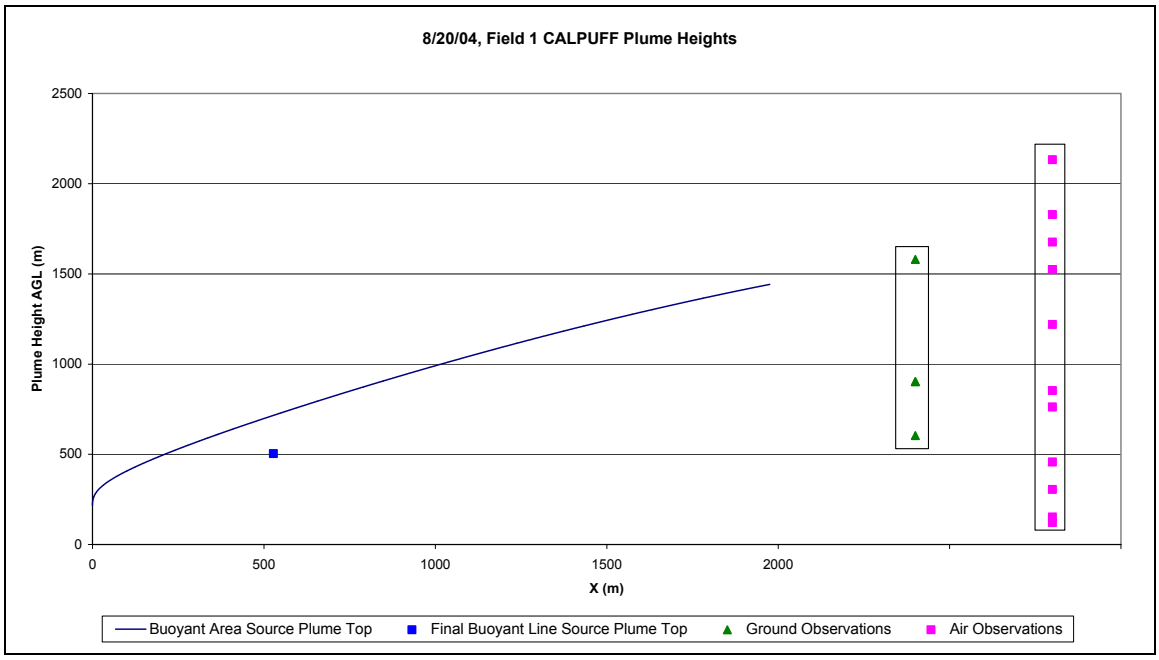

Figure A.3: CALPUFF plume heights versus downwind distance (X) and the ranges of air and ground observations are displayed in the boxes on the right side of the graph.

Case Study 4 (August 20, 2004 – Field 2)

Table A.5: 8/20/04, Field 2 - Top of Plume Heights From Plane

Time (PDT)	Burn Description	Top of Plume AGL (m)
14:36	Burn Started	
14:38		91
14:39		305
14:41		610
14:42		914
14:43		1067
14:46		1067
14:49		1311
14:52		1463
14:53		1616
14:54		1616
14:56		1768
14:57		1921
14:58		2012
14:59		2073
15:01		2073
15:03		2256
15:12	Burn Finished	
Average Elevation Of Field 2 = 975 meters ASL		

Table A.6: 8/20/04, Field 2 - Top of Plume Heights From Surface

Time (PDT)	Burn Description	Top of Plume AGL (m)
14:36	Burn Started	
14:41		258
14:49		387
14:55		645
14:57		957
15:12	Burn Finished	
Distance Between Field Center And Ground-crew = 1300 m		

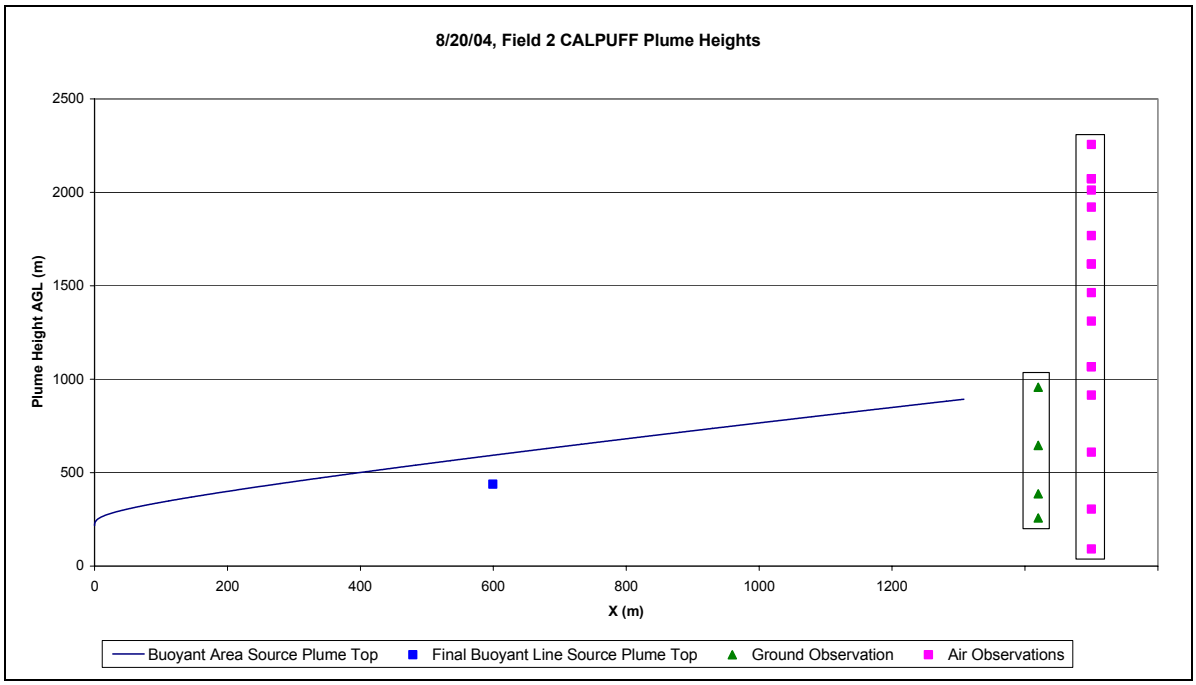

Figure A.4: CALPUFF plume heights versus downwind distance (X) and the ranges of air and ground observations are displayed in the boxes on the right side of the graph.

Case Study 5 (August 20, 2004 – Field 3)

Table A.7: 8/20/04, Field 3 - Top of Plume Heights From Plane

Time (PDT)	Burn Description	Top of Plume AGL (m)
15:17	Burn Started	
15:19		91
15:19		244
15:23		951
15:26		951
15:34		152
15:36		457
15:37		555
15:38		555
15:40		860
15:41		1012
15:42		1165
15:49		860
15:50		1012
15:51		1256
15:52		1622
15:53		1622
15:54		1774
15:56		1927
16:08		1988
16:09		2170
16:09		2262
16:12		2384
16:15		2689
16:16		2811
16:18	Burn Finished	
Average Elevation Of Field 3 = 969 meters ASL		

Table A.8: 8/20/04, Field 3 - Top of Plume Heights From Surface

Time (PDT)	Burn Description	Top of Plume AGL (m)
15:17	Burn Start	
16:04		387
16:05		709
16:05		771
16:06		1029
16:08		1580
16:15		2404
16:18	Burn Finish	
Distance Between Field Center And Ground-crew = 1300 m		

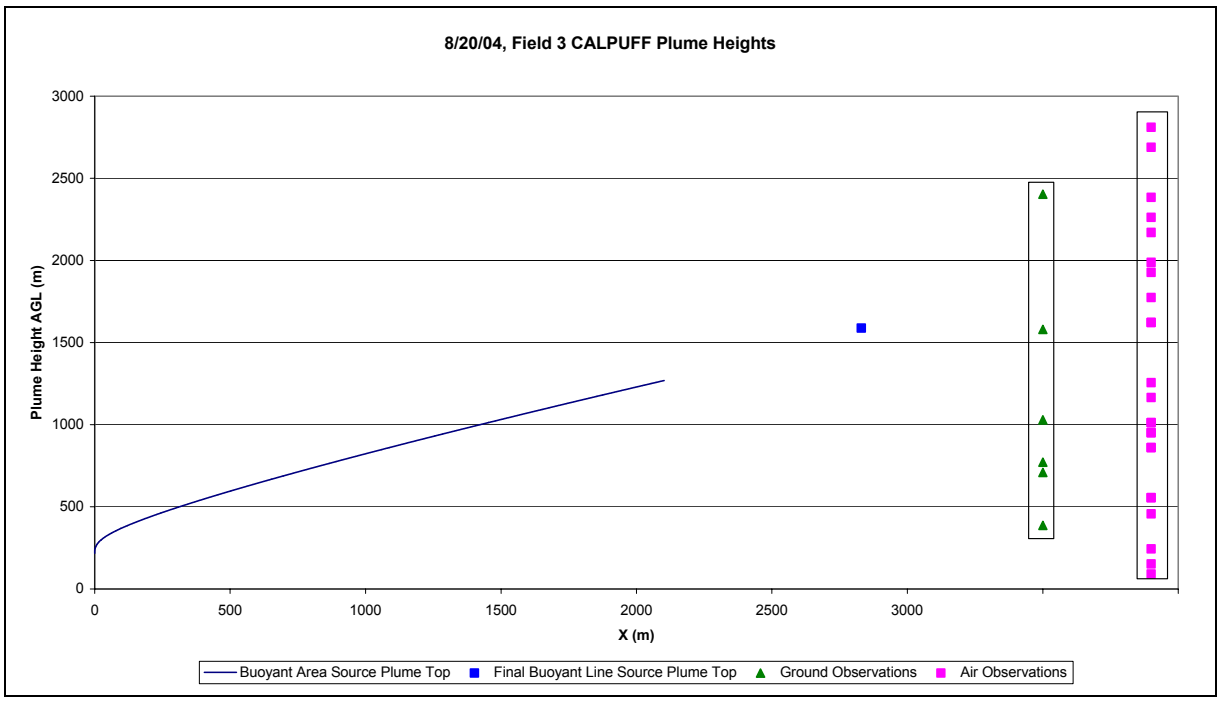

Figure A.5: CALPUFF plume heights versus downwind distance (X) and the ranges of air and ground observations are displayed in the boxes on the right side of the graph.

Case Study 6 (September 8, 2004 – Field 1)

Table A.9: 9/8/04, Field 1 - Top of Plume Heights From Plane

Time (PDT)	Burn Description	Top of Plume AGL (m)
12:05	Burn start, southern edge	128
12:06		189
12:07		280
12:08		280
12:09		280
12:11		280
12:12		280
12:15		402
12:19		402
12:19		402
12:20		402
12:21		463
12:21		494
12:24		615
12:26		707
12:28		737
12:31		798
12:33		890
12:34		1042
12:34		1195
12:36		1286
12:39		1347
12:41		1438
12:43		1438
12:45		1438
12:47		1438
12:52		1377
13:02		1347
13:03		1347
13:09	Burn Finished	
Average Elevation Of Field 1 = 939 meters ASL		

Table A.10: 9/8/04, Field 1 - Top of Plume Heights From Surface

Time (PDT)	Burn Description	Top of Plume AGL (m)
12:05	Burn start, southern edge	
12:19		447
12:23		804
12:30		614
12:33		759
12:35		946
12:40		1006
12:44		1006
12:46		896
12:50		2606
12:57		2606
13:06		782
13:09	Burn Finish	
Distance Between Field Center And Ground-crew = 1120 m		

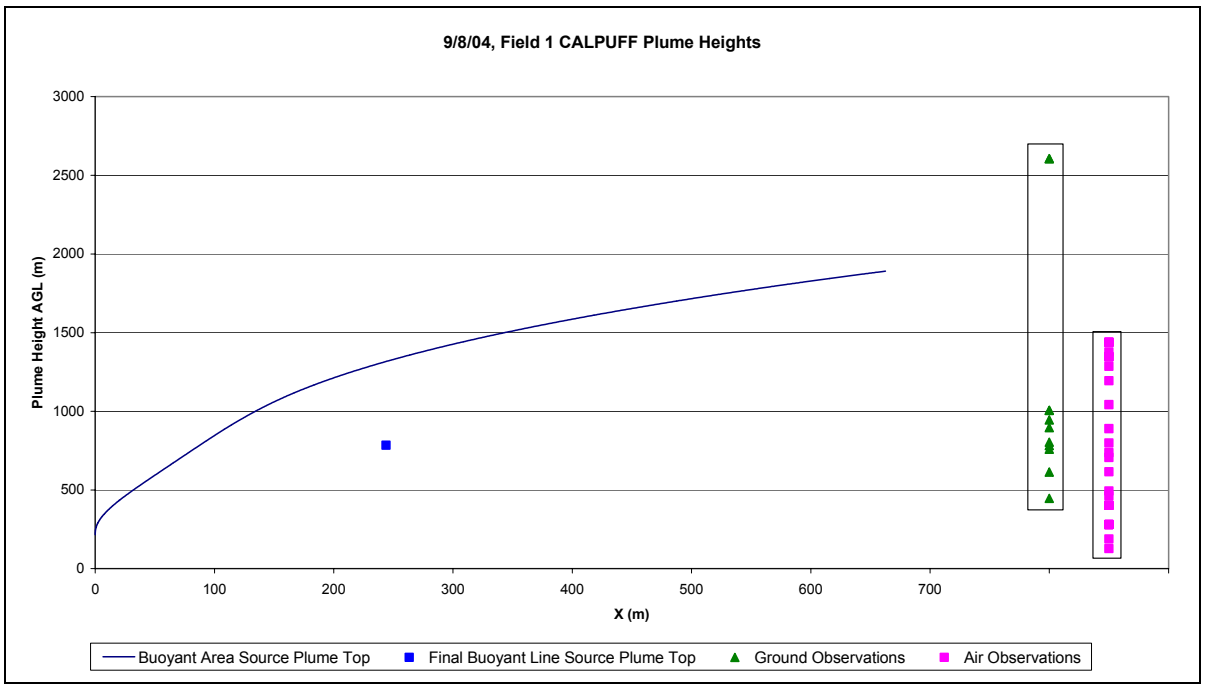

Figure A.6: CALPUFF plume heights versus downwind distance (X) and the ranges of air and ground observations are displayed in the boxes on the right side of the graph.

Case Study 7 (September 8, 2004 – Field 2)

Table A.11: 9/8/04, Field 2 - Top of Plume Heights From Plane

Time (PDT)	Burn Description	Top of Plume AGL (m)
13:50	Burn started, west edge	
13:58		177
14:00		177
14:01		207
14:03		238
14:07		603
14:09		695
14:12		725
14:14		725
14:18		512
14:19		512
14:25		512
14:27		664
14:28		664
14:30		695
14:32		756
14:33		817
14:33		908
14:34		908
14:38		1152
14:41		1304
14:45		1304
14:48	Plume settled into canyon	
15:09	No plume, data collection finished	
Average Elevation Of Field 2 = 1012 meters ASL		

Table A.12: 9/8/04, Field 2 - Top of Plume Heights From Surface

Time (PDT)	Burn Description	Top of Plume AGL (m)
13:50	Burn started, west edge	
14:22		243
14:25		390
14:29		405
14:33		454
14:35		439
14:37		472
14:40		343
14:45		325
14:50		343
14:54		260
14:57		293
14:48	Plume settled into canyon	
15:09	No plume, data collection finished	
Distance Between Field Center And Ground-crew = 1630 m		

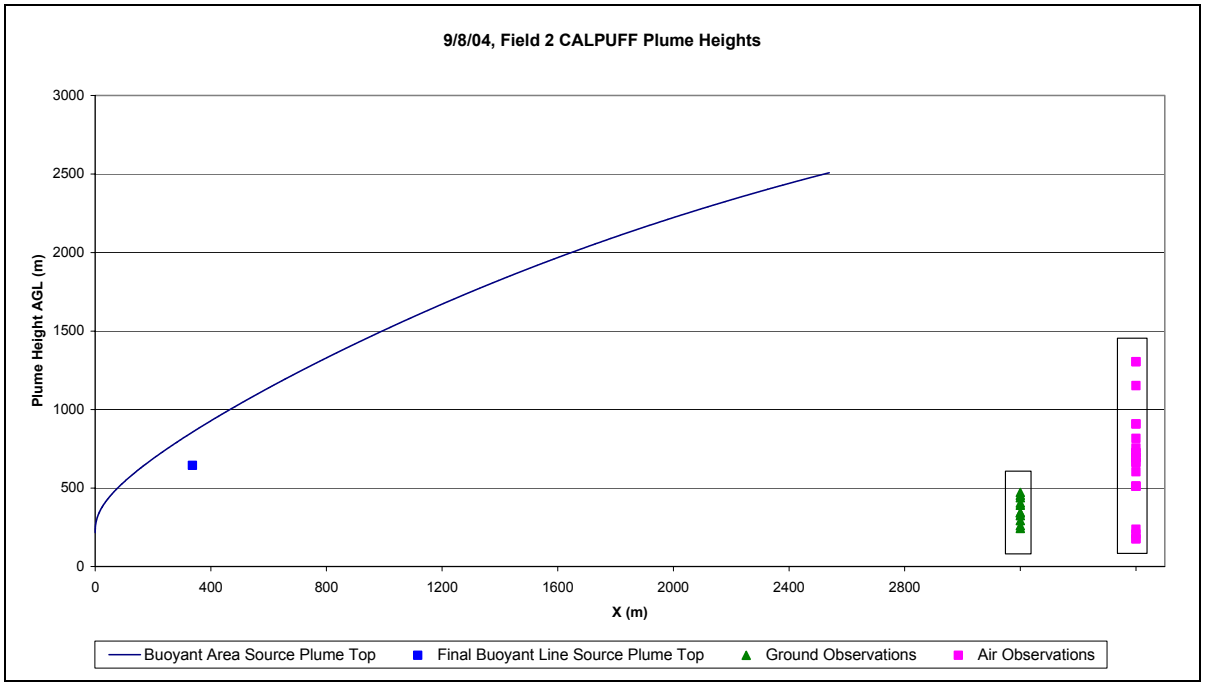

Figure A.7: CALPUFF plume heights versus downwind distance (X) and the ranges of air and ground observations are displayed in the boxes on the right side of the graph.

Case Study 8 (September 29, 2004 – Field 1)

Table A.13: 9/29/04, Field 1 - Top of Plume Heights From Plane

Time (PDT)	Burn Description	Top of Plume AGL (m)
11:54	Burn start, northern edge	
12:20		320
12:21		320
12:22		381
12:25		503
12:26		655
12:30	1/3 of field ignited	655
12:36		1082
12:38		1234
12:39		1387
12:40	Another 1/3 of field ignited	
12:46	Last 1/3 of field ignited	
12:54	Burn Finished	
Average Elevation Of Field 1 = 655 meters ASL		

Table A.14: 9/29/04, Field 1 - Top of Plume Heights From Surface

Time (PDT)	Burn Description	Top of Plume AGL (m)
11:54	Burn start, northern edge	
12:18		148
12:21		171
12:25		191
12:28		218
12:30	1/3 of field ignited	
12:33		372
12:37		237
12:41	Another 1/3 of field ignited	368
12:42		439
12:43	Last 1/3 of field ignited	494
12:49		774
12:52		386
12:54	Burn Finished	
Distance Between Field Center And Ground-crew = 590 m		

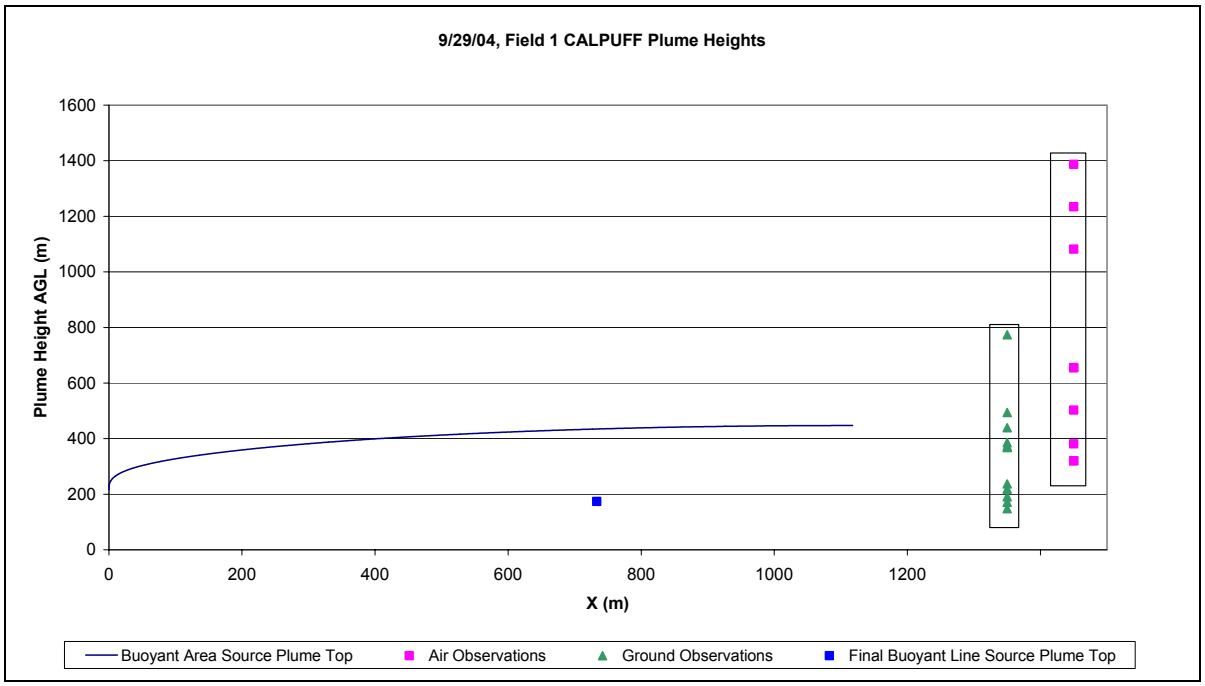

Figure A.8: CALPUFF plume heights versus downwind distance (X) and the ranges of air and ground observations are displayed in the boxes on the right side of the graph.

Case Study 9 (September 29, 2004 – Field 2)

Table A.15: 9/29/04, Field 2 - Top of Plume Heights From Plane

Time (PDT)	Burn Description	Top of Plume AGL (m)
14:53	Burn Start, eastern edge	
15:11		229
15:15		321
15:19		626
15:21	Southern edge ignited	
15:23		1113
15:25		1205
15:27		1449
15:27		1601
15:29		1814
15:29		1906
15:31		2058
15:37		1784
15:43		1540
15:50		1692
15:52	Burn Finished	
Average Elevation Of Field 2 = 685 meters ASL		

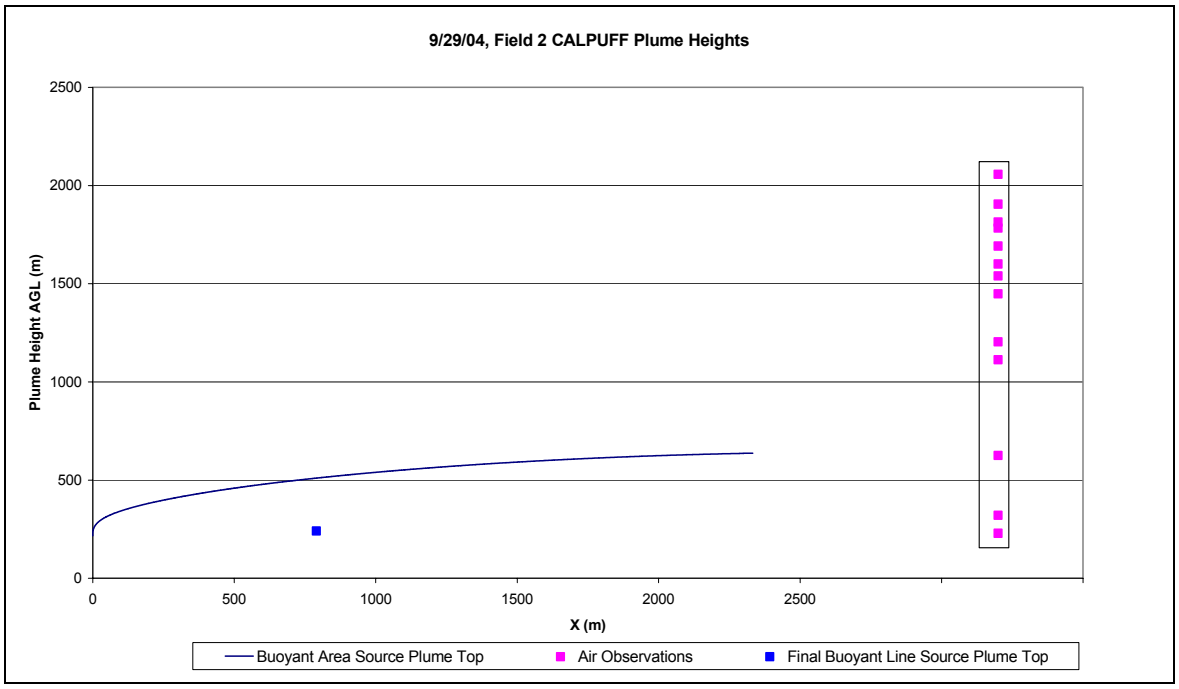

Figure A.9: CALPUFF plume heights versus downwind distance (X) and the range of air observations are displayed in a box on the right side of the graph.

APPENDIX B

Ensemble Meteorology and Ensemble $PM_{2.5}$ Forecasts for August 17, 2004

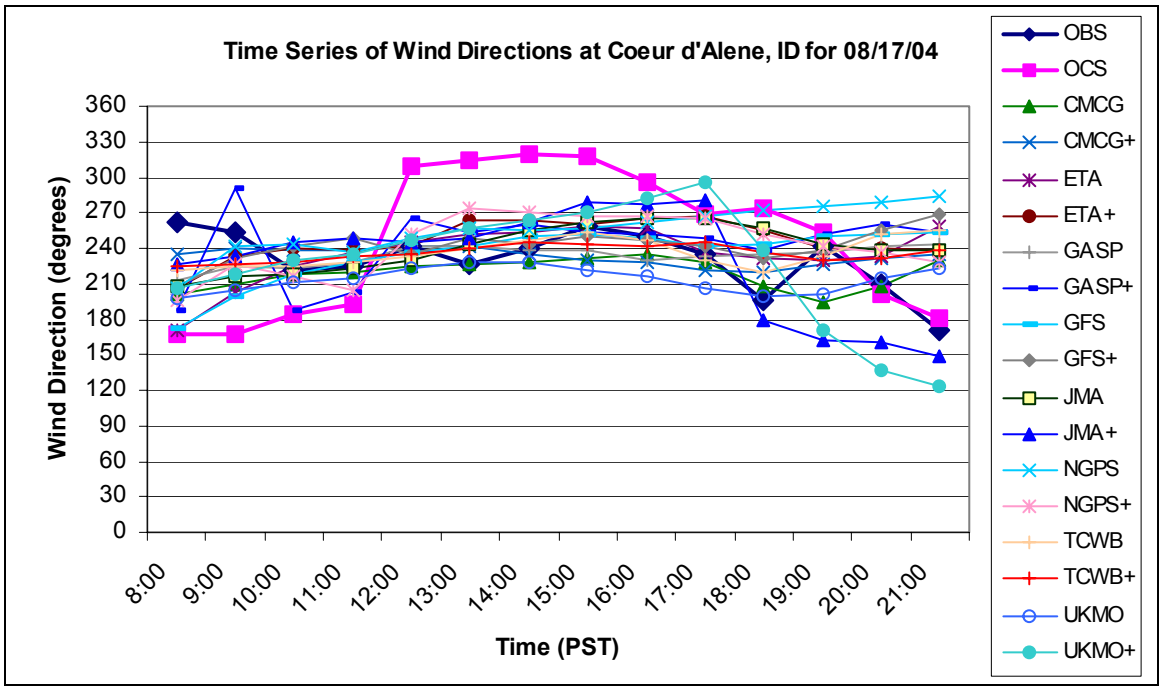

Figure B.1: Time series of wind directions at Coeur d'Alene, ID monitoring site for August 17, 2004. Observations (OBS) and original ClearSky (OCS) are shown with the 16 ensemble ClearSky members.

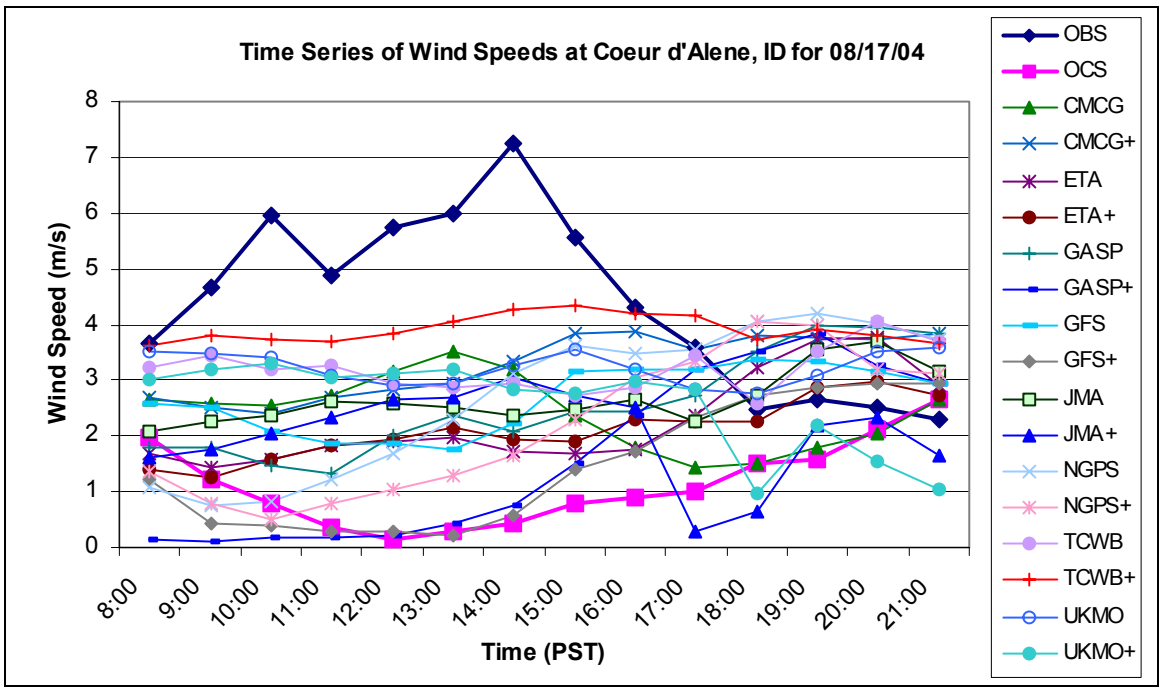

Figure B.2: Time series of wind speeds at Coeur d'Alene, ID for August 17, 2004. Observations (OBS) and original ClearSky (OCS) are shown with the 16 ensemble ClearSky members.

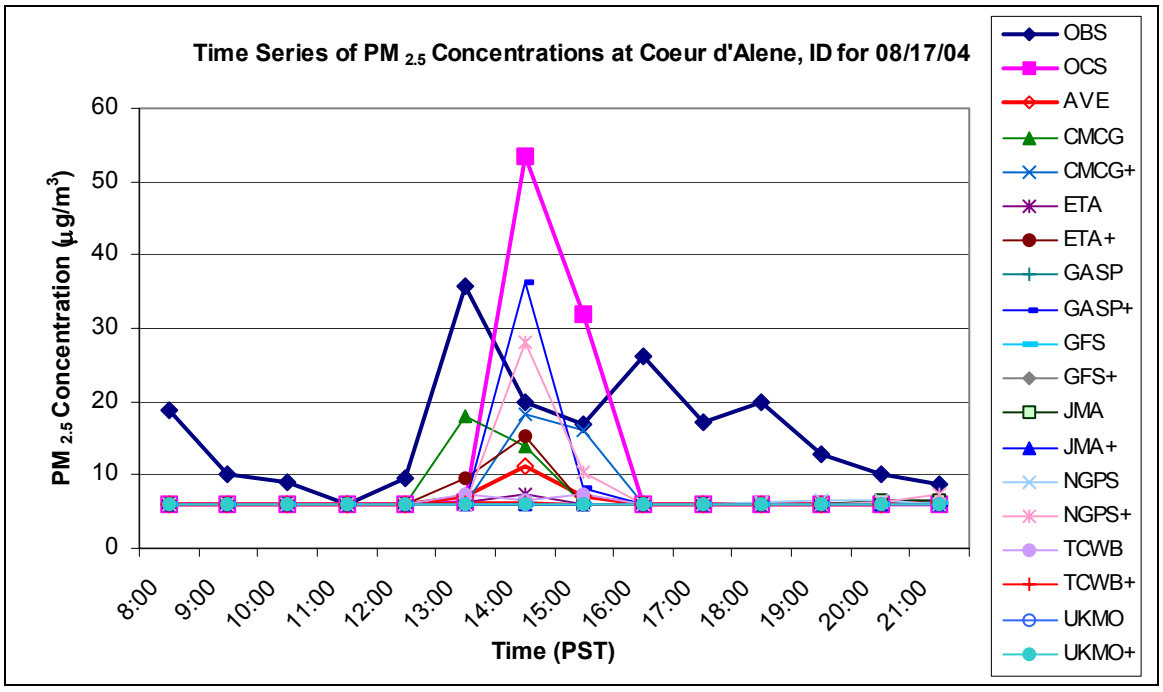

Figure B.3: Time series of ensemble $PM_{2.5}$ concentrations at Coeur d'Alene, ID monitoring site for August 17, 2004. Observations (OBS), original ClearSky (OCS), and ensemble average (AVE) are shown with the 16 ensemble ClearSky members.

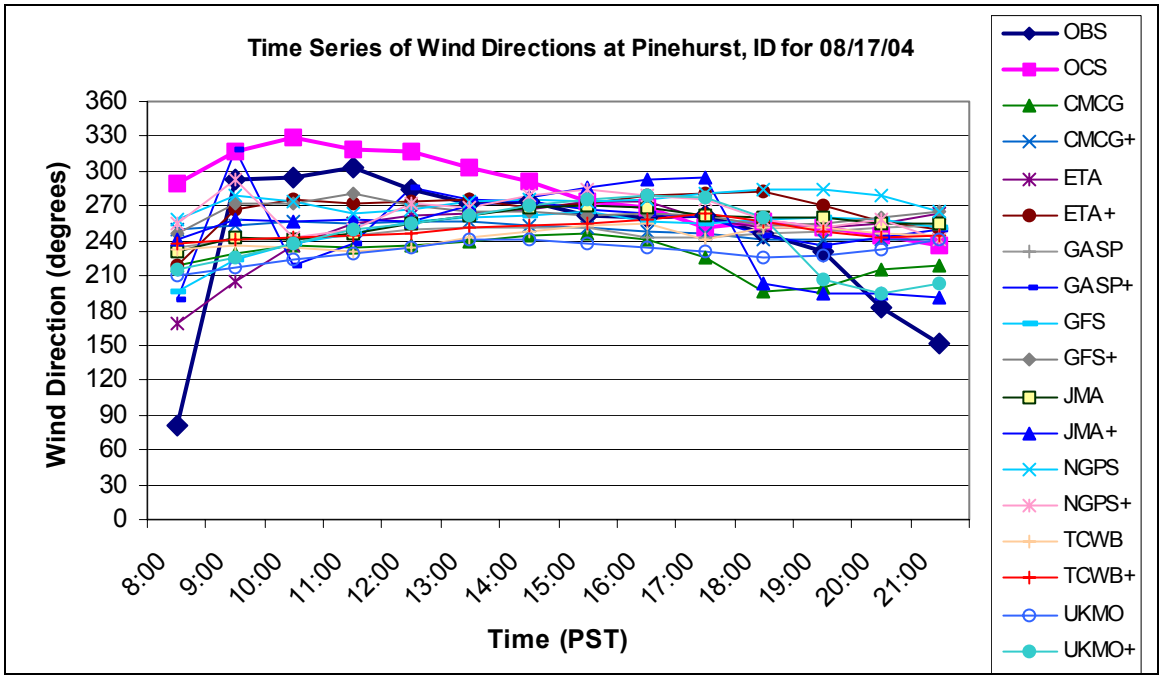

Figure B.4: Time series of wind directions at Pinehurst, ID monitoring site for August 17, 2004. Observations (OBS) and original ClearSky (OCS) are shown with the 16 ensemble ClearSky members.

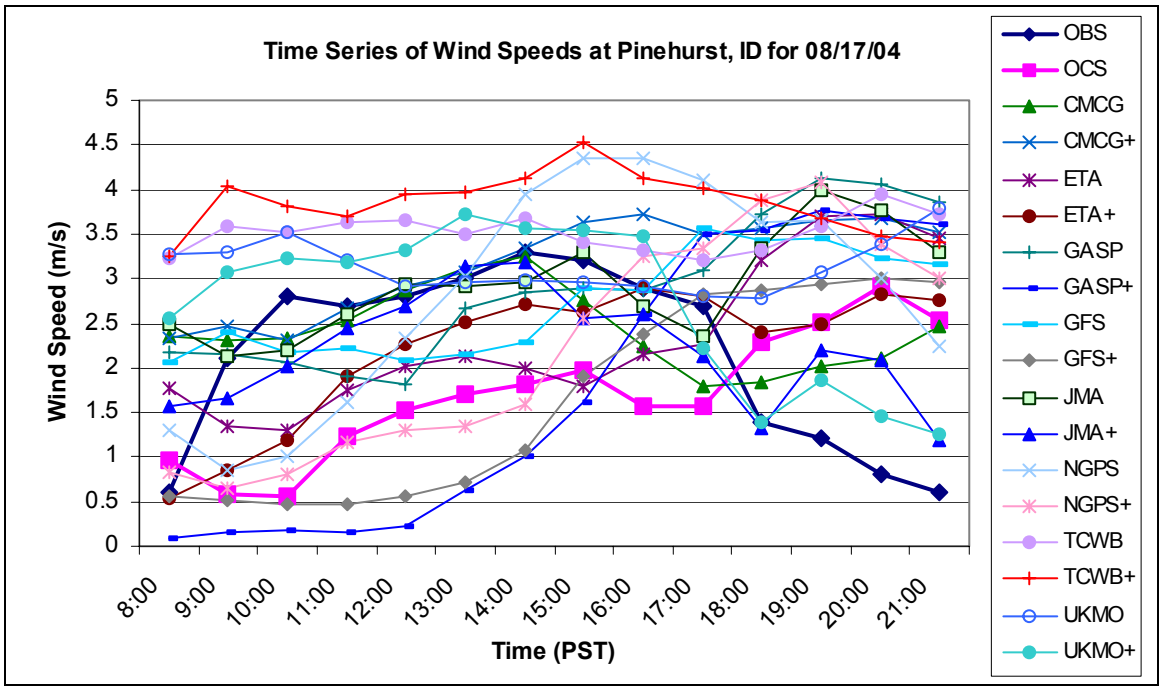

Figure B.5: Time series of wind speeds at Pinehurst, ID for August 17, 2004. Observations (OBS) and original ClearSky (OCS) are shown with the 16 ensemble ClearSky members.

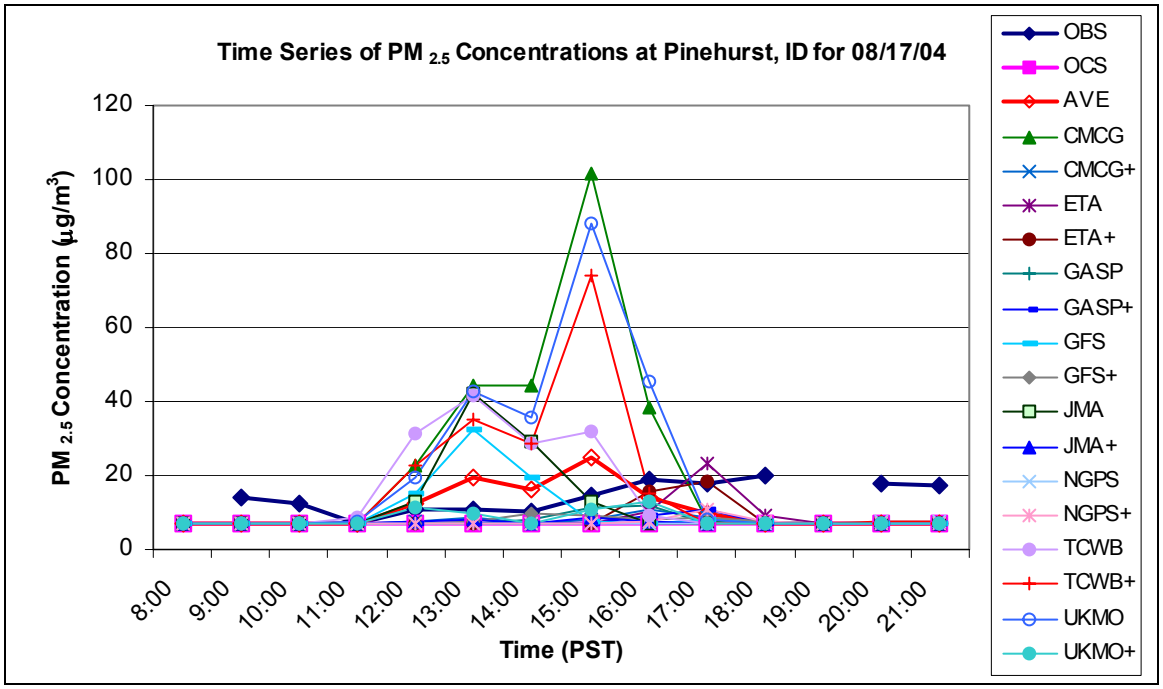

Figure B.6: Time series of ensemble $PM_{2.5}$ concentrations at Pinehurst, ID monitoring site for August 17, 2004. Observations (OBS), original ClearSky (OCS), and ensemble average (AVE) are shown with the 16 ensemble ClearSky members.

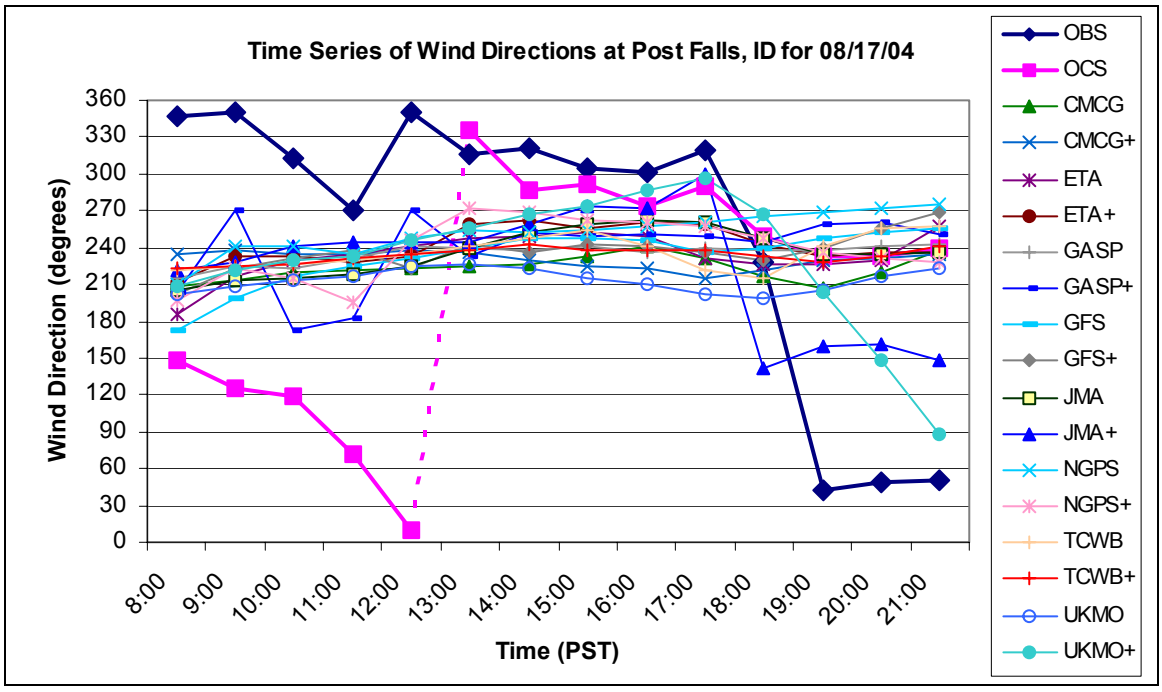

Figure B.7: Time series of wind directions at Post Falls, ID monitoring site for August 17, 2004. Observations (OBS) and original ClearSky (OCS) are shown with the 16 ensemble ClearSky members. Dashed lines represent a shift from 0 to 360 degrees.

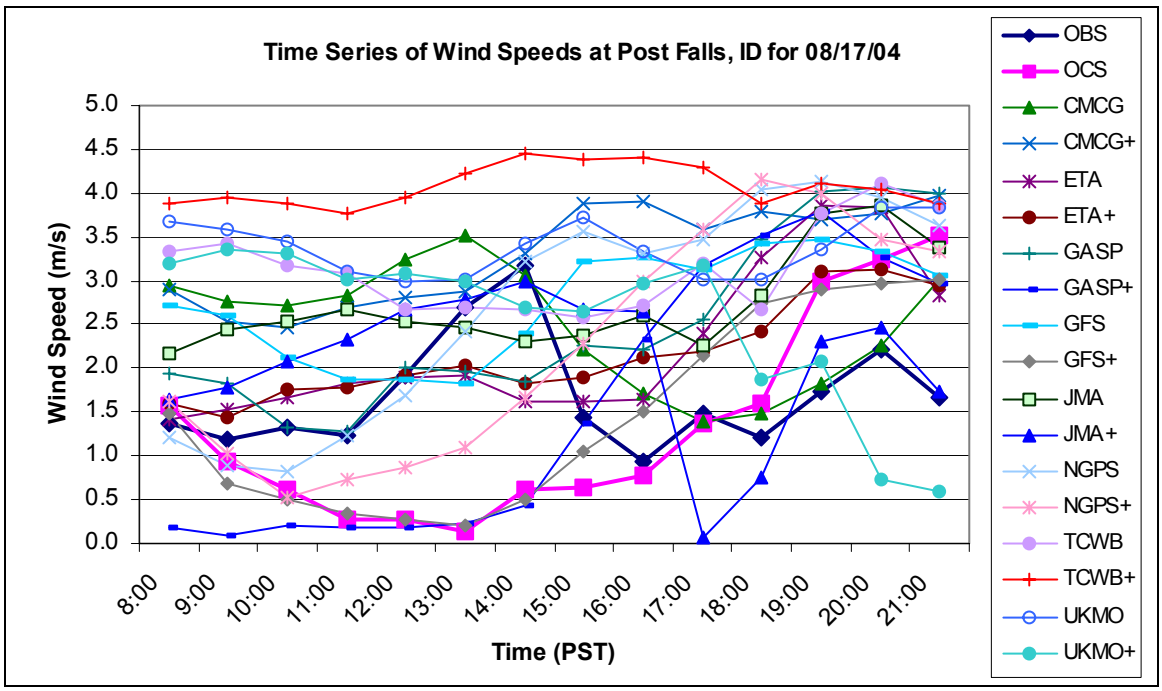

Figure B.8: Time series of wind speeds at Post Falls, ID for August 17, 2004. Observations (OBS) and original ClearSky (OCS) are shown with the 16 ensemble ClearSky members.

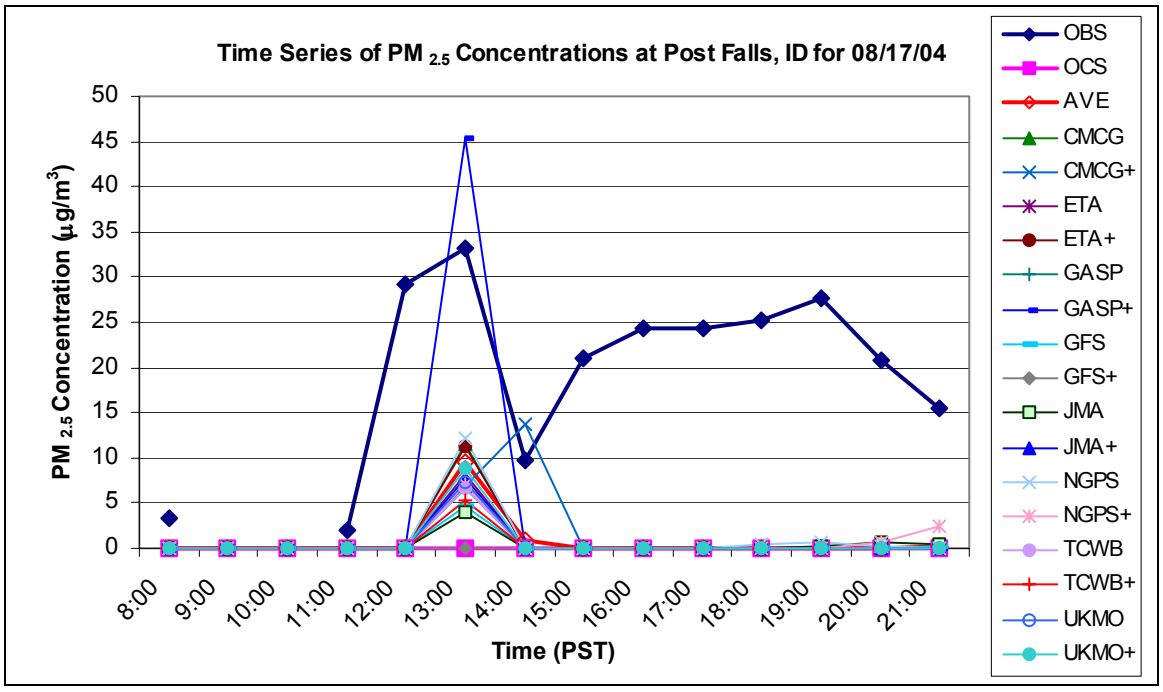

Figure B.9: Time series of ensemble $PM_{2.5}$ concentrations at Post Falls, ID monitoring site for August 17, 2004. Observations (OBS), original ClearSky (OCS), and ensemble average (AVE) are shown with the 16 ensemble ClearSky members.

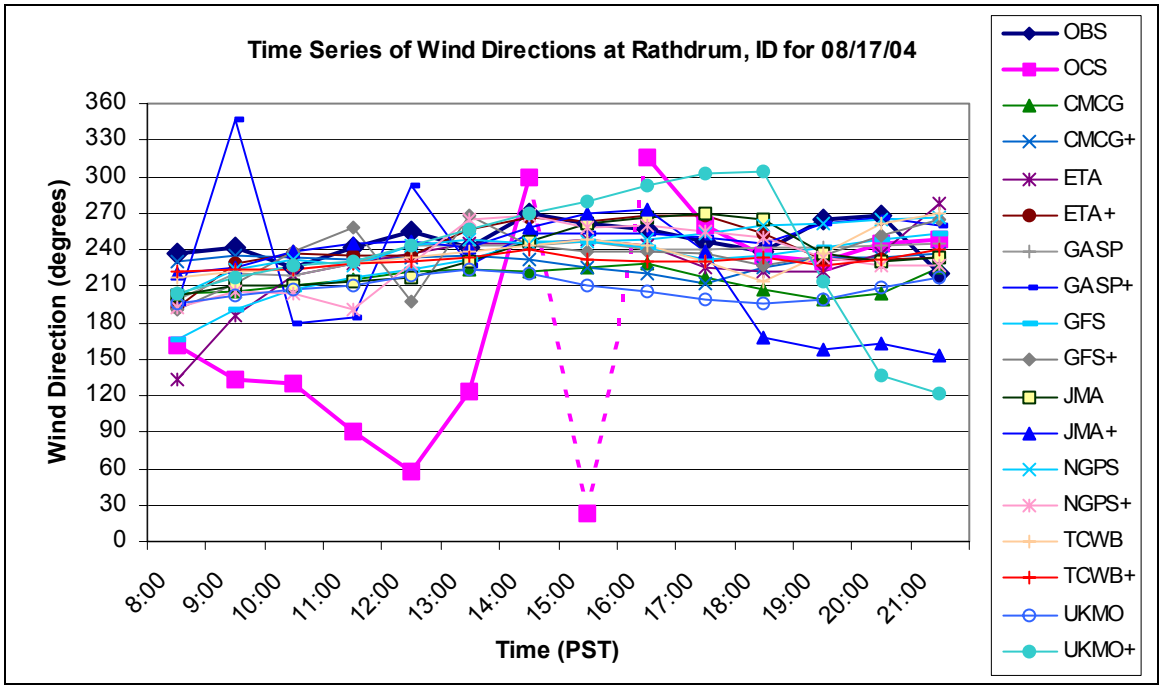

Figure B.10: Time series of wind directions at Rathdrum, ID monitoring site for August 17, 2004. Observations (OBS) and original ClearSky (OCS) are shown with the 16 ensemble ClearSky members. Dashed lines represent a shift from 0 to 360 degrees.

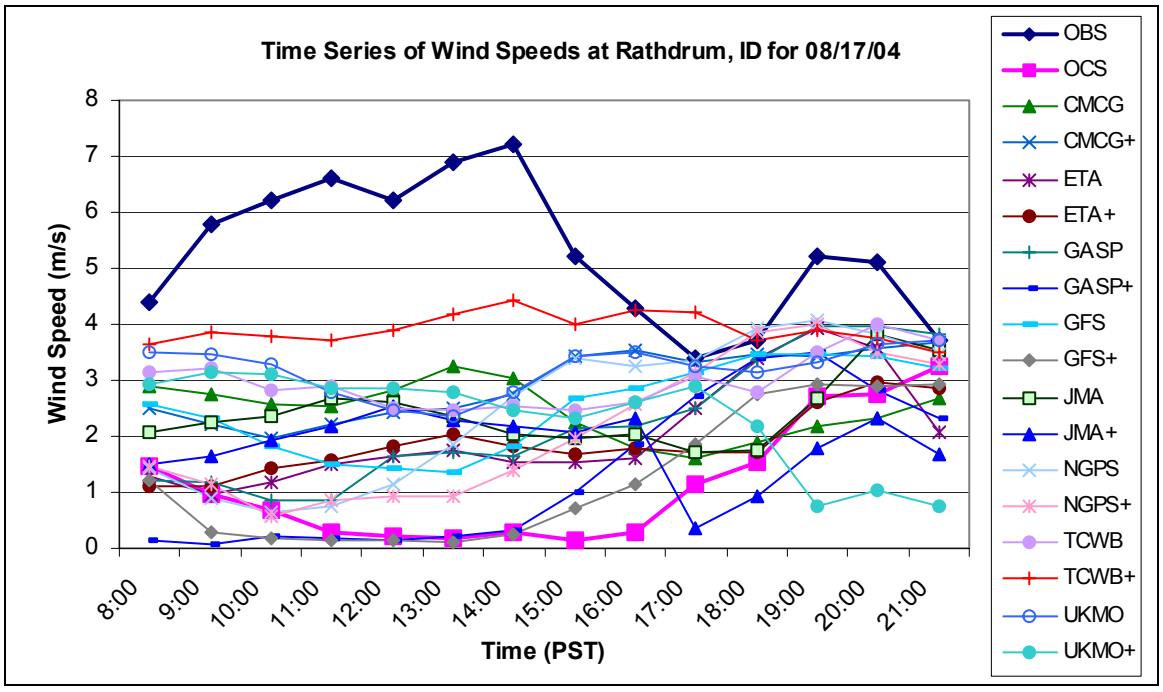

Figure B.11: Time series of wind speeds at Rathdrum, ID for August 17, 2004. Observations (OBS) and original ClearSky (OCS) are shown with the 16 ensemble ClearSky members.

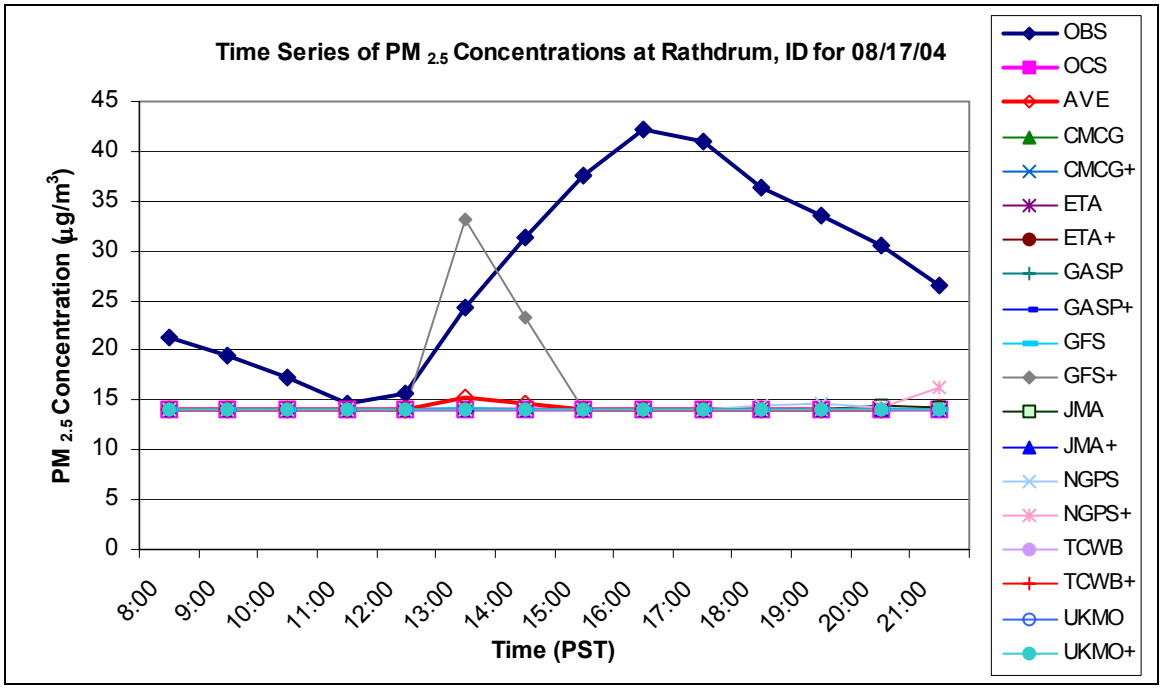

Figure B.12: Time series of ensemble $PM_{2.5}$ concentrations at Rathdrum, ID monitoring site for August 17, 2004. Observations (OBS), original ClearSky (OCS), and ensemble average (AVE) are shown with the 16 ensemble ClearSky members.

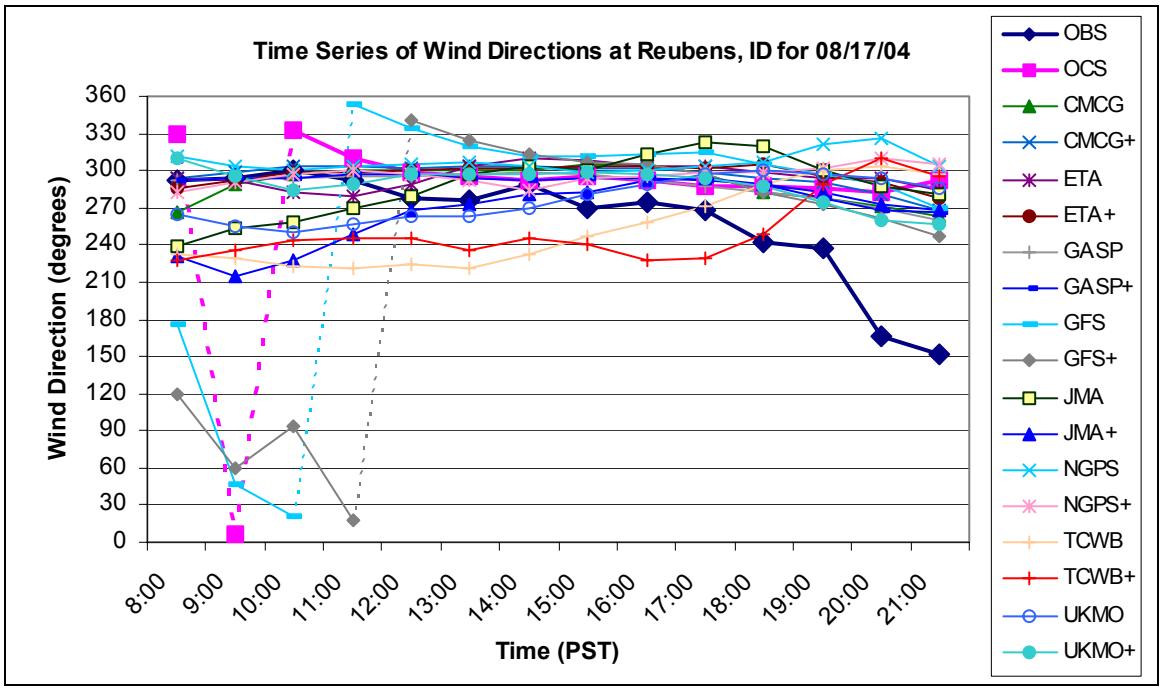

Figure B.13: Time series of wind directions at Reubens, ID monitoring site for August 17, 2004. Observations (OBS) and original ClearSky (OCS) are shown with the 16 ensemble ClearSky members. Dashed lines represent a shift from 0 to 360 degrees.

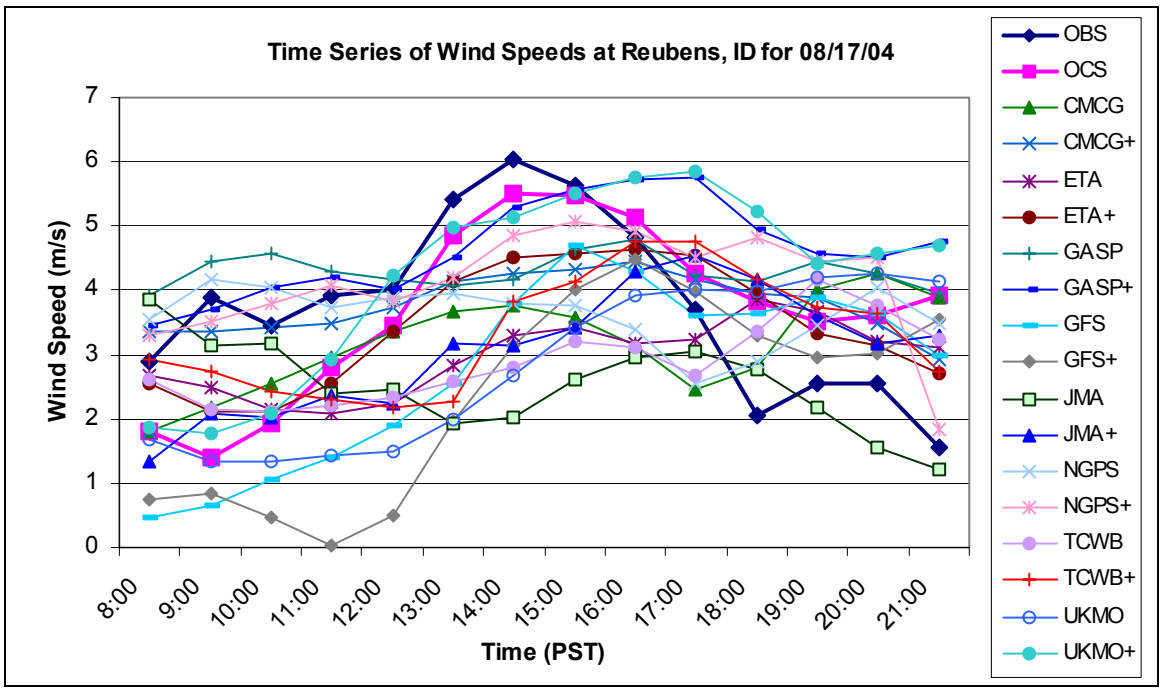

Figure B.14: Time series of wind speeds at Reubens, ID for August 17, 2004. Observations (OBS) and original ClearSky (OCS) are shown with the 16 ensemble ClearSky members.

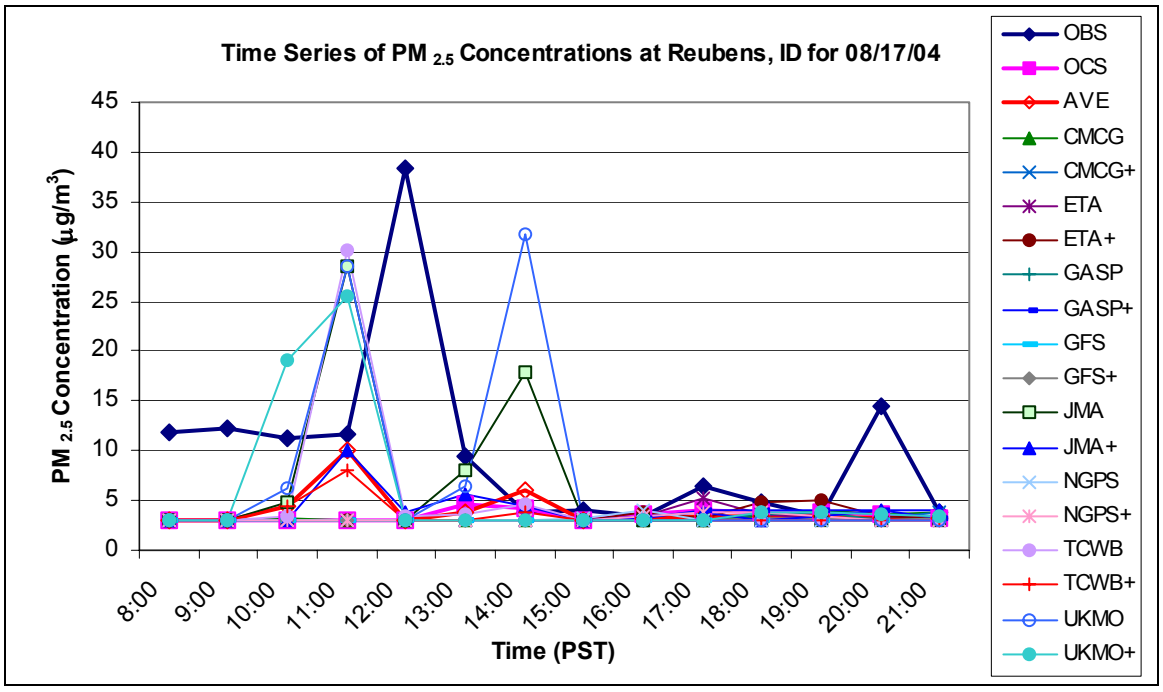

Figure B.15: Time series of ensemble $PM_{2.5}$ concentrations at Reubens, ID monitoring site for August 17, 2004. Observations (OBS), original ClearSky (OCS), and ensemble average (AVE) are shown with the 16 ensemble ClearSky members.

APPENDIX C

Ensemble Meteorology and Ensemble $PM_{2.5}$ Forecasts for September 8, 2004

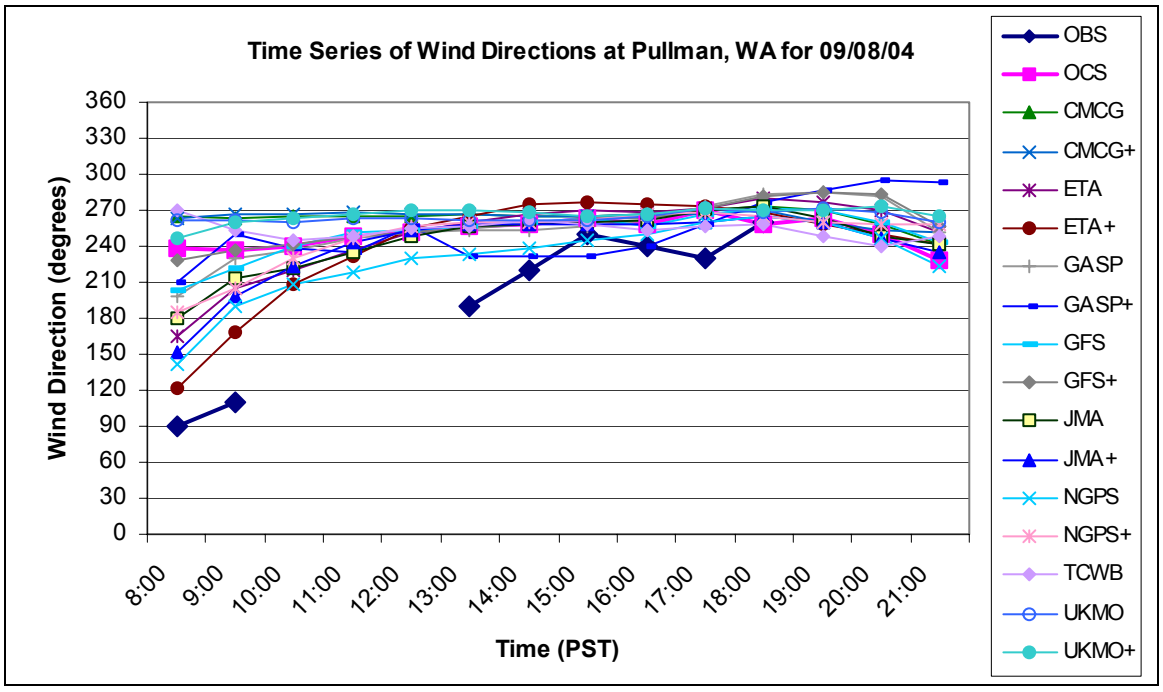

Figure C.1: Time series of wind directions at Pullman, WA monitoring site for September 8, 2004. Observations (OBS) and original ClearSky (OCS) are shown with the 15 ensemble ClearSky members.

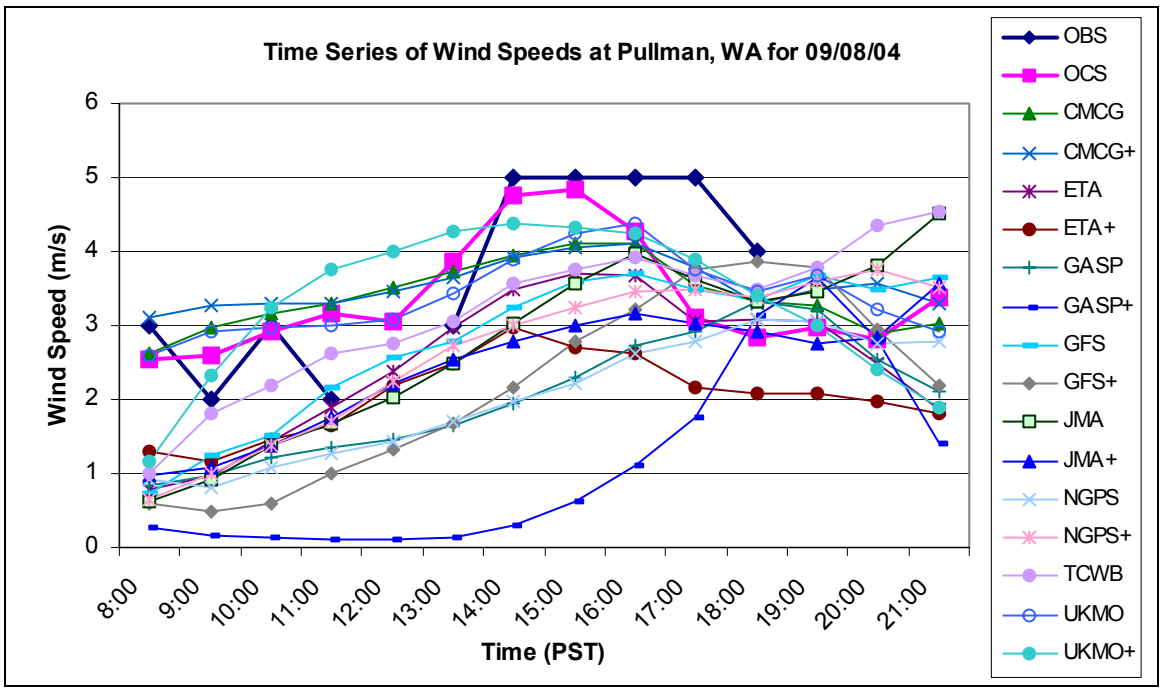

Figure C.2: Time series of wind speeds at Pullman, WA for September 8, 2004. Observations (OBS) and original ClearSky (OCS) are shown with the 15 ensemble ClearSky members.

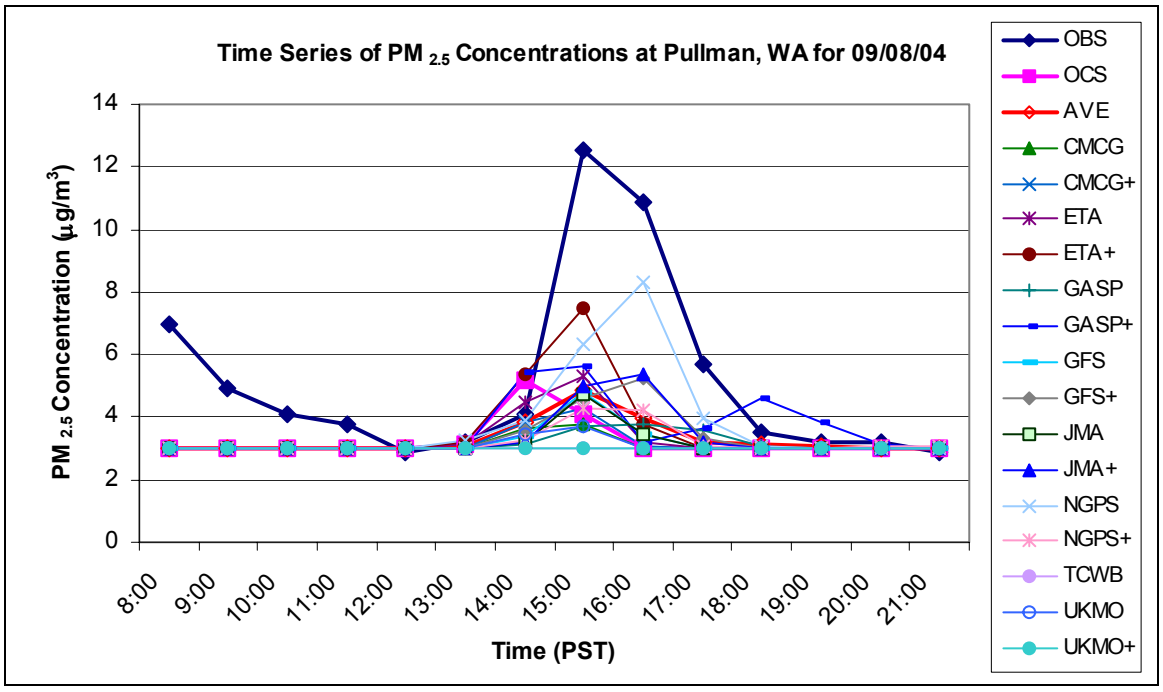

Figure C.3: Time series of ensemble $PM_{2.5}$ concentrations at Pullman, WA monitoring site for September 8, 2004. Observations (OBS), original ClearSky (OCS), and ensemble average (AVE) are shown with the 15 ensemble ClearSky members.

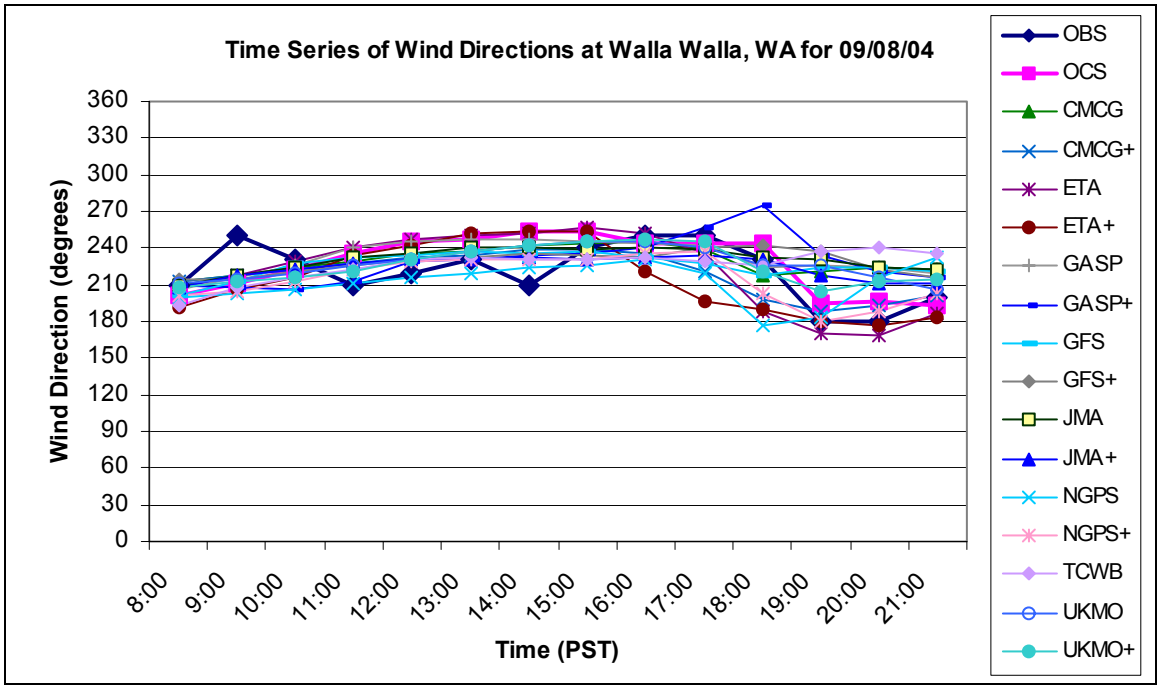

Figure C.4: Time series of wind directions at Walla Walla, WA monitoring site for September 8, 2004. Observations (OBS) and original ClearSky (OCS) are shown with the 15 ensemble ClearSky members.

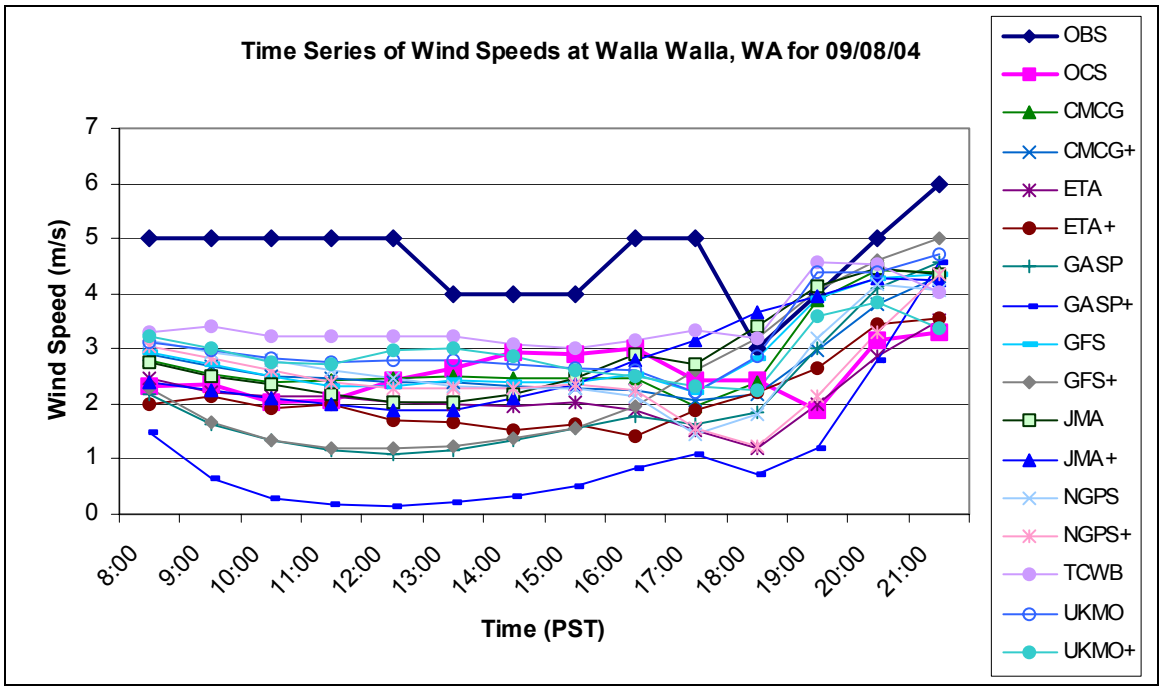

Figure C.5: Time series of wind speeds at Walla Walla, WA for September 8, 2004. Observations (OBS) and original ClearSky (OCS) are shown with the 15 ensemble ClearSky members.

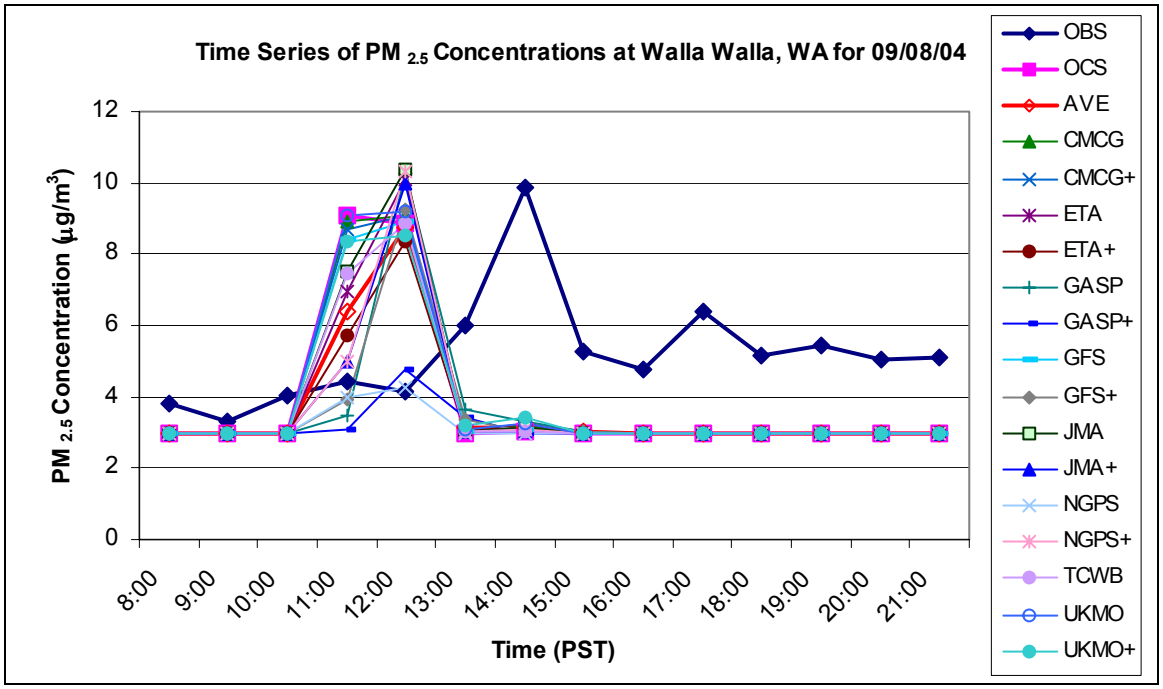

Figure C.6: Time series of ensemble $PM_{2.5}$ concentrations at Walla Walla, WA monitoring site for September 8, 2004. Observations (OBS), original ClearSky (OCS), and ensemble average (AVE) are shown with the 15 ensemble ClearSky members.

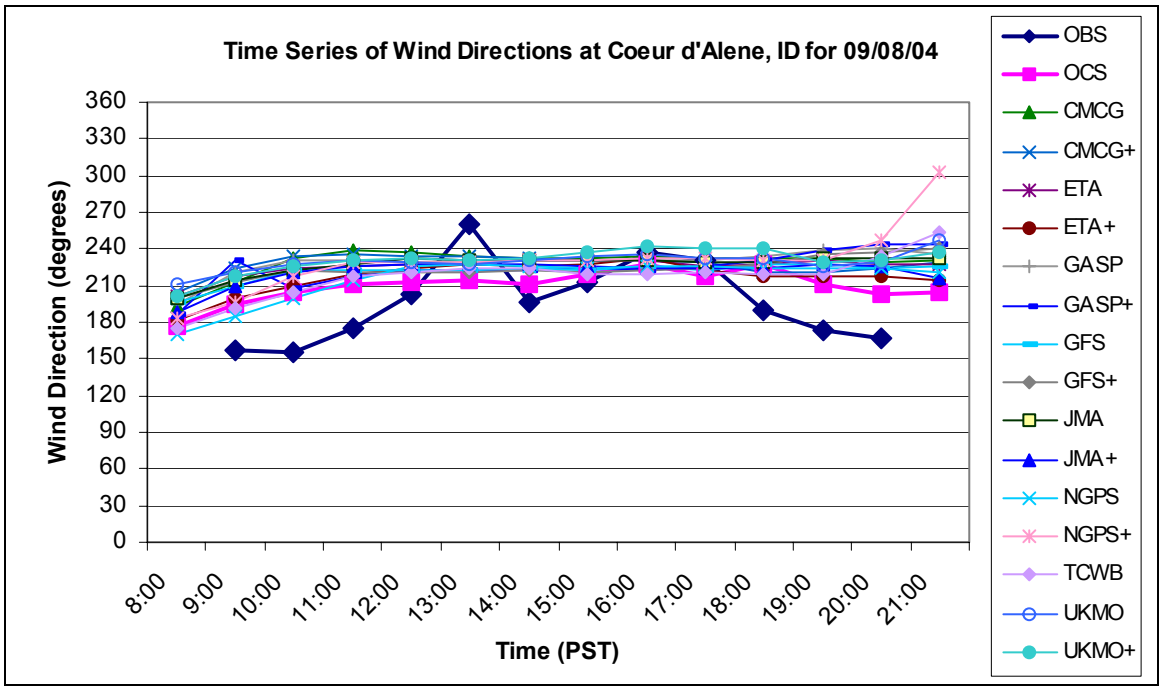

Figure C.7: Time series of wind directions at Coeur d'Alene, ID monitoring site for September 8, 2004. Observations (OBS) and original ClearSky (OCS) are shown with the 15 ensemble ClearSky members.

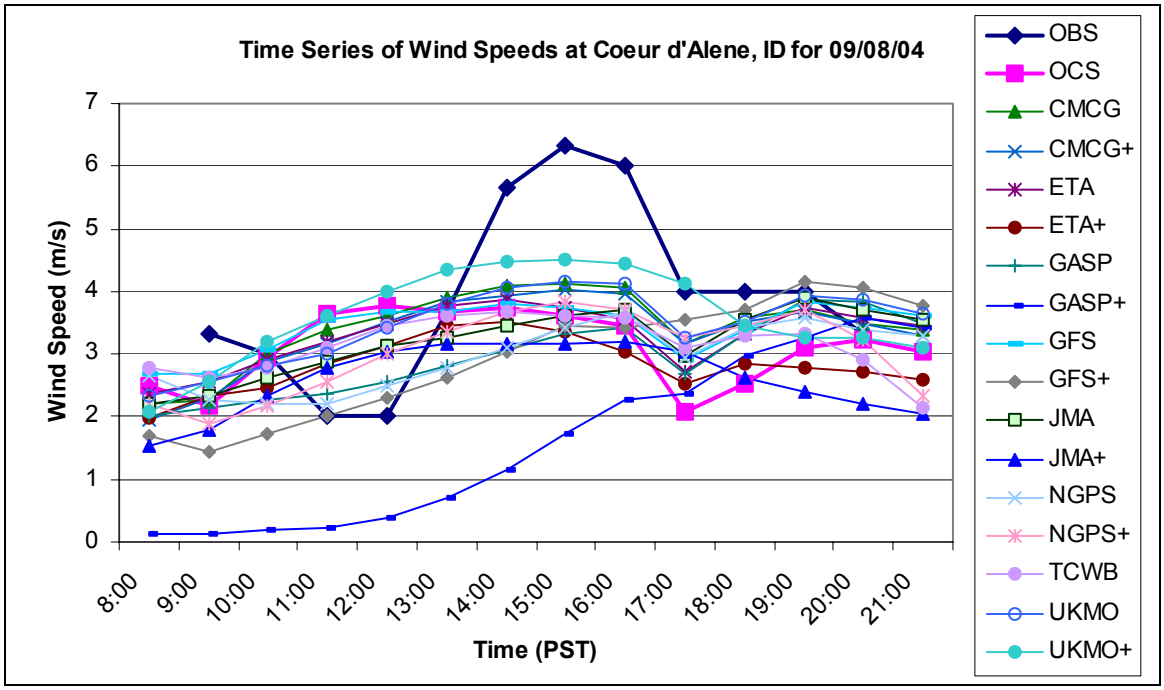

Figure C.8: Time series of wind speeds at Coeur d'Alene, ID for September 8, 2004. Observations (OBS) and original ClearSky (OCS) are shown with the 15 ensemble ClearSky members.

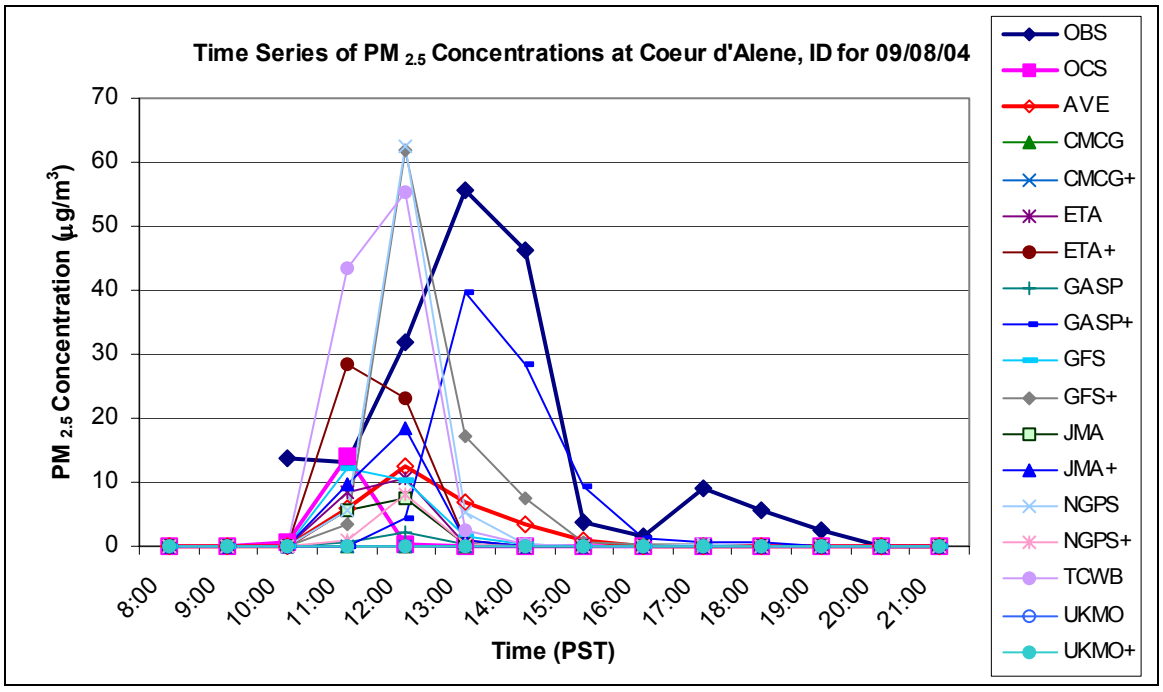

Figure C.9: Time series of ensemble $PM_{2.5}$ concentrations at Coeur d'Alene, ID monitoring site for September 8, 2004. Observations (OBS), original ClearSky (OCS), and ensemble average (AVE) are shown with the 15 ensemble ClearSky members.

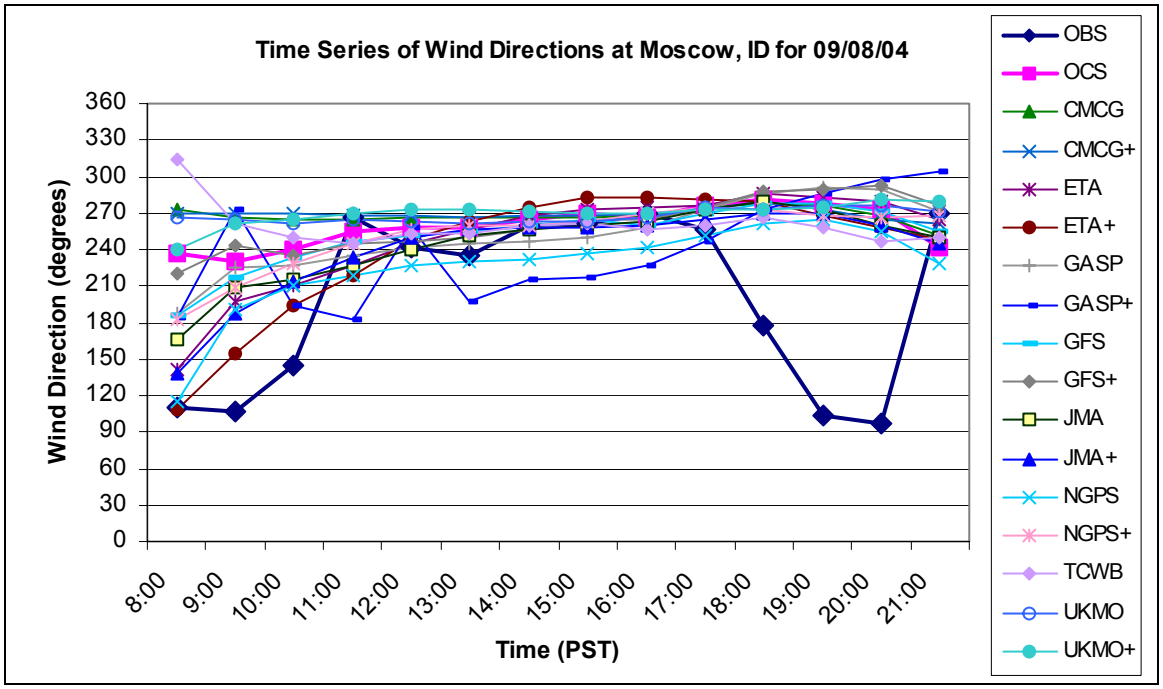

Figure C.10: Time series of wind directions at Moscow, ID monitoring site for September 8, 2004. Observations (OBS) and original ClearSky (OCS) are shown with the 15 ensemble ClearSky members.

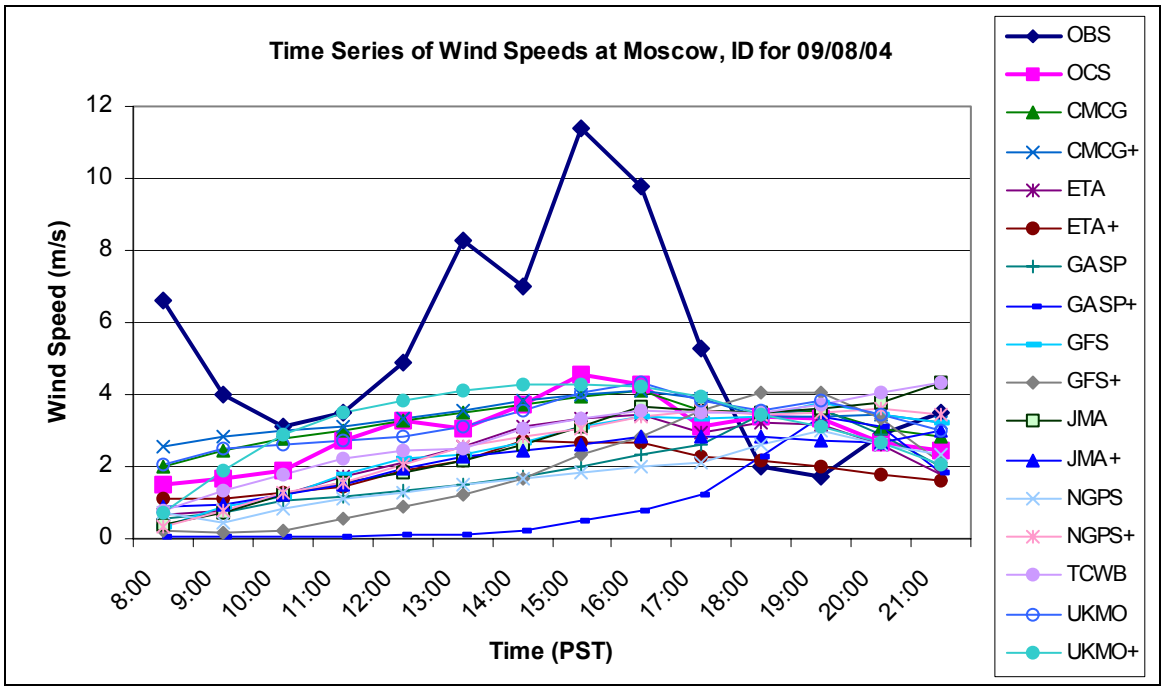

Figure C.11: Time series of wind speeds at Moscow, ID for September 8, 2004. Observations (OBS) and original ClearSky (OCS) are shown with the 15 ensemble ClearSky members.

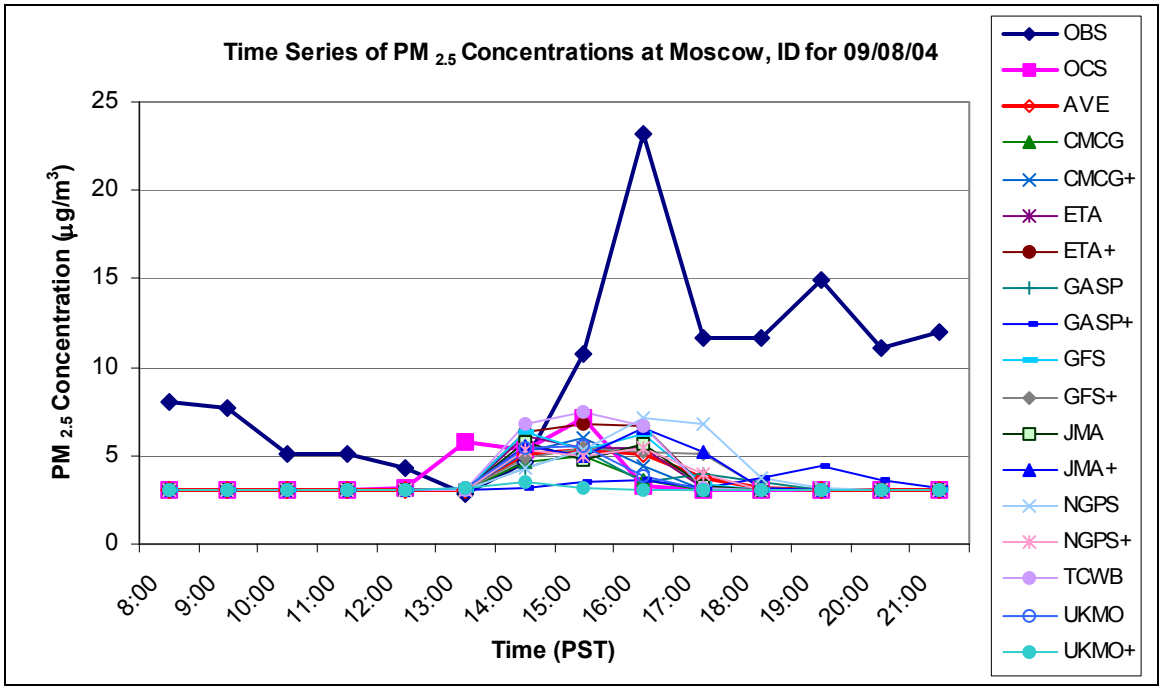

Figure C.12: Time series of ensemble $PM_{2.5}$ concentrations at Moscow, ID monitoring site for September 8, 2004. Observations (OBS), original ClearSky (OCS), and ensemble average (AVE) are shown with the 15 ensemble ClearSky members.

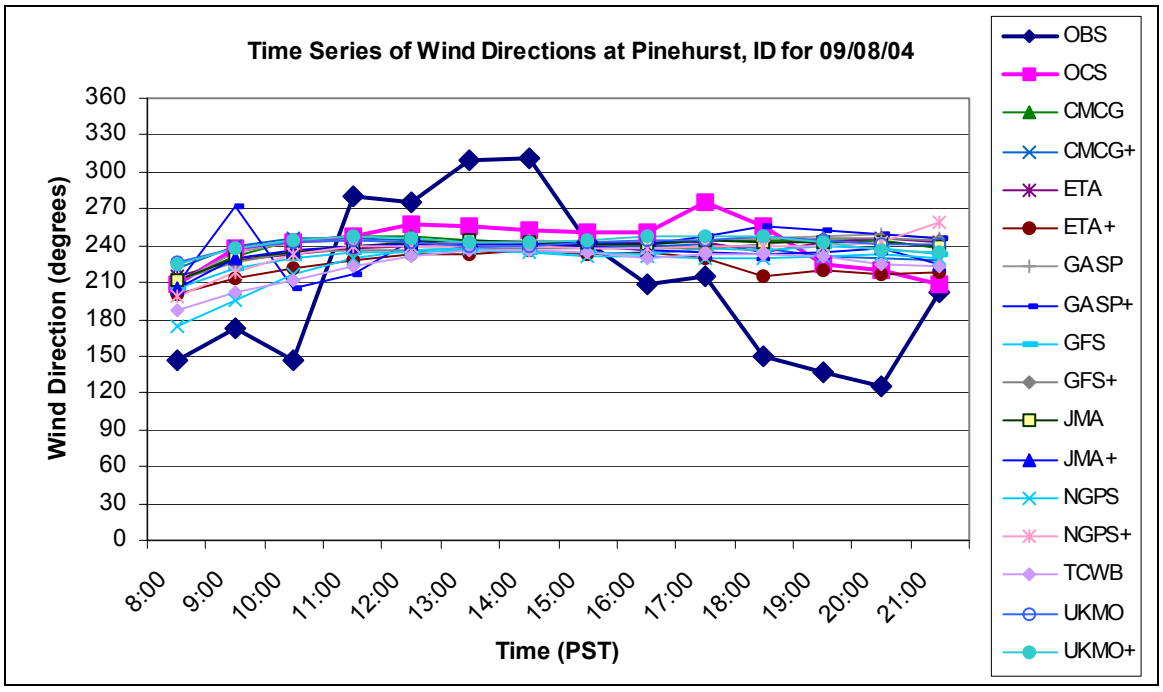

Figure C.13: Time series of wind directions at Pinehurst, ID monitoring site for September 8, 2004. Observations (OBS) and original ClearSky (OCS) are shown with the 15 ensemble ClearSky members.

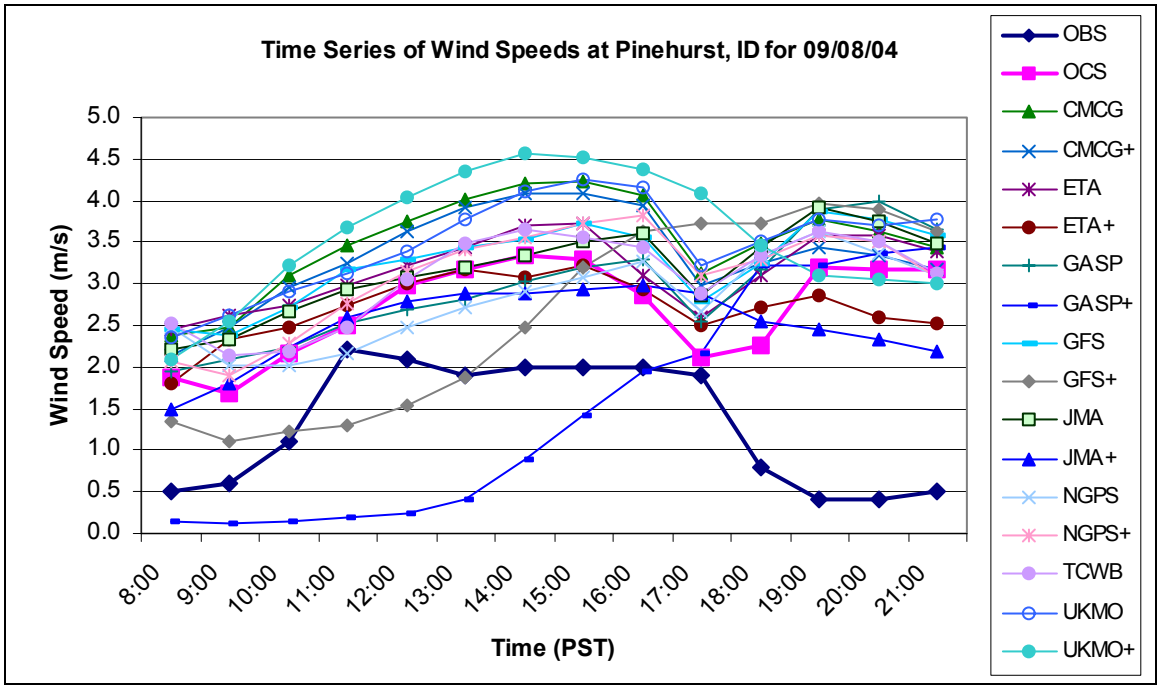

Figure C.14: Time series of wind speeds at Pinehurst, ID for September 8, 2004. Observations (OBS) and original ClearSky (OCS) are shown with the 15 ensemble ClearSky members.

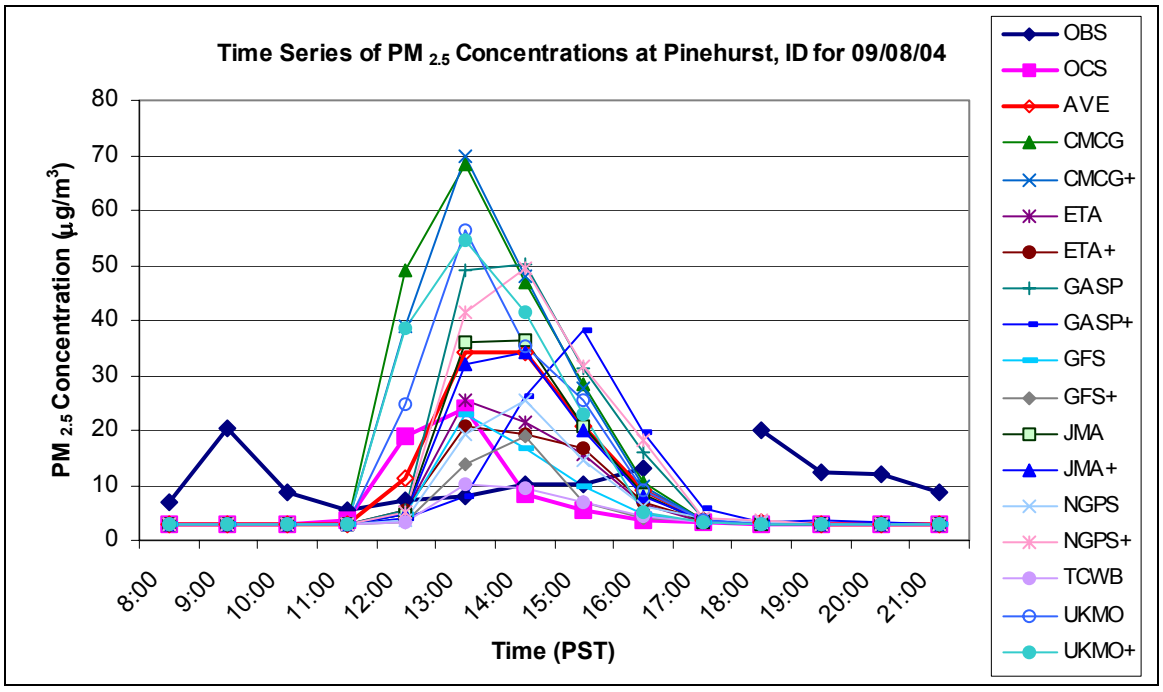

Figure C.15: Time series of ensemble $PM_{2.5}$ concentrations at Pinehurst, ID monitoring site for September 8, 2004. Observations (OBS), original ClearSky (OCS), and ensemble average (AVE) are shown with the 15 ensemble ClearSky members.

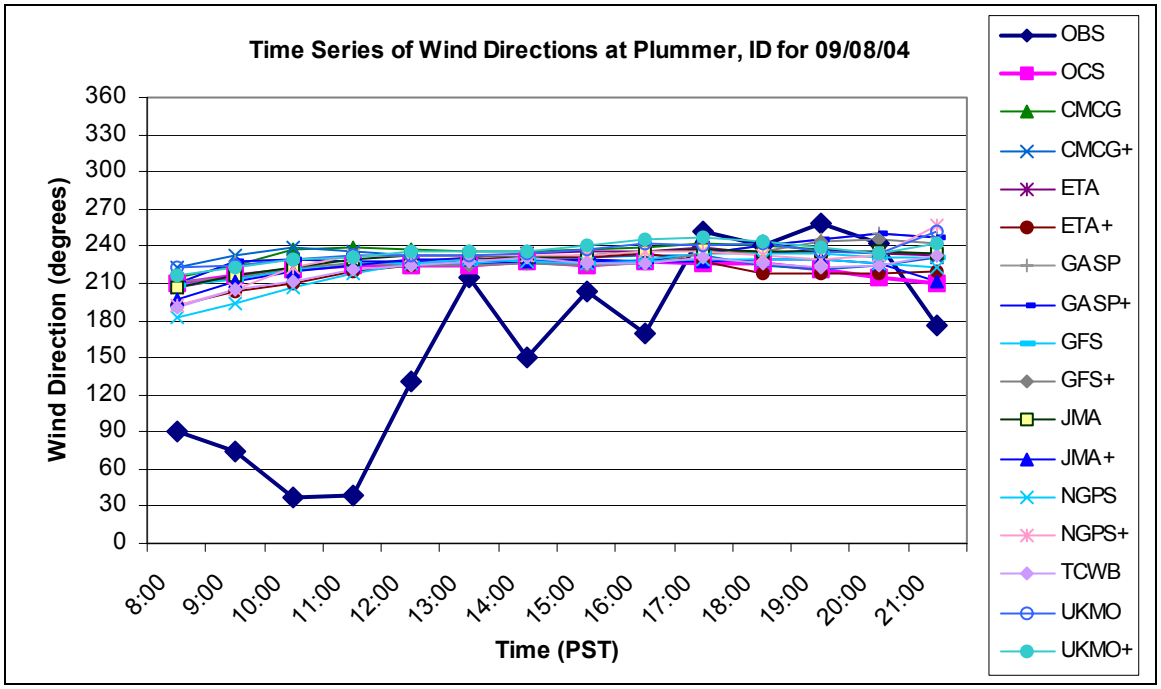

Figure C.16: Time series of wind directions at Plummer, ID monitoring site for September 8, 2004. Observations (OBS) and original ClearSky (OCS) are shown with the 15 ensemble ClearSky members.

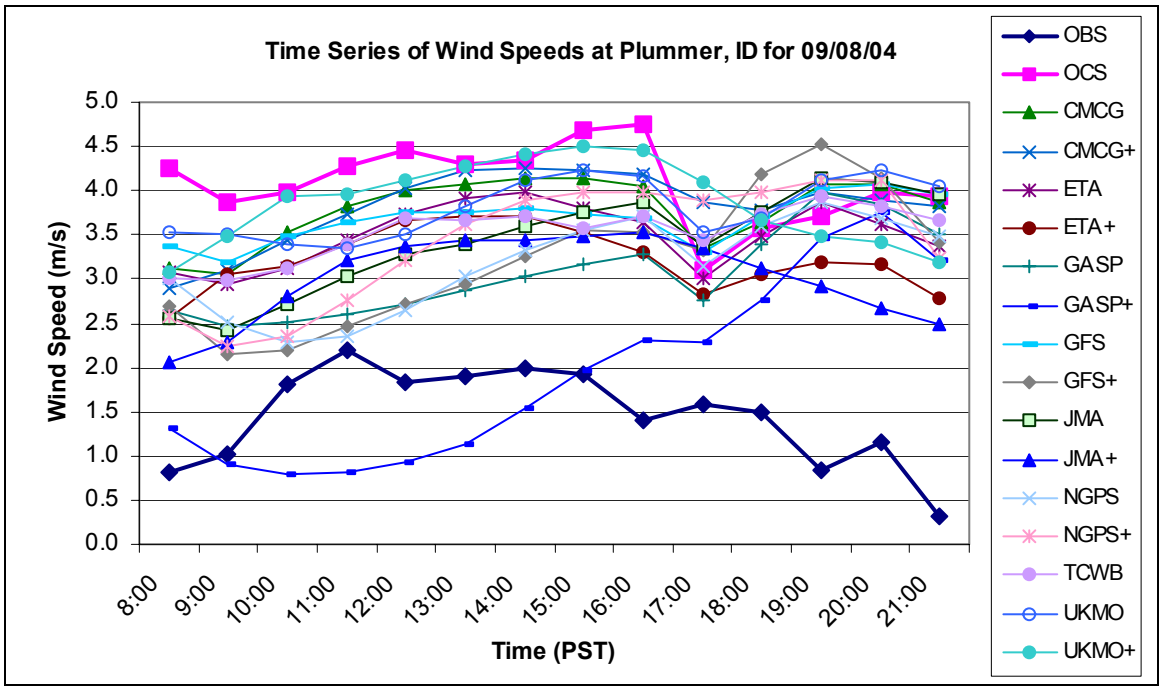

Figure C.17: Time series of wind speeds at Plummer, ID for September 8, 2004. Observations (OBS) and original ClearSky (OCS) are shown with the 15 ensemble ClearSky members.

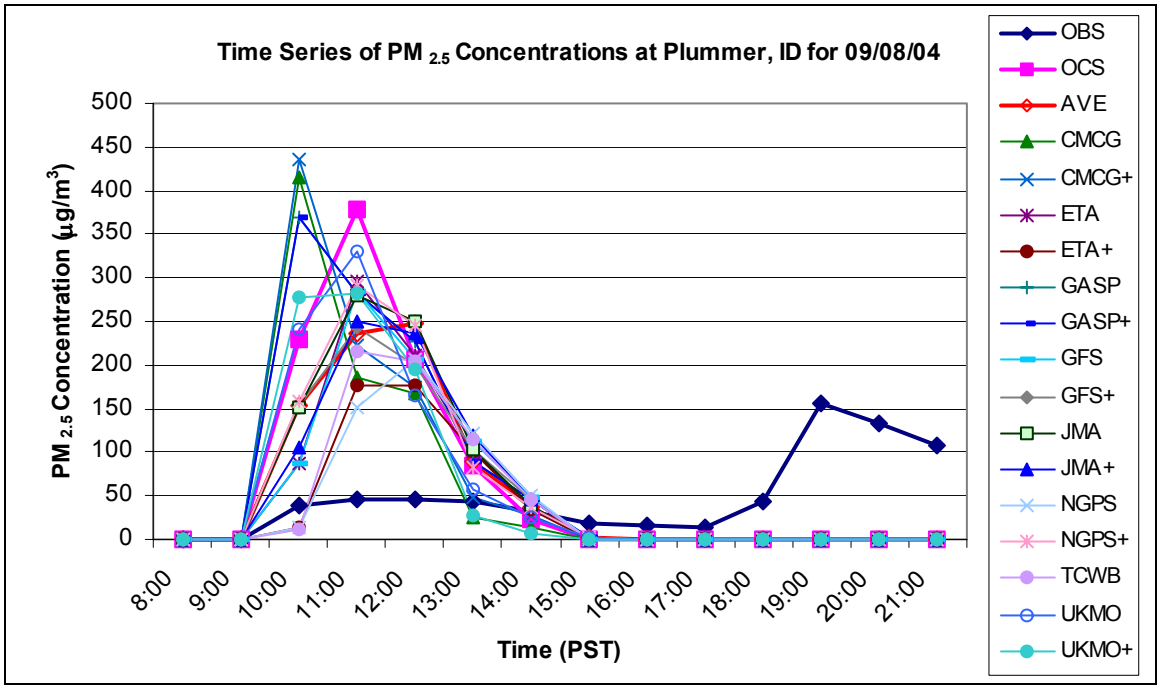

Figure C.18: Time series of ensemble $PM_{2.5}$ concentrations at Plummer, ID monitoring site for September 8, 2004. Observations (OBS), original ClearSky (OCS), and ensemble average (AVE) are shown with the 15 ensemble ClearSky members.

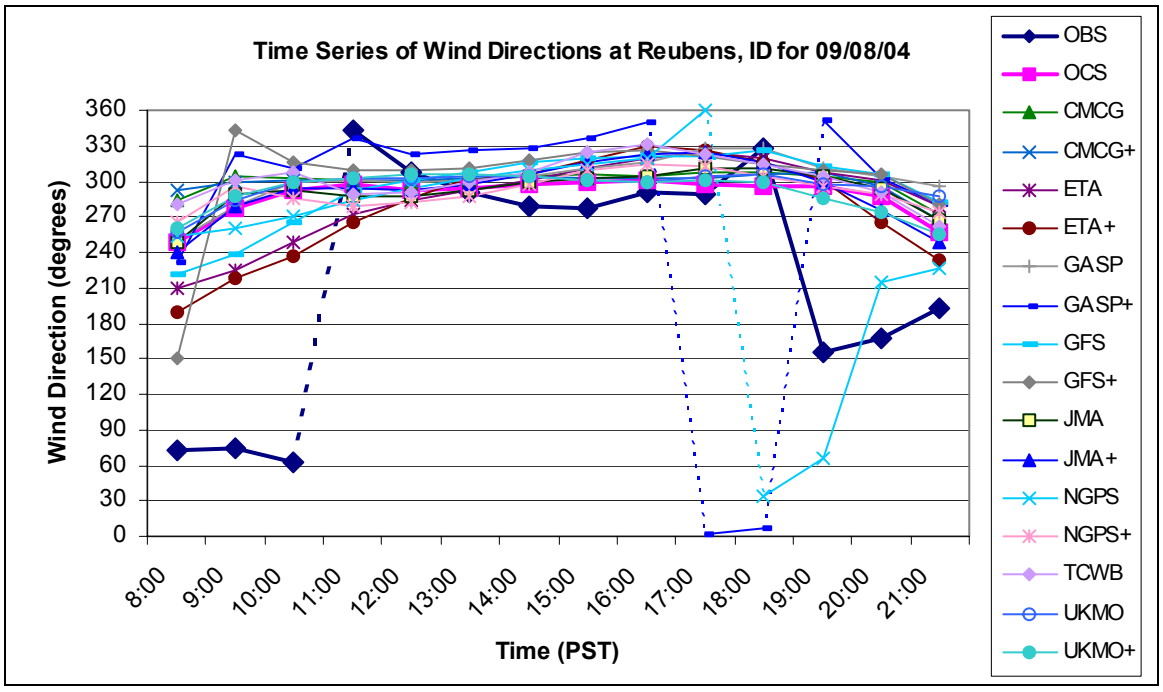

Figure C.19: Time series of wind directions at Reubens, ID monitoring site for September 8, 2004. Observations (OBS) and original ClearSky (OCS) are shown with the 15 ensemble ClearSky members. Dashed lines represent the shift from 0 to 360 degrees.

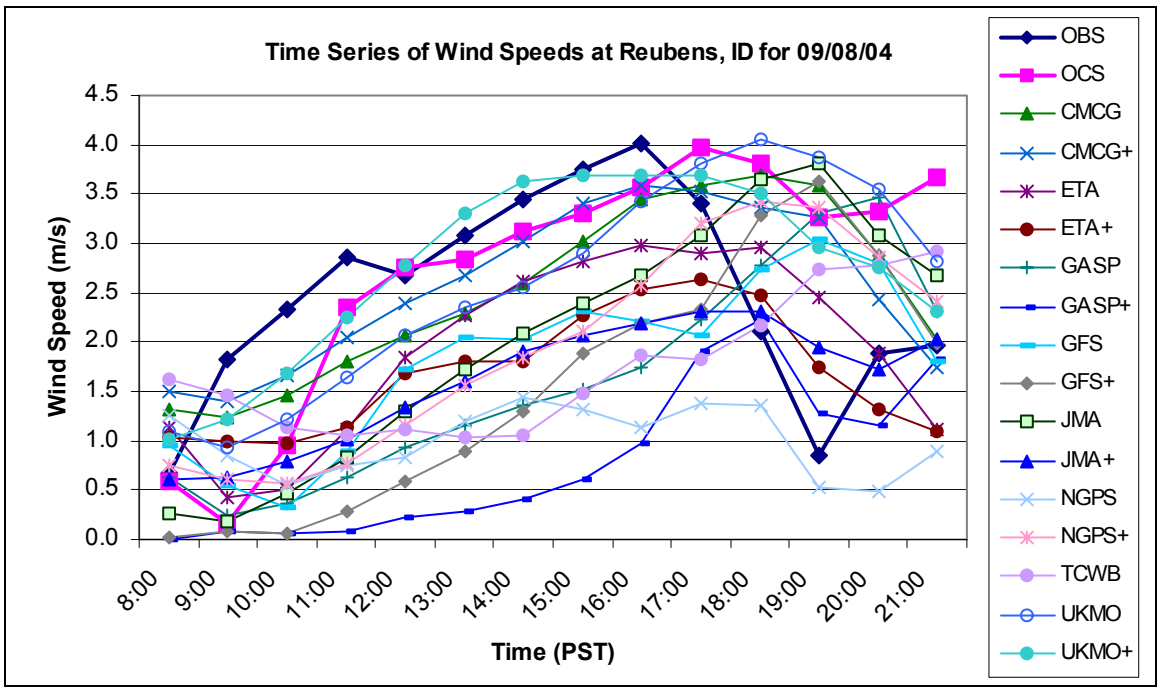

Figure C.20: Time series of wind speeds at Reubens, ID for September 8, 2004. Observations (OBS) and original ClearSky (OCS) are shown with the 15 ensemble ClearSky members.

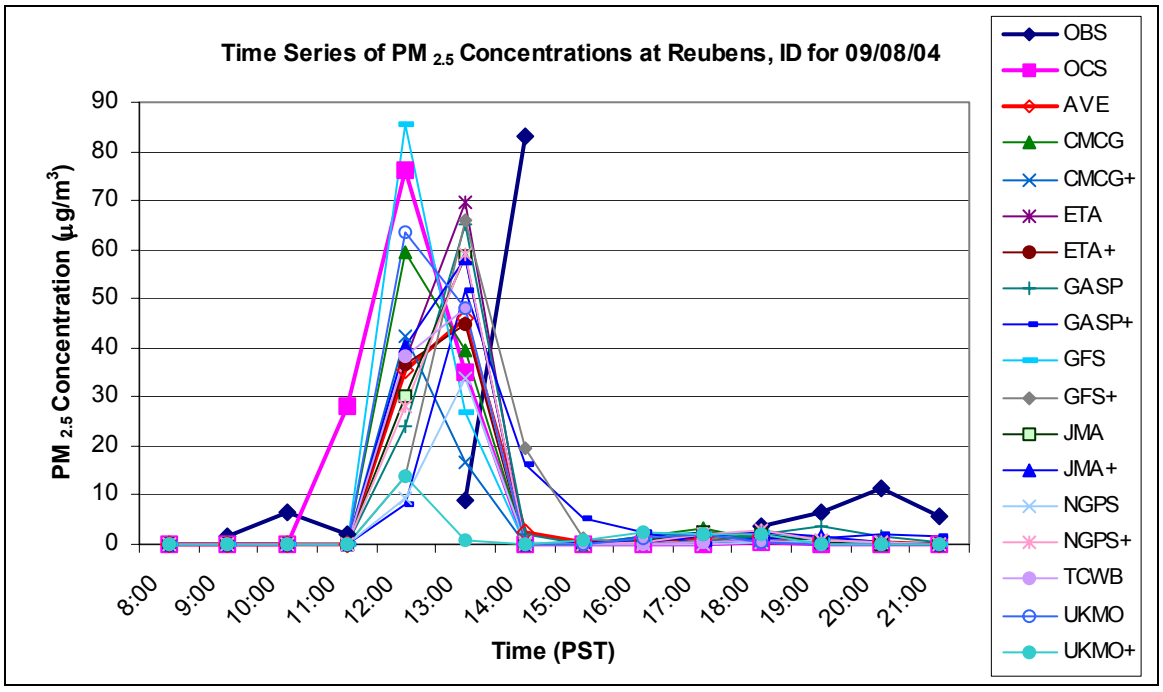

Figure C.21: Time series of ensemble $PM_{2.5}$ concentrations at Reubens, ID monitoring site for September 8, 2004. Observations (OBS), original ClearSky (OCS), and ensemble average (AVE) are shown with the 15 ensemble ClearSky members.